ISSN 1948-0210 (online)

World Journal of *Stem Cells*

World J Stem Cells 2020 February 26; 12(2): 100-167

Published by Baishideng Publishing Group Inc

WJSC

World Journal of Stem Cells

Contents

Monthly Volume 12 Number 2 February 26, 2020

Contents

World Journal of Stem Cells

Volume 12 Number 2 February 26, 2020

ABOUT COVER

Editorial Board Member of *World Journal of Stem Cells*, Pietro Gentile, MD, PhD, Professor, Senior Researcher, Department of Surgical Science, Plastic and Reconstructive Surgery, "Tor Vergata" University, Rome 00173, Italy

AIMS AND SCOPE

The primary aim of *World Journal of Stem Cells* (*WJSC*, *World J Stem Cells*) is to provide scholars and readers from various fields of stem cells with a platform to publish high-quality basic and clinical research articles and communicate their research findings online.

WJSC publishes articles reporting research results obtained in the field of stem cell biology and regenerative medicine, related to the wide range of stem cells including embryonic stem cells, germline stem cells, tissue-specific stem cells, adult stem cells, mesenchymal stromal cells, induced pluripotent stem cells, embryoid bodies, embryonal carcinoma stem cells, hemangioblasts, hematopoietic stem cells, lymphoid progenitor cells, myeloid progenitor cells, *etc*.

INDEXING/ABSTRACTING

The *WJSC* is now indexed in PubMed, PubMed Central, Science Citation Index Expanded (also known as SciSearch®), Journal Citation Reports/Science Edition, Biological Abstracts, and BIOSIS Previews. The 2019 Edition of Journal Citation Reports cites the 2018 impact factor for *WJSC* as 3.534 (5-year impact factor: N/A), ranking *WJSC* as 16 among 26 journals in Cell and Tissue Engineering (quartile in category Q3), and 94 among 193 journals in Cell Biology (quartile in category Q2).

RESPONSIBLE EDITORS FOR THIS ISSUE

Responsible Electronic Editor: *Yan-Xia Xing*

Proofing Production Department Director: *Yun-Xiaojian Wu*

NAME OF JOURNAL
World Journal of Stem Cells

ISSN
ISSN 1948-0210 (online)

LAUNCH DATE
December 31, 2009

FREQUENCY
Monthly

EDITORS-IN-CHIEF
Tong Cao, Shengwen Calvin Li, Carlo Ventura

EDITORIAL BOARD MEMBERS
https://www.wjgnet.com/1948-0210/editorialboard.htm

EDITORIAL OFFICE
Jin-Lei Wang, Director

PUBLICATION DATE
February 26, 2020

INSTRUCTIONS TO AUTHORS
https://www.wjgnet.com/bpg/gerinfo/204

GUIDELINES FOR ETHICS DOCUMENTS
https://www.wjgnet.com/bpg/GerInfo/287

GUIDELINES FOR NON-NATIVE SPEAKERS OF ENGLISH
https://www.wjgnet.com/bpg/gerinfo/240

PUBLICATION MISCONDUCT
https://www.wjgnet.com/bpg/gerinfo/208

ARTICLE PROCESSING CHARGE
https://www.wjgnet.com/bpg/gerinfo/242

STEPS FOR SUBMITTING MANUSCRIPTS
https://www.wjgnet.com/bpg/GerInfo/239

ONLINE SUBMISSION
https://www.f6publishing.com

World Journal of Stem Cells

Submit a Manuscript: https://www.f6publishing.com

World J Stem Cells 2020 February 26; 12(2): 100-109

DOI: 10.4252/wjsc.v12.i2.100

ISSN 1948-0210 (online)

OPINION REVIEW

Mesenchymal stem cells from different sources and their derived exosomes: A pre-clinical perspective

María Álvarez-Viejo

ORCID number: María Álvarez-Viejo (0000-0003-4248-0164).

Author contributions: Álvarez-Viejo M wrote the paper.

Conflict-of-interest statement: Author declare no conflicts of interest related to this article.

Manuscript source: Invited manuscript

Received: August 29, 2019
Peer-review started: August 29, 2019
First decision: November 12, 2019
Revised: December 18, 2019
Accepted: January 14, 2020
Article in press: January 14, 2020
Published online: February 26, 2020

P-Reviewer: Grawish M, Valenti MT, Zheng TW
S-Editor: Zhang L
L-Editor: Webster JR
E-Editor: Xing YX

María Álvarez-Viejo, Unidad de Terapia Celular y Medicina Regenerativa, Servicio de Hematología y Hemoterapia, Hospital Universitario Central de Asturias, Oviedo 33011, Spain

María Álvarez-Viejo, Plataforma de Terapias Avanzadas, Instituto de Investigación Sanitaria del Principado de Asturias, Oviedo 33011, Spain

Corresponding author: María Álvarez-Viejo, PhD, Associate Professor, Unidad de Terapia Celular y Medicina Regenerativa, Servicio de Hematología y Hemoterapia, Hospital Universitario Central de Asturias, Oviedo 33011, Spain. maria.alvarezv@sespa.es

Abstract

Since the introduction of cell therapy as a strategy for the treatment of many diseases, mesenchymal stem cells have emerged as ideal candidates, yet the underlying mechanisms of their beneficial effects are only partially understood. At the start of the 21st century, a paracrine effect was proposed as a mechanism of tissue repair by these cells. In addition, a role was suggested for a heterogeneous population of extracellular vesicles in cell-to-cell communication. Some of these vesicles including exosomes have been isolated from most fluids and cells, as well as from supernatants of *in vitro* cell cultures. Recent research in the field of regenerative medicine suggests that exosomes derived from mesenchymal stem cells could be a powerful new therapeutic tool. This review examines the therapeutic potential of these exosomes obtained from the sources most used in cell therapy: bone marrow, adipose tissue, and umbilical cord.

Key words: Mesenchymal stem cells; Exosomes; Cellular therapy

Core tip: This article reviews the use of exosomes derived from mesenchymal stem cells to treat various disease states and discusses their possible clinical applications.

Citation: Álvarez-Viejo M. Mesenchymal stem cells from different sources and their derived exosomes: A pre-clinical perspective. *World J Stem Cells* 2020; 12(2): 100-109
URL: https://www.wjgnet.com/1948-0210/full/v12/i2/100.htm
DOI: https://dx.doi.org/10.4252/wjsc.v12.i2.100

INTRODUCTION

At the start of the 21st century, cell therapy, defined as a series of strategies based on the use of living cells for therapeutic purposes, emerged as a promising tool in the field of biomedicine. The aim of cell therapy is to repair, replace or restore the biological functions of an organ or of damaged tissue. Research efforts in regenerative medicine have mainly focused on the use of mesenchymal stem cells (MSC).

Friedenstein and co-workers were the first to discover MSC. These authors showed that bone marrow (BM) contains a population of cells with a high proliferative capacity that adheres to plastic in culture[1]. Since this observation in the 1970s, many studies have focused on this type of adult stem cell. However, there was no defined approach to characterize MSC and different methods of isolation, expansion and characterization were reported. This made it difficult to compare findings between independent laboratories. To resolve this issue, in 2006, the Mesenchymal and Tissue Stem Cell Committee of the International Society for Cellular Therapy proposed minimal criteria to define human MSC: They should be plastic-adherent when maintained in standard culture conditions; they must express specific surface antigens; and they should also show multipotent cell differentiation potential *in vitro*[2]. These criteria facilitated the work of many groups which continued their research with this cell type. MSC have been successfully obtained from many sources including adipose tissue, Wharton's Jelly, placenta, dental pulp or amniotic fluid among others[3]. Furthermore, throughout the years, the regenerative capacity of MSC and their immunoregulatory properties have been well documented[4].

Due to their characteristics, MSC offer great therapeutic potential and many therapies based on these cells have been developed to treat a wide range of disorders. However, despite good results, the underlying mechanisms of their beneficial impacts are only partially understood. One hypothesis is that MSC induce tissue regeneration through their capacity to migrate to the site of injury and then to differentiate into the corresponding cells in the damaged tissue. In 2005, Gnecchi *et al*[5] were among the first to propose a paracrine effect of MSC in tissue regeneration[5]. Since then, many studies have shown these effects of MSC[6,7] and it is recognized today that, besides releasing cytokines and growth factors, MSC also secrete extracellular vesicles (EV), which are thought to play an important role in tissue regeneration and immunomodulation[4]. Based on these data, recent research has focused on EV derived from MSC as a form of non-cellular therapy[8].

The term EV refers to a heterogeneous population of vesicles[9]. For several decades, the presence of membrane-enclosed vesicles outside solid tissue cells, as well as biological fluids such as blood or semen, was described[10]. These vesicles were considered a vehicle for the cell to discard unwanted proteins[11]. In the first decade of the 21st century, two independent research groups demonstrated the presence of RNA, including miRNA in EV. This finding has rekindled interest in EV as possible mediators of cell-to-cell communication[12,13]. The International Society for Extracellular Vesicles proposed minimum criteria for their definition: EV is the generic term for particles naturally released from the cell that are delimited by a lipid bilayer and cannot replicate, *i.e.* they do not contain a functional nucleus[14]. To date, EV have been isolated from most fluids and cells[15] and from supernatants of *in vitro* cell cultures[16]. It has also been established that the release of EV is an evolutionarily well-conserved mechanism that the cells exploit for the exchange of bioactive proteins, lipids and nucleic acids[17].

The term EV encompasses microvesicles/nanoparticles/vesicles, apoptotic bodies and exosomes[16]. Exosomes are small EV generated thought inward budding of endosomal membranes. While the definition of exosomes is not completely clear, they are negatively charged lipid-bilayer vesicles of diameter 30-100 nm and density 1.13-1.19 g/mL. Exosomes are secreted by fusion of the multivesicular body containing exosomes with the plasma membrane[18]. The protein content of exosomes has been extensively studied since their initial description. So far, it is known that the composition of exosomal proteins varies among cell types. However, proteins such as Alix, Tsg101 and tetraspanins including CD9, CD63 or CD81 are frequent components and are often used as exosome markers[19].

Several studies have suggested that exosomes derived from MSC could serve as a novel therapeutic tool in the field of regenerative medicine. The main benefit proposed is that as no cells are introduced, mutated or damaged genetic material that could negatively affect the recipient is avoided. Another advantage is that exosomes lack immunogenicity[20]. As a shortcoming, exosomes are static and do not reproduce *in vivo*[21].

While MSC can be found in most adult tissues, the major sources of MSC for therapeutic use have been bone marrow, adipose tissue and umbilical cord[22]. This review updates research addressing the therapeutic potential of exosomes derived

from MSC obtained from these tissues.

EXOSOMES DERIVED FROM BONE MARROW MSC

MSC derived from bone marrow are probably the most commonly used stem cells in clinical trials. The use of bone marrow MSC derived exosomes (BM MSC-Ex) as a promising tool for future therapies has been examined in experimental models of various pathologies. In a model of liver disease, Damania *et al*[23] employed rat BM MSC conditioned medium in *in vitro* and *in vivo* experiments. The rich exosome fraction obtained through ultracentrifugation of this medium was found to have antiapoptotic and antioxidant effects in *in vitro* models of liver injury and to improve liver regeneration and recovery from liver injury *in vivo*. These results are in accordance with those reported by Rong *et al*[24] who, using a rat model of liver fibrosis, observed that the administration of BM MSC-Ex improved this fibrosis. Furthermore, these authors proposed that the beneficial effects of these exosomes consisted of inhibition of the Wnt/β-catenin signaling pathway and suggested their use to treat liver disease in a clinical setting[24]. The therapeutic potential of BM MSC-Ex in degenerative diseases, such as intervertebral disc degeneration (IDD), has been advocated by several researchers. IDD is a cause of lower back pain related to degenerative musculoskeletal disorders affecting large numbers of patients. Liao *et al*[25], using human BM MSC-Ex in a rat tail model proposed that exosomes may delay or prevent disc degeneration. Exosomes could modulate endoplasmic reticulum stress and protect against nucleus pulposus cell death. The therapeutic effects of BM MSC-Ex on IDD are supported by the findings of another study conducted in an IDD model in rabbits. In this work, Xia *et al*[26] proposed that the use of BM MSC-Ex significantly prevents the progression of degeneration *via* anti-oxidant and anti-inflammatory effects. The use of BM MSC-Ex for the treatment of cancer has also been explored by several groups. Recently, BM MSC-Ex overexpressing (exogenous) miR-34a, a recognized tumor suppressor, were reported to ameliorate glioblastoma in a mouse model[27]. In another experimental study on pancreatic cancer, Wu *et al*[28] observed that BM MSC-Ex-derived miRNA-126-3p blocked the progression of this cancer.

Zhu *et al*[29] found that exosomes derived from different cell types had different therapeutic effects. This hypothesis is consistent with recently published data by the same group. When comparing the effects of exosomes obtained from healthy or diabetic rats in a rat calvarial defect, these authors observed a more positive effect when exosomes from rats without type-1 diabetes were used. Accordingly, they proposed that for patients with type-1 diabetes, the autologous transplantation of BM MSC-Ex to promote regeneration could be inappropriate[30].

According to the literature, the potential of BM MSC-Ex for the treatment of various pathologies seems evident. However, in terms of clinical applications we have only found a letter to the Editor in which their use to treat graft *vs* host disease (GvHD) is described. BM-MSC have been employed in the treatment of GvHD in clinical practice since Blanc *et al*[31] published their encouraging results for the treatment of refractory GvHD. In one patient, Kordelas *et al*[32] used an exosome-enriched fraction processed from collected MSC supernatants instead of administering the MSC themselves. The patient was stable for several months post-exosome application. Although the patient died of pneumonia 7 months after treatment, the authors concluded that BM MSC-Ex could be a new safe tool to treat therapy-refractory GvHD and most likely other inflammation-associated diseases[32]. The improvement observed in this patient is supported by work conducted in mouse models[33,34].

EXOSOMES DERIVED FROM ADIPOSE MSC

As with BM MSC-Ex, there are many literature descriptions of the use of exosomes derived from adipose MSC (AMSC-Ex), in which a paracrine effect is produced both *in vivo* and *in vitro*. Several research groups have reported positive effects of AMSC-Ex in various skin disorders. Cho *et al*[35] were the first to investigate the therapeutic effect of AMSC-Ex in an atopic dermatitis mouse model. Taken together, the results suggested that AMSC-Ex could be a novel cell-free treatment for atopic dermatitis. The limitations reported by these authors were that AMSC donor age seemed to affect their immunomodulatory properties. Accordingly, they proposed to continue working on this issue to determine whether the potential of AMSC-Ex could be influenced by age[35]. Treatment of cutaneous wound healing has also been explored using exosomes derived from AMSC. To improve the retention of exosomes in the target area, Liu *et al*[36] proposed the use of hyaluronic acid and examined the effect of

AMSC-Ex combined with hyaluronic acid for acute cutaneous wound healing in nude mice. These authors concluded that this preparation of exosomes combined with appropriate scaffolds was effective. Their results showed that AMSC-Ex could markedly promote fibroblast activities, re-epithelialization and vascularization in wound healing[36]. Other studies have shown that AMSC-Ex accelerate wound healing *via* optimizing fibroblast function and collagen deposition[37]. Furthermore, Shen *et al*[38] detected a role for AMSC-Ex in corneal stromal cell and extracellular matrix remodeling.

Other disease states such as heart and neural conditions or cancer have also been examined as targets of AMSC-Ex therapy. The results of *in vitro* experiments by Liu *et al*[39] indicated that apoptosis induced by oxidative stress in the cardiomyocyte was blocked by AMSC-Ex. Others have reported the inhibition of ovarian cancer cell proliferation by exosomes collected from AMSC conditioned medium[40]. Feng *et al*[41] also argued that the use of AMSC-Ex to inhibit the activation of microglia cells and prevent neuroinflammation could be a promising therapeutic strategy for nerve injury.

EXOSOMES DERIVED FROM UMBILICAL CORD MSC

Umbilical cord MSC and their exosomes have also been examined as potential therapeutic tools in regenerative medicine. However, as for exosomes derived from other sources, the underlying mechanisms are still not well understood. Zhang *et al*[42] suggested that exosomes derived from umbilical cord MSC (UcMSC-Ex) enhanced angiogenesis through the Wnt4/β-catenin pathway, which could be an important mechanism responsible for cutaneous wound healing. This positive effect on angiogenesis has also been reported by another group. Hence, the authors of a recent study reported that transplantation of UcMSC-Ex markedly enhanced angiogenesis and bone healing in a rat model of femoral fracture. Their results unveiled a novel role of exosomes in accelerating fracture healing *via* the promotion of angiogenesis[43]. The results of both these studies are in accordance with the data reported by Zhou *et al*[44]. These last authors explored the impacts of human UcMSC-Ex on fracture healing by acting on the Wnt signaling pathway. They concluded that UcMSC-Ex could participate in repairing fractures in rats through this pathway.

Mao *et al*[45] investigated the effects of UcMSC-Ex in a model of induced inflammatory bowel disease. According to their findings, UcMSC-Ex are able to substantially alleviate induced inflammatory bowel disease in mice and may exert their impact through IL-7 expression modulation in macrophages. Other authors have assessed the immunosuppression and therapeutic effects of UcMSC-Ex used to treat colitis in a mouse model. Exosomes were obtained from MSC cultures in defined medium thus avoiding the use of fetal bovine serum. The results indicated that UcMSC-Ex alleviate colon damage in an animal disease model and have immunosuppressive effects *in vitro*[46]. These results have interesting implications for the clinical use of this type of therapy. Due to their immunosuppressive activity, autoimmune diseases have been a popular target of MSC therapy. This activity has been related to the secretion of soluble factors. Bai *et al*[47] analyzed the effect of UcMSC-Ex in an experimental model of autoimmune uveitis. The results revealed the therapeutic potential of exosomes for this condition. Bearing in mind that this is a major cause of visual impairment worldwide, these are promising results. Zhang *et al*[48] in 2018 addressed the clinical treatment of another common cause of visual impairment, idiopathic macular hole. This work is interesting because, as previously mentioned, the translation of exosome-based therapies to clinical practice is still very limited. Five patients with large, long-standing idiopathic macular holes were treated with an intravitreal UcMSC-Ex injection. The authors proposed that these exosomes could improve anatomic and visual outcomes of surgery for that disease, and suggested the need for a clinical trial with a greater number of patients[48]. In a mouse model of acute liver failure, Jiang *et al*[49] observed that UcMSC-Ex decreased the expression of the NLRP3 inflammasome and improved acute liver failure in that model. Animal models have also been used to examine the treatment of ischemic heart disease using exosomes. In a recent study, Han *et al*[50] encapsulated UcMSC-Ex in a functional peptide hydrogel designed to increase the retention and stability of exosomes. The hydrogel containing UcMSC-Ex was then used in a rat myocardial infarction model, injecting it into the infarcted border of the heart. The authors concluded that this is an effective way of harnessing exosomes for cardiac regeneration[50].

The data available in the literature related to the use of exosomes derived from different MSC to treat various pathologies are practically all at the experimental stage.

These data supporting their therapeutic potential are summarized in Table 1, Table 2 and Table 3. Although many studies have interesting clinical implications, there are still few data on the clinical use of exosomes including very few registered trials (www.ClinicalTrials.gov).

There is still much work to do. The optimization and standardization of obtaining exosomes is an important goal. Some authors advocate inducing hypoxia or stress in exosome-producing cells to increase exosome production[18]. This could be an interesting way of generating exosomes for clinical applications. Another interesting issue is related to adjusting doses for treatment. Further questions that need to be addressed are: Which is the ideal time to administer exosomes? Will scaffolds be necessary in some applications? The different laboratories are presently working on these issues to standardize how exosomes are obtained.

CONCLUSION

In summary, cell therapy "without cells", is an emerging field. While still at the experimental level, recent research efforts are starting to explore its translation to clinical practice. In the meantime, research into MSC cell therapy continues and there are hundreds of registered trials at different stages. We envisage that clinical trials in the near future will compare the benefits and shortcomings of cell therapy with and without cells.

Table 1 Exosomes derived from bone marrow mesenchymal stem cells

	In vitro study	*In vivo* study (animal model / clinical use)	Results	Ref.
Liver disease	+	Liver injury model (Rat)	Improves liver regeneration and recovery	Damania *et al*[23], 2018
Liver disease	+	Liver fibrosis model (Rat)	Reduces liver fibrosis	Rong *et al*[24], 2019
Intervertebral disc degeneration	-	Tail model (Rat)	Prevents disc degeneration progression	Liao *et al*[25], 2019
Intervertebral disc degeneration	+	IDD model (Rabbit)	Prevents the progression of degeneration *via* anti-oxidant and anti-inflammatory effects	Xia *et al*[26], 2019
Cancer	+	Xenografted with glioblastoma cells (Nude mice)	Improves glioblastoma	Wang *et al*[27], 2019
Cancer	+	Pancreatic cancer cells xenografted (Nude mice)	Inhibits cancer development	Wu *et al*[28], 2019
Bone regeneration	+	Calvarian defect (Rat)	Promotes bone regeneration and neovascularization	Zhu *et al*[30], 2019
Graft *vs* host disease	+	GvHD model (Mouse)	Enhances Treg production *in vitro* and *in vivo*	Zhang *et al*[34], 2018
Graft *vs* host disease	+	GvHD model (Mouse)	Ameliorates aGvHD *via* the therapeutic infusion of BM MSC-Ex	Fuji *et al*[33], 2018
Graft *vs* host disease	-	Clinical patient	Patient stable for several months after exosome application	Kordelas *et al*[32], 2014

GvHD: Graft *vs* host disease; BM MSC-Ex: Bone marrow mesenchymal stem cells derived exosomes; IDD: Intervertebral disc degeneration.

Table 2 Exosomes derived from adipose mesenchymal stem cells

Condition	*In vitro* study	*In vivo* study (animal model / clinical use)	Results	Ref.
Atopic dermatitis	-	Atopic dermatitis model (Mouse)	Reduces clinical symptoms	Cho *et al*[35], 2018
Acute cutaneous wound healing	-	Acute cutaneous wound healing (Nude mice)	Promotes fibroblast activities, re-epithelialization, vascularization in wound healing	Liu *et al*[36], 2019
Wound healing	+	Mouse full-thickness incision wound model	Accelerates wound healing by optimizing fibroblast function	Zhang *et al*[37], 2018
Corneal stromal cells	+	-	Role of ASC-Ex in corneal stromal cell and extra cellular matrix remodeling	Shen *et al*[38], 2018
Apoptosis in cardiomyocyte caused by oxidative stress	+	-	Prevents apoptosis	Liu *et al*[39], 2019
Ovarian cancer	+	-	Ovarian cancer cells inhibited by exosomes	Reza *et al*[40], 2016
Neural injury	+	-	Could inhibit the activation of microglia cells and prevent neuroinflammation	Feng *et al*[41], 2019

ASC-Ex: Exosomes derived from adipose mesenchymal stem cells.

Table 3 Exosomes derived from umbilical cord mesenchymal stem cells

Condition	*In vitro* study	*In vivo* study (animal model / clinical use)	Results	Ref.
Cutaneous wound healing	+	Wound model (Rat)	Proangiogenic effect	Zhang *et al*[42], 2015
Bone healing	+	Femoral fracture model (Rat)	Accelerated fracture healing *via* the promotion of angiogenesis	Zhang *et al*[43], 2019
Bone healing	-	Fracture model (Rat)	Repairs fractures in rats through the Wnt signaling pathway	Zhou *et al*[44], 2019
Inflammatory bowel disease	+	Inflammatory bowel disease model (Mouse)	Alleviates induced inflammatory bowel disease	Mao *et al*[45], 2017
Acute liver failure	+	Liver injury model (Mouse)	Decreases acute liver failure in that model	Jiang *et al*[49], 2019
Colitis	+	Colitis model (Mouse)	Improves colon damage in an animal disease model and has immunosuppressive effects *in vitro*	Ma *et al*[46], 2019
Autoimmune uveitis	+	Autoimmune uveitis model (Rat)	Ameliorates autoimmune uveitis by inhibiting the migration of inflammatory cells	Bai *et al*[47], 2017
Idiopathic macular hole	-	Clinical patients (5)	May improve anatomic and visual outcomes of surgery for that disease	Zhang *et al*[48], 2018
Myocardial infarction	+	Myocardial infarction model (Rat)	UcMSC-Ex encapsulated in a functional peptide hydrogel could be effective for cardiac regeneration	Han *et al*[50], 2019

UcMSC-Ex: Exosomes derived from umbilical cord mesenchymal stem cells.

ACKNOWLEDGEMENTS

The author would like to thank Roberto Garcia Gomez for reviewing the text and Cristina Martin Martin for her suggestions.

REFERENCES

1 **Friedenstein AJ**, Chailakhjan RK, Lalykina KS. The development of fibroblast colonies in monolayer cultures of guinea-pig bone marrow and spleen cells. *Cell Tissue Kinet* 1970; **3**: 393-403 [PMID: 5523063 DOI: 10.1111/j.1365-2184.1970.tb00347.x]
2 **Dominici M**, Le Blanc K, Mueller I, Slaper-Cortenbach I, Marini F, Krause D, Deans R, Keating A, Prockop Dj, Horwitz E. Minimal criteria for defining multipotent mesenchymal stromal cells. The International Society for Cellular Therapy position statement. *Cytotherapy* 2006; **8**: 315-317 [PMID: 16923606 DOI: 10.1080/14653240600855905]
3 **Altanerova U**, Jakubechova J, Repiska V, Altaner C. Exosomes of human mesenchymal stem/stromal/medicinal signaling cells. *Neoplasma* 2017; **64**: 809-815 [PMID: 28895404 DOI: 10.4149/neo_2017_601]
4 **Phan J**, Kumar P, Hao D, Gao K, Farmer D, Wang A. Engineering mesenchymal stem cells to improve their exosome efficacy and yield for cell-free therapy. *J Extracell Vesicles* 2018; **7**: 1522236 [PMID: 30275938 DOI: 10.1080/20013078.2018.1522236]
5 **Gnecchi M**, He H, Liang OD, Melo LG, Morello F, Mu H, Noiseux N, Zhang L, Pratt RE, Ingwall JS, Dzau VJ. Paracrine action accounts for marked protection of ischemic heart by Akt-modified mesenchymal stem cells. *Nat Med* 2005; **11**: 367-368 [PMID: 15812508 DOI: 10.1038/nm0405-367]
6 **Beer L**, Mildner M, Ankersmit HJ. Cell secretome based drug substances in regenerative medicine: when regulatory affairs meet basic science. *Ann Transl Med* 2017; **5**: 170 [PMID: 28480206 DOI: 10.21037/atm.2017.03.50]
7 **Fu X**, Liu G, Halim A, Ju Y, Luo Q, Song AG. Mesenchymal Stem Cell Migration and Tissue Repair. *Cells* 2019; 8 [PMID: 31357692 DOI: 10.3390/cells8080784]
8 **Rani S**, Ryan AE, Griffin MD, Ritter T. Mesenchymal Stem Cell-derived Extracellular Vesicles: Toward Cell-free Therapeutic Applications. *Mol Ther* 2015; **23**: 812-823 [PMID: 25868399 DOI: 10.1038/mt.2015.44]
9 **Samuelson I**, Vidal-Puig AJ. Fed-EXosome: extracellular vesicles and cell-cell communication in metabolic regulation. *Essays Biochem* 2018; **62**: 165-175 [PMID: 29717059 DOI: 10.1042/EBC20170087]
10 **Colombo M**, Raposo G, Théry C. Biogenesis, secretion, and intercellular interactions of exosomes and other extracellular vesicles. *Annu Rev Cell Dev Biol* 2014; **30**: 255-289 [PMID: 25288114 DOI: 10.1146/annurev-cellbio-101512-122326]

11 **Lou G**, Chen Z, Zheng M, Liu Y. Mesenchymal stem cell-derived exosomes as a new therapeutic strategy for liver diseases. *Exp Mol Med* 2017; **49**: e346 [PMID: 28620221 DOI: 10.1038/emm.2017.63]

12 **Ratajczak J**, Miekus K, Kucia M, Zhang J, Reca R, Dvorak P, Ratajczak MZ. Embryonic stem cell-derived microvesicles reprogram hematopoietic progenitors: evidence for horizontal transfer of mRNA and protein delivery. *Leukemia* 2006; **20**: 847-856 [PMID: 16453000 DOI: 10.1038/sj.leu.2404132]

13 **Valadi H**, Ekström K, Bossios A, Sjöstrand M, Lee JJ, Lötvall JO. Exosome-mediated transfer of mRNAs and microRNAs is a novel mechanism of genetic exchange between cells. *Nat Cell Biol* 2007; **9**: 654-659 [PMID: 17486113 DOI: 10.1038/ncb1596]

14 **Théry C**, Witwer KW, Aikawa E, Alcaraz MJ, Anderson JD, Andriantsitohaina R, Antoniou A, Arab T, Archer F, Atkin-Smith GK, Ayre DC, Bach JM, Bachurski D, Baharvand H, Balaj L, Baldacchino S, Bauer NN, Baxter AA, Bebawy M, Beckham C, Bedina Zavec A, Benmoussa A, Berardi AC, Bergese P, Bielska E, Blenkiron C, Bobis-Wozowicz S, Boilard E, Boireau W, Bongiovanni A, Borràs FE, Bosch S, Boulanger CM, Breakefield X, Breglio AM, Brennan MÁ, Brigstock DR, Brisson A, Broekman ML, Bromberg JF, Bryl-Górecka P, Buch S, Buck AH, Burger D, Busatto S, Buschmann D, Bussolati B, Buzás EI, Byrd JB, Camussi G, Carter DR, Caruso S, Chamley LW, Chang YT, Chen C, Chen S, Cheng L, Chin AR, Clayton A, Clerici SP, Cocks A, Cocucci E, Coffey RJ, Cordeiro-da-Silva A, Couch Y, Coumans FA, Coyle B, Crescitelli R, Criado MF, D'Souza-Schorey C, Das S, Datta Chaudhuri A, de Candia P, De Santana EF, De Wever O, Del Portillo HA, Demaret T, Deville S, Devitt A, Dhondt B, Di Vizio D, Dieterich LC, Dolo V, Dominguez Rubio AP, Dominici M, Dourado MR, Driedonks TA, Duarte FV, Duncan HM, Eichenberger RM, Ekström K, El Andaloussi S, Elie-Caille C, Erdbrügger U, Falcón-Pérez JM, Fatima F, Fish JE, Flores-Bellver M, Försönits A, Frelet-Barrand A, Fricke F, Fuhrmann G, Gabrielsson S, Gámez-Valero A, Gardiner C, Gärtner K, Gaudin R, Gho YS, Giebel B, Gilbert C, Gimona M, Giusti I, Goberdhan DC, Görgens A, Gorski SM, Greening DW, Gross JC, Gualerzi A, Gupta GN, Gustafson D, Handberg A, Haraszti RA, Harrison P, Hegyesi H, Hendrix A, Hill AF, Hochberg FH, Hoffmann KF, Holder B, Holthofer H, Hosseinkhani B, Hu G, Huang Y, Huber V, Hunt S, Ibrahim AG, Ikezu T, Inal JM, Isin M, Ivanova A, Jackson HK, Jacobsen S, Jay SM, Jayachandran M, Jenster G, Jiang L, Johnson SM, Jones JC, Jong A, Jovanovic-Talisman T, Jung S, Kalluri R, Kano SI, Kaur S, Kawamura Y, Keller ET, Khamari D, Khomyakova E, Khvorova A, Kierulf P, Kim KP, Kislinger T, Klingeborn M, Klinke DJ 2nd, Kornek M, Kosanović MM, Kovács ÁF, Krämer-Albers EM, Krasemann S, Krause M, Kurochkin IV, Kusuma GD, Kuypers S, Laitinen S, Langevin SM, Languino LR, Lannigan J, Lässer C, Laurent LC, Lavieu G, Lázaro-Ibáñez E, Le Lay S, Lee MS, Lee YXF, Lemos DS, Lenassi M, Leszczynska A, Li IT, Liao K, Libregts SF, Ligeti E, Lim R, Lim SK, Linē A, Linnemannstöns K, Llorente A, Lombard CA, Lorenowicz MJ, Lörincz ÁM, Lötvall J, Lovett J, Lowry MC, Loyer X, Lu Q, Lukomska B, Lunavat TR, Maas SL, Malhi H, Marcilla A, Mariani J, Mariscal J, Martens-Uzunova ES, Martin-Jaular L, Martinez MC, Martins VR, Mathieu M, Mathivanan S, Maugeri M, McGinnis LK, McVey MJ, Meckes DG Jr, Meehan KL, Mertens I, Minciacchi VR, Möller A, Møller Jørgensen M, Morales-Kastresana A, Morhayim J, Mullier F, Muraca M, Musante L, Mussack V, Muth DC, Myburgh KH, Najrana T, Nawaz M, Nazarenko I, Nejsum P, Neri C, Neri T, Nieuwland R, Nimrichter L, Nolan JP, Nolte-'t Hoen EN, Noren Hooten N, O'Driscoll L, O'Grady T, O'Loghlen A, Ochiya T, Olivier M, Ortiz A, Ortiz LA, Osteikoetxea X, Østergaard O, Ostrowski M, Park J, Pegtel DM, Peinado H, Perut F, Pfaffl MW, Phinney DG, Pieters BC, Pink RC, Pisetsky DS, Pogge von Strandmann E, Polakovicova I, Poon IK, Powell BH, Prada I, Pulliam L, Quesenberry P, Radeghieri A, Raffai RL, Raimondo S, Rak J, Ramirez MI, Raposo G, Rayyan MS, Regev-Rudzki N, Ricklefs FL, Robbins PD, Roberts DD, Rodrigues SC, Rohde E, Rome S, Rouschop KM, Rughetti A, Russell AE, Saá P, Sahoo S, Salas-Huenuleo E, Sánchez C, Saugstad JA, Saul MJ, Schiffelers RM, Schneider R, Schøyen TH, Scott A, Shahaj E, Sharma S, Shatnyeva O, Shekari F, Shelke GV, Shetty AK, Shiba K, Siljander PR, Silva AM, Skowronek A, Snyder OL 2nd, Soares RP, Sódar BW, Soekmadji C, Sotillo J, Stahl PD, Stoorvogel W, Stott SL, Strasser EF, Swift S, Tahara H, Tewari M, Timms K, Tiwari S, Tixeira R, Tkach M, Toh WS, Tomasini R, Torrecilhas AC, Tosar JP, Toxavidis V, Urbanelli L, Vader P, van Balkom BW, van der Grein SG, Van Deun J, van Herwijnen MJ, Van Keuren-Jensen K, van Niel G, van Royen ME, van Wijnen AJ, Vasconcelos MH, Vechetti IJ Jr, Veit TD, Vella LJ, Velot É, Verweij FJ, Vestad B, Viñas JL, Visnovitz T, Vukman KV, Wahlgren J, Watson DC, Wauben MH, Weaver A, Webber JP, Weber V, Wehman AM, Weiss DJ, Welsh JA, Wendt S, Wheelock AM, Wiener Z, Witte L, Wolfram J, Xagorari A, Xander P, Xu J, Yan X, Yáñez-Mó M, Yin H, Yuana Y, Zappulli V, Zarubova J, Žėkas V, Zhang JY, Zhao Z, Zheng L, Zheutlin AR, Zickler AM, Zimmermann P, Zivkovic AM, Zocco D, Zuba-Surma EK. Minimal information for studies of extracellular vesicles 2018 (MISEV2018): a position statement of the International Society for Extracellular Vesicles and update of the MISEV2014 guidelines. *J Extracell Vesicles* 2018; **7**: 1535750 [PMID: 30637094 DOI: 10.1080/20013078.2018.1535750]

15 **Yáñez-Mó M**, Siljander PR, Andreu Z, Zavec AB, Borràs FE, Buzas EI, Buzas K, Casal E, Cappello F, Carvalho J, Colás E, Cordeiro-da Silva A, Fais S, Falcon-Perez JM, Ghobrial IM, Giebel B, Gimona M, Graner M, Gursel I, Gursel M, Heegaard NH, Hendrix A, Kierulf P, Kokubun K, Kosanovic M, Kralj-Iglic V, Krämer-Albers EM, Laitinen S, Lässer C, Lener T, Ligeti E, Linē A, Lipps G, Llorente A, Lötvall J, Manček-Keber M, Marcilla A, Mittelbrunn M, Nazarenko I, Nolte-'t Hoen EN, Nyman TA, O'Driscoll L, Olivan M, Oliveira C, Pállinger É, Del Portillo HA, Reventós J, Rigau M, Rohde E, Sammar M, Sánchez-Madrid F, Santarém N, Schallmoser K, Ostenfeld MS, Stoorvogel W, Stukelj R, Van der Grein SG, Vasconcelos MH, Wauben MH, De Wever O. Biological properties of extracellular vesicles and their physiological functions. *J Extracell Vesicles* 2015; **4**: 27066 [PMID: 25979354 DOI: 10.3402/jev.v4.27066]

16 **Pinheiro A**, Silva AM, Teixeira JH, Gonçalves RM, Almeida MI, Barbosa MA, Santos SG. Extracellular vesicles: intelligent delivery strategies for therapeutic applications. *J Control Release* 2018; **289**: 56-69 [PMID: 30261205 DOI: 10.1016/j.jconrel.2018.09.019]

17 **Camussi G**, Deregibus MC, Cantaluppi V. Role of stem-cell-derived microvesicles in the paracrine action of stem cells. *Biochem Soc Trans* 2013; **41**: 283-287 [PMID: 23356298 DOI: 10.1042/BST20120192]

18 **Yamashita T**, Takahashi Y, Takakura Y. Possibility of Exosome-Based Therapeutics and Challenges in Production of Exosomes Eligible for Therapeutic Application. *Biol Pharm Bull* 2018; **41**: 835-842 [PMID: 29863072 DOI: 10.1248/bpb.b18-00133]

19 **Pols MS**, Klumperman J. Trafficking and function of the tetraspanin CD63. *Exp Cell Res* 2009; **315**: 1584-1592 [PMID: 18930046 DOI: 10.1016/j.yexcr.2008.09.020]

20 **Elahi FM**, Farwell DG, Nolta JA, Anderson JD. Preclinical translation of exosomes derived from mesenchymal stem/stromal cells. *Stem Cells* 2019 [PMID: 31381842 DOI: 10.1002/stem.3061]

21 **Phinney DG**, Pittenger MF. Concise Review: MSC-Derived Exosomes for Cell-Free Therapy. *Stem Cells*

2017; **35**: 851-858 [PMID: 28294454 DOI: 10.1002/stem.2575]
22 **Williams AR**, Hare JM. Mesenchymal stem cells: biology, pathophysiology, translational findings, and therapeutic implications for cardiac disease. *Circ Res* 2011; **109**: 923-940 [PMID: 21960725 DOI: 10.1161/CIRCRESAHA.111.243147]
23 **Damania A**, Jaiman D, Teotia AK, Kumar A. Mesenchymal stromal cell-derived exosome-rich fractionated secretome confers a hepatoprotective effect in liver injury. *Stem Cell Res Ther* 2018; **9**: 31 [PMID: 29409540 DOI: 10.1186/s13287-017-0752-6]
24 **Rong X**, Liu J, Yao X, Jiang T, Wang Y, Xie F. Human bone marrow mesenchymal stem cells-derived exosomes alleviate liver fibrosis through the Wnt/β-catenin pathway. *Stem Cell Res Ther* 2019; **10**: 98 [PMID: 30885249 DOI: 10.1186/s13287-019-1204-2]
25 **Liao Z**, Luo R, Li G, Song Y, Zhan S, Zhao K, Hua W, Zhang Y, Wu X, Yang C. Exosomes from mesenchymal stem cells modulate endoplasmic reticulum stress to protect against nucleus pulposus cell death and ameliorate intervertebral disc degeneration in vivo. *Theranostics* 2019; **9**: 4084-4100 [PMID: 31281533 DOI: 10.7150/thno.33638]
26 **Xia C**, Zeng Z, Fang B, Tao M, Gu C, Zheng L, Wang Y, Shi Y, Fang C, Mei S, Chen Q, Zhao J, Lin X, Fan S, Jin Y, Chen P. Mesenchymal stem cell-derived exosomes ameliorate intervertebral disc degeneration via anti-oxidant and anti-inflammatory effects. *Free Radic Biol Med* 2019; **143**: 1-15 [PMID: 31351174 DOI: 10.1016/j.freeradbiomed.2019.07.026]
27 **Wang B**, Wu ZH, Lou PY, Chai C, Han SY, Ning JF, Li M. Human bone marrow-derived mesenchymal stem cell-secreted exosomes overexpressing microRNA-34a ameliorate glioblastoma development via down-regulating MYCN. *Cell Oncol (Dordr)* 2019; **42**: 783-799 [PMID: 31332647 DOI: 10.1007/s13402-019-00461-z]
28 **Wu DM**, Wen X, Han XR, Wang S, Wang YJ, Shen M, Fan SH, Zhang ZF, Shan Q, Li MQ, Hu B, Lu J, Chen GQ, Zheng YL. Bone Marrow Mesenchymal Stem Cell-Derived Exosomal MicroRNA-126-3p Inhibits Pancreatic Cancer Development by Targeting ADAM9. *Mol Ther Nucleic Acids* 2019; **16**: 229-245 [PMID: 30925451 DOI: 10.1016/j.omtn.2019.02.022]
29 **Zhu Y**, Wang Y, Zhao B, Niu X, Hu B, Li Q, Zhang J, Ding J, Chen Y, Wang Y. Comparison of exosomes secreted by induced pluripotent stem cell-derived mesenchymal stem cells and synovial membrane-derived mesenchymal stem cells for the treatment of osteoarthritis. *Stem Cell Res Ther* 2017; **8**: 64 [PMID: 28279188 DOI: 10.1186/s13287-017-0510-9]
30 **Zhu Y**, Jia Y, Wang Y, Xu J, Chai Y. Impaired Bone Regenerative Effect of Exosomes Derived from Bone Marrow Mesenchymal Stem Cells in Type 1 Diabetes. *Stem Cells Transl Med* 2019; **8**: 593-605 [PMID: 30806487 DOI: 10.1002/sctm.18-0199]
31 **Le Blanc K**, Rasmusson I, Sundberg B, Götherström C, Hassan M, Uzunel M, Ringdén O. Treatment of severe acute graft-versus-host disease with third party haploidentical mesenchymal stem cells. *Lancet* 2004; **363**: 1439-1441 [PMID: 15121408 DOI: 10.1016/S0140-6736(04)16104-7]
32 **Kordelas L**, Rebmann V, Ludwig AK, Radtke S, Ruesing J, Doeppner TR, Epple M, Horn PA, Beelen DW, Giebel B. MSC-derived exosomes: a novel tool to treat therapy-refractory graft-versus-host disease. *Leukemia* 2014; **28**: 970-973 [PMID: 24445866 DOI: 10.1038/leu.2014.41]
33 **Fujii S**, Miura Y, Fujishiro A, Shindo T, Shimazu Y, Hirai H, Tahara H, Takaori-Kondo A, Ichinohe T, Maekawa T. Graft-Versus-Host Disease Amelioration by Human Bone Marrow Mesenchymal Stromal/Stem Cell-Derived Extracellular Vesicles Is Associated with Peripheral Preservation of Naive T Cell Populations. *Stem Cells* 2018; **36**: 434-445 [PMID: 29239062 DOI: 10.1002/stem.2759]
34 **Zhang B**, Yeo RWY, Lai RC, Sim EWK, Chin KC, Lim SK. Mesenchymal stromal cell exosome-enhanced regulatory T-cell production through an antigen-presenting cell-mediated pathway. *Cytotherapy* 2018; **20**: 687-696 [PMID: 29622483 DOI: 10.1016/j.jcyt.2018.02.372]
35 **Cho BS**, Kim JO, Ha DH, Yi YW. Exosomes derived from human adipose tissue-derived mesenchymal stem cells alleviate atopic dermatitis. *Stem Cell Res Ther* 2018; **9**: 187 [PMID: 29996938 DOI: 10.1186/s13287-018-0939-5]
36 **Liu K**, Chen C, Zhang H, Chen Y, Zhou S. ASC-Derived Exosomes in Combination with Hyaluronic Acid Accelerate Wound Healing through Enhancing Re-epithelialization and Vascularization. *Br J Dermatol* 2019 [DOI: 10.1111/bjd.17984]
37 **Zhang W**, Bai X, Zhao B, Li Y, Zhang Y, Li Z, Wang X, Luo L, Han F, Zhang J, Han S, Cai W, Su L, Tao K, Shi J, Hu D. Cell-free therapy based on adipose tissue stem cell-derived exosomes promotes wound healing via the PI3K/Akt signaling pathway. *Exp Cell Res* 2018; **370**: 333-342 [PMID: 29964051 DOI: 10.1016/j.yexcr.2018.06.035]
38 **Shen T**, Zheng QQ, Shen J, Li QS, Song XH, Luo HB, Hong CY, Yao K. Effects of Adipose-derived Mesenchymal Stem Cell Exosomes on Corneal Stromal Fibroblast Viability and Extracellular Matrix Synthesis. *Chin Med J (Engl)* 2018; **131**: 704-712 [PMID: 29521294 DOI: 10.4103/0366-6999.226889]
39 **Liu Z**, Xu Y, Wan Y, Gao J, Chu Y, Li J. Exosomes from adipose-derived mesenchymal stem cells prevent cardiomyocyte apoptosis induced by oxidative stress. *Cell Death Discov* 2019; **5**: 79 [PMID: 30911413 DOI: 10.1038/s41420-019-0159-5]
40 **Reza AMMT**, Choi YJ, Yasuda H, Kim JH. Human adipose mesenchymal stem cell-derived exosomal-miRNAs are critical factors for inducing anti-proliferation signalling to A2780 and SKOV-3 ovarian cancer cells. *Sci Rep* 2016; **6**: 38498 [PMID: 27929108 DOI: 10.1038/srep38498]
41 **Feng N**, Jia Y, Huang X. Exosomes from adipose-derived stem cells alleviate neural injury caused by microglia activation via suppressing NF-kB and MAPK pathway. *J Neuroimmunol* 2019; **334**: 576996 [PMID: 31260950 DOI: 10.1016/j.jneuroim.2019.576996]
42 **Zhang B**, Wu X, Zhang X, Sun Y, Yan Y, Shi H, Zhu Y, Wu L, Pan Z, Zhu W, Qian H, Xu W. Human umbilical cord mesenchymal stem cell exosomes enhance angiogenesis through the Wnt4/β-catenin pathway. *Stem Cells Transl Med* 2015; **4**: 513-522 [PMID: 25824139 DOI: 10.5966/sctm.2014-0267]
43 **Zhang Y**, Hao Z, Wang P, Xia Y, Wu J, Xia D, Fang S, Xu S. Exosomes from human umbilical cord mesenchymal stem cells enhance fracture healing through HIF-1α-mediated promotion of angiogenesis in a rat model of stabilized fracture. *Cell Prolif* 2019; **52**: e12570 [PMID: 30663158 DOI: 10.1111/cpr.12570]
44 **Zhou J**, Liu HX, Li SH, Gong YS, Zhou MW, Zhang JH, Zhu GY. Effects of human umbilical cord mesenchymal stem cells-derived exosomes on fracture healing in rats through the Wnt signaling pathway. *Eur Rev Med Pharmacol Sci* 2019; **23**: 4954-4960 [PMID: 31210331 DOI: 10.26355/eurrev_201906_18086]
45 **Mao F**, Wu Y, Tang X, Kang J, Zhang B, Yan Y, Qian H, Zhang X, Xu W. Exosomes Derived from Human Umbilical Cord Mesenchymal Stem Cells Relieve Inflammatory Bowel Disease in Mice. *Biomed*

Res Int 2017; **2017**: 5356760 [PMID: 28589143 DOI: 10.1155/2017/5356760]
46 **Ma ZJ**, Wang YH, Li ZG, Wang Y, Li BY, Kang HY, Wu XY. Immunosuppressive Effect of Exosomes from Mesenchymal Stromal Cells in Defined Medium on Experimental Colitis. *Int J Stem Cells* 2019; **12**: 440-448 [PMID: 31242720 DOI: 10.15283/ijsc18139]
47 **Bai L**, Shao H, Wang H, Zhang Z, Su C, Dong L, Yu B, Chen X, Li X, Zhang X. Effects of Mesenchymal Stem Cell-Derived Exosomes on Experimental Autoimmune Uveitis. *Sci Rep* 2017; **7**: 4323 [PMID: 28659587 DOI: 10.1038/s41598-017-04559-y]
48 **Zhang X**, Liu J, Yu B, Ma F, Ren X, Li X. Effects of mesenchymal stem cells and their exosomes on the healing of large and refractory macular holes. *Graefes Arch Clin Exp Ophthalmol* 2018; **256**: 2041-2052 [PMID: 30167916 DOI: 10.1007/s00417-018-4097-3]
49 **Jiang L**, Zhang S, Hu H, Yang J, Wang X, Ma Y, Jiang J, Wang J, Zhong L, Chen M, Wang H, Hou Y, Zhu R, Zhang Q. Exosomes derived from human umbilical cord mesenchymal stem cells alleviate acute liver failure by reducing the activity of the NLRP3 inflammasome in macrophages. *Biochem Biophys Res Commun* 2019; **508**: 735-741 [PMID: 30528233 DOI: 10.1016/j.bbrc.2018.11.189]
50 **Han C**, Zhou J, Liang C, Liu B, Pan X, Zhang Y, Wang Y, Yan B, Xie W, Liu F, Yu XY, Li Y. Human umbilical cord mesenchymal stem cell derived exosomes encapsulated in functional peptide hydrogels promote cardiac repair. *Biomater Sci* 2019; **7**: 2920-2933 [PMID: 31090763 DOI: 10.1039/c9bm00101h]

World Journal of Stem Cells

Submit a Manuscript: https://www.f6publishing.com

World J Stem Cells 2020 February 26; 12(2): 110-122

DOI: 10.4252/wjsc.v12.i2.110

ISSN 1948-0210 (online)

MINIREVIEWS

Cartilage and bone tissue engineering using adipose stromal/stem cells spheroids as building blocks

Gabriela S Kronemberger, Renata Akemi Morais Matsui, Guilherme de Almeida Santos de Castro e Miranda, José Mauro Granjeiro, Leandra Santos Baptista

ORCID number: Gabriela S Kronemberger (0000-0002-0953-221X); Renata Akemi Morais Matsui (0000-0003-4200-0175); Guilherme de Almeida Santos de Castro e Miranda (0000-0002-8698-1342); José Mauro Granjeiro (0000-0002-8027-8293); Leandra Santos Baptista (0000-0001-9998-8044).

Author contributions: Kronemberger GS drafted the article, contributed to the conception and design of the manuscript and wrote the article. Matsui RAM drafted and wrote the article. Miranda GASC drafted and wrote the article. Granjeiro JM contributed to the writing of the manuscript, made critical revisions related to relevant intellectual content of the manuscript and approved the final version of the article. Baptista LS drafted the article, contributed to the conception and design of the manuscript, contributed to the writing of the manuscript, made critical revisions related to relevant intellectual content of the manuscript and approved the final version of the article.

Supported by the Coordination for the Improvement of Higher Education Personnel (CAPES), No. 88882.366181/2019-01; the Carlos Chagas Filho Foundation for Research Support of the State of Rio de Janeiro (FAPERJ), No. E-26/202.682/2018; National Council for Scientific and Technological Development (CNPq), No. 467513/2014-7.

Gabriela S Kronemberger, Renata Akemi Morais Matsui, Guilherme de Almeida Santos de Castro e Miranda, José Mauro Granjeiro, Leandra Santos Baptista, Laboratory of Tissue Bioengineering, Directory of Metrology Applied to Life Sciences, National Institute of Metrology, Quality and Technology (INMETRO), Duque de Caxias, RJ 25250-020, Brazil

Gabriela S Kronemberger, Leandra Santos Baptista, Post-graduate Program in Translational Biomedicine (Biotrans), Unigranrio, Campus I, Duque de Caxias, RJ 25250-020, Brazil

Renata Akemi Morais Matsui, José Mauro Granjeiro, Leandra Santos Baptista, Post-graduate Program in Biotechnology, National Institute of Metrology, Quality and Technology (INMETRO), Duque de Caxias, RJ 25250-020, Brazil

Guilherme de Almeida Santos de Castro e Miranda, Federal University of Rio de Janeiro (UFRJ), Campus Duque de Caxias, Duque de Caxias, RJ 25250-020, Brazil

José Mauro Granjeiro, Laboratory of Clinical Research in Odontology, Fluminense Federal University (UFF), Niterói 25255-030 Brazil

Leandra Santos Baptista, Multidisciplinary Center for Biological Research (Numpex-Bio), Federal University of Rio de Janeiro (UFRJ) Campus Duque de Caxias, Duque de Caxias, RJ 25245-390, Brazil

Corresponding author: Leandra Santos Baptista, PhD, Associate Professor, Laboratory of Tissue Bioengineering, Directory of Metrology Applied to Life Sciences, National Institute of Metrology, Quality and Technology (INMETRO), Duque de Caxias, RJ 25250-020, Brazil. leandrabaptista@xerem.ufrj.br

Abstract

Scaffold-free techniques in the developmental tissue engineering area are designed to mimic *in vivo* embryonic processes with the aim of biofabricating, *in vitro*, tissues with more authentic properties. Cell clusters called spheroids are the basis for scaffold-free tissue engineering. In this review, we explore the use of spheroids from adult mesenchymal stem/stromal cells as a model in the developmental engineering area in order to mimic the developmental stages of cartilage and bone tissues. Spheroids from adult mesenchymal stromal/stem cells lineages recapitulate crucial events in bone and cartilage formation during embryogenesis, and are capable of spontaneously fusing to other spheroids, making them ideal building blocks for bone and cartilage tissue engineering. Here, we discuss data from ours and other labs on the use of adipose stromal/stem cell spheroids in chondrogenesis and osteogenesis *in vitro*. Overall,

Conflict-of-interest statement: The authors declare no conflict of interest.

Manuscript source: Invited manuscript

Received: May 18, 2019
Peer-review started: May 20, 2019
First decision: August 23,2019
Revised: October 19, 2019
Accepted: January 14, 2020
Article in press: January 14, 2020
Published online: February 26, 2020

P-Reviewer: Alonso MBD, Huang YC, Hassan A
S-Editor: Dou Y
L-Editor: Webster JR
E-Editor: Xing YX

recent studies support the notion that spheroids are ideal "building blocks" for tissue engineering by "bottom-up" approaches, which are based on tissue assembly by advanced techniques such as three-dimensional bioprinting. Further studies on the cellular and molecular mechanisms that orchestrate spheroid fusion are now crucial to support continued development of bottom-up tissue engineering approaches such as three-dimensional bioprinting.

Key words: Adipose stromal/stem cells; Spheroids; Building-blocks; Bottom-up; Developmental tissue engineering; Cartilage and bone

Core tip: Classic approaches to tissue engineering rely on scaffold-based strategies, which have limited ability to recapitulate organogenesis *in vitro* and are not capable of generating hierarchical engineered tissues. Scaffold-free strategies, in particular those using spheroids, are appealing, mainly due to the capacity of spheroids to recapitulate three main embryonic processes: (1) Cell-to-cell and cell-to-extracellular matrix interactions; (2) Cell differentiation; and (3) Fusion. The use of spheroids to recapitulate embryonic tissue formation *in vitro* represents a potent strategy in developmental tissue engineering. In particular, the fusion capacity of spheroids allows their use as building-blocks in bottom-up tissue engineering through three-dimensional bioprinting techniques.

Citation: Kronemberger GS, Matsui RAM, Miranda GASCE, Granjeiro JM, Baptista LS. Cartilage and bone tissue engineering using adipose stromal/stem cells spheroids as building blocks. *World J Stem Cells* 2020; 12(2): 110-122
URL: https://www.wjgnet.com/1948-0210/full/v12/i2/110.htm
DOI: https://dx.doi.org/10.4252/wjsc.v12.i2.110

INTRODUCTION

Classic approaches to tissue engineering rely on scaffold-based strategies, which have limited ability to recapitulate organogenesis *in vitro*[1,2]. In scaffold-based approaches, limitations are related to the replication of morphological, biomechanical and biochemical signs that occur *in vivo*, mainly because of the prevalence of cell interactions with scaffolds instead of cell-cell and cell-extracellular matrix interactions found in the natural tissues microenvironment[1]. Other disadvantages of scaffold-based approaches are (1) The homogeneous distribution of cells to fill the entire area of the scaffold; (2) The final density of the cells reached in the scaffold area; (3) The diffusion of nutrients; and (4) The cost and time to produce a proper design of the desired scaffold to support the desired regeneration *in vivo*[3-5]. The emerging approach of scaffold-free tissue engineering often relies on the cultivation of cells as spherical clusters known as "spheroids", which mimic the physiological conditions of tissues *in vitro*[6]. During spheroid formation, cells aggregate by cadherins-based interactions in the absence of a fixation medium, in a process known as self-assembly[7]. Spheroids can be used in developmental tissue engineering due to their capacity to form hierarchical tissue structures by recapitulating embryonic processes *in vitro*.

As a result of their three-dimensional (3D) architecture, spheroids have improved cell biological properties such as increased cell viability and proliferative capacity, more stable morphology and polarization, and improved metabolic functions (as compared to 2D cultures)[2]. Consequently, adult stem cell spheroids show distinct properties suitable for regenerative medicine approaches, such as high adhesion capacity and the secretion of a variety of growth factors[8]. Spheroids can be formed from different cell types, including mature cells[9-11]; however, for tissue engineering approaches, spheroids formed of mesenchymal stromal/stem cells (MSCs) are particularly appealing, due to the regenerative and multipotential properties of these adult stem cells[6].

The subcutaneous adipose tissue is an abundant source of MSCs, recently termed adipose derived stem/stromal cells (ASCs)[12]. Various studies have reported that ASCs have osteogenic[13-17] as well as chondrogenic[18-20] potential for use in scaffold-based approaches of tissue engineering. In agreement with these studies, ASCs were

used successfully in pre-clinical and clinical trials for bone and cartilage repair[21-30].

Despite the osteogenic and chondrogenic potential of ASCs, the use of spheroids of ASCs (or other MSCs) in bone tissue engineering is still in its infancy[31]. Saburina *et al*[32] reported that ASC spheroids express osteoblast markers such as osteocalcin and osteopontin, and have angiogenic potential and calcium deposits. In addition, the use of scaffold-free 3D culture, including spheroids, in chondrogenesis studies led to the identification of important molecular markers of cartilage formation[33-35]. Spheroids have the capacity to express crucial extracellular matrix molecules such as collagen type II, tenascin-C, collagen type IX and aggrecan[36], recapitulating cartilage formation. Spheroids also secrete COMP (cartilage oligomeric matrix), a thrombospondin family protein (TSP-5)[37,38] recognized as a biomarker for chondrogenesis[39].

Our research group recently reported the production of a stably engineered cartilage using ASC spheroids under chondrogenic and hypoxic conditions[35]. In addition, we have recently established a hypertrophic engineered cartilage (manuscript submitted) for future use in bone engineering[31]. Although hypertrophic cartilage has been used as a template for osteogenesis *in vivo* based on different strategies[40-42], hypertrophic cartilage made from spheroids has not been tested in this context.

Finally, spheroids have already been used as building blocks for the biofabrication of different tissues (such as nervous and cardiac tissues) and recent data support their potential use in 3D bioprinting approaches[43,44].

USE OF SPHEROIDS FOR CARTILAGE AND BONE ENGINEERING

Cultures of MSCs as 2D monolayers are widely used and suitable for cell expansion. However, 2D cultures have numerous limitations; in particular, these cultures have limited cell differentiation potential[45,46]. *In vivo*, stem cells dwell in specific compartments of tissue microenvironments known as "niches", which regulate cell physiology[47]. In 3D cultures - particularly in scaffold-free strategies such as spheroids (Figure 1) - niche conditions can be recreated[48].

The use of 3D scaffold-free cultures, including spheroids, as an *in vitro* cartilage model has been widely explored in the past few years[49,50], because the hypoxia gradient found inside spheroids mimics the microenvironment of native cartilage, favoring the differentiation of MSCs and ASCs down the chondrogenic pathway[51].

Yoon *et al*[52] showed that ASCs in 3D cultures have improved chondrogenic potential when compared with monolayers. More recently, Occhetta *et al*[53] showed that the downregulation of bone morphogenetic protein (BMP) signaling in bone marrow MSCs guides embryonic progenitors towards articular cartilage formation, and is responsible for stable chondrogenesis, protecting against vessel invasion and, consequently, bone formation. In a co-culture approach, spheroids composed of a mixture of chondrocytes and ASCs had upregulated expression of chondrogenic markers[54]. Importantly, Dikina *et al*[55] successfully used a modular system based on MSC spheroids to engineer cartilaginous scaffold-free tissue for tracheal tissue replacement. MSC differentiation was optimized by delivering TGF-β entrapped in gelatin microspheres, and MSC spheroids were guided to form a cartilaginous tube structure with mechanical properties similar to those of native trachea.

Our research group isolated and characterized human cartilage progenitor cells (CPCs) capable of spontaneous chondrogenesis *in vitro*[56] in the absence of exogenous stimuli of chondrogenic growth factors, when using a 3D scaffold and serum-free culture[57]. Recently, we modified our 3D culture system to a scalable methodology using micro-molded, non-adhesive hydrogel[58]. This methodology prevents cell attachment, and encourages cell-cell interactions, improving chondrogenic differentiation[59]. The micro-molded hydrogel strategy showed promising results not only for chondrogenesis, but also for the formation of spheroids of homogeneous size and shape, and with high cell viability[58].

ASC spheroids made using micro-molded hydrogel are also homogeneous in size, shape and have increased cell viability[35]. Induced ASC spheroids showed a chondrogenic potential similar to that of CPC spheroids, as validated by proteomic analysis of spheroid culture supernatants, known as "secretomes"[35]. When *in vivo*, these spheroids might be able to secrete cartilage specific extracellular molecular proteins and bioactive molecules, in order to promote the formation of cartilage tissue (Figure 2). Interestingly, our secretome data on differentiated ASC spheroids revealed the absence of collagen type X, a classic marker of chondrocyte hypertrophy[60]. Furthermore, comparative secretome analysis revealed that induced ASC spheroids

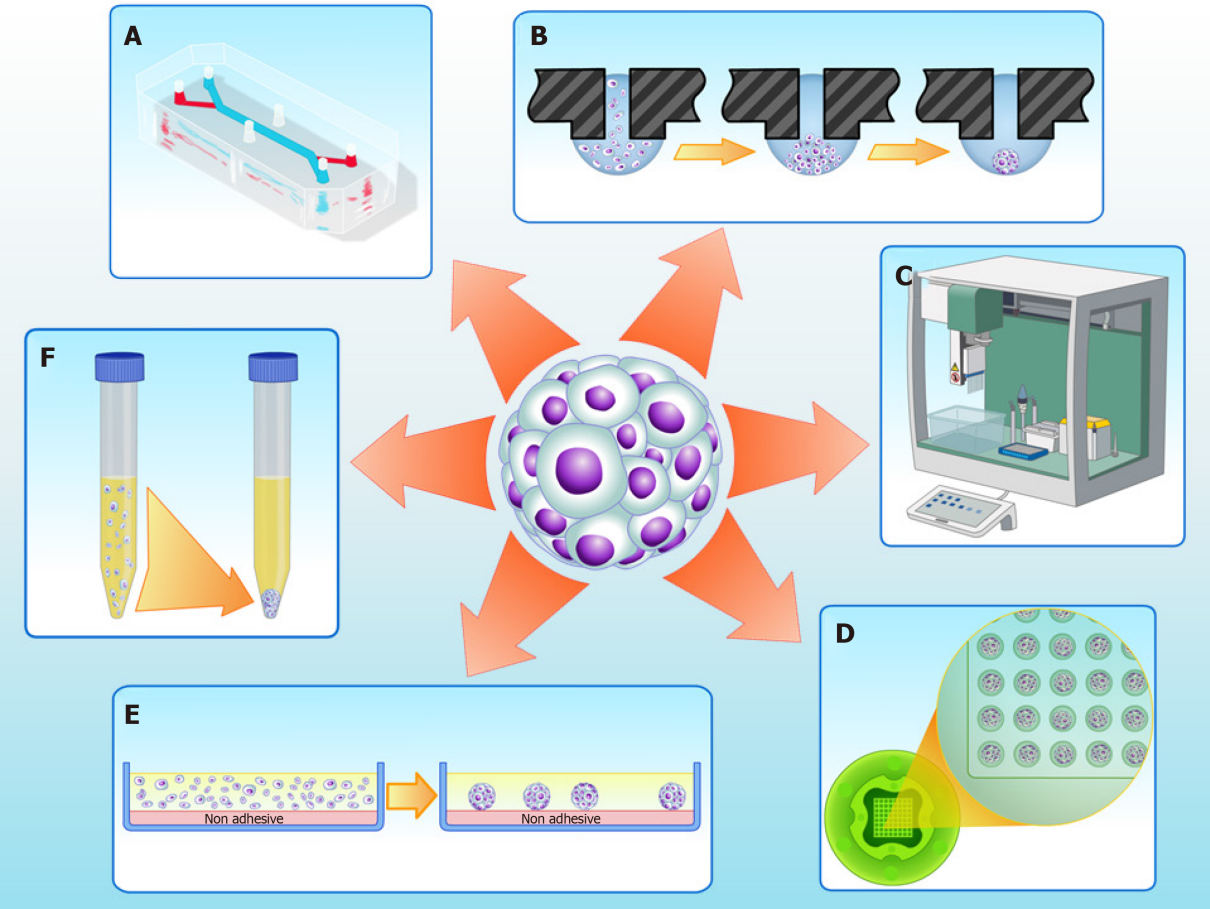

Figure 1 Three-dimensional cell culture techniques to fabricate spheroids *in vitro*. A: Microfluidics; B: Hanging drop; C: Automatic platforms; D: Non-adherent agarose micromolded hydrogel produced from a silicone mold (3D Petri dish®, Microtissues); E: Non adhesive surfaces; F: Pellet culture.

secreted higher levels of the chondrogenesis biomarkers collagen type II and COMP than CPC spheroids. Induced ASC spheroids also had increased secretion of a new biomarker of chondrogenesis - TSP-1[35] - an anti-angiogenic protein recently described as anti-hypertrophic[61].

While several studies have reported successful chondrogenic differentiation using spheroids, only a few studies have reported the use MSC or ASC spheroids in bone engineering[31]. Osteogenic differentiation is commonly reached by the addition of inducers to the culture medium. Hildebrandt *et al*[62] showed that MSC spheroids induced using dexamethasone, ascorbic acid and β-glycerophosphate had a widespread distribution of collagen type I, the main collagen found in bone extracellular matrix. In addition, Shen *et al*[63] reported that ASC spheroids induced into the osteogenic pathway using a cocktail of vitamin D3, ascorbic acid, dexamethasone and β-glycerophosphate developed calcium deposits (stained with Alizarin red); these deposits were associated preferentially with the inner spheroid cells. In agreement with these data, Gurumurthy *et al*[64] observed that growth as spheroids improved the synthesis of calcium deposits by ASCs. In that study, ASC spheroids and monolayers were maintained in medium containing ascorbic acid, dexamethasone, β-glycerophosphate and 10% fetal bovine serum. Recently, Rumiński *et al*[65], compared the osteogenic potential of ASCs by culturing them as monolayer, spheroids or seeded in a scaffold. The results showed that ASCs spheroids presented an up-regulation of osteogenic markers. In addition, after the induction of cells to later osteogenic differentiation events, cells dissociated from spheroids produced mineral and osteocalcin. In this study, ASCs spheroids were kept in a medium containing the inducing factors 10 nmol dexamethasone, 50 μg/mL ascorbic acid 2-phosphate and 3 mmol NaH_2PO_4. During the induction of later differentiation events, the medium was supplemented with 10 nmol 1α,25-dihydroxyvitamin D3.

BMP-7 stimulates bone metabolism, as well as modulating the proliferation and differentiation of MSCs into bone tissue cells[66]. According to our preliminary results, ASC spheroids induced using BMP-7 had calcium deposits, they were negative for typical bone extracellular matrix components, showing a restricted area of positivity for osteocalcin. Nevertheless, even in the absence of BMP-7, ASC spheroids had

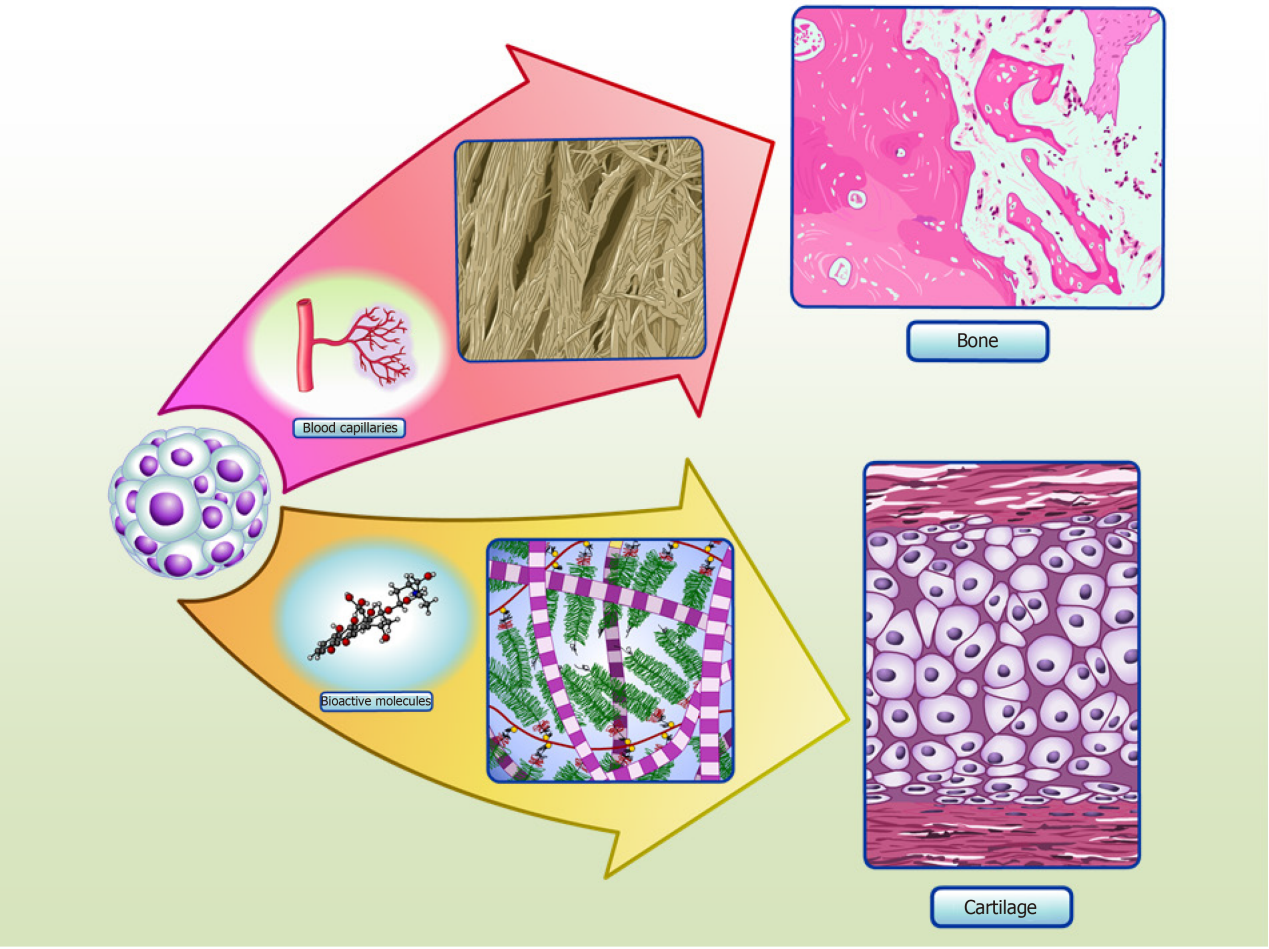

Figure 2 Spheroids in cartilage and bone tissue microenvironments. Adipose stem/stromal cells (ASCs) spheroids delivered to defect area *in vivo* can secrete bioactive molecules and synthetize typical extracellular matrix proteins of cartilage, promoting regeneration. Our group have detected collagen type II and COMP in the secretome of *in vitro* ASCs spheroids, as the production of typical extracellular matrix proteins of cartilage *in situ*[35]. ASCs spheroids delivered to critical-size bone defects can stimulate angiogenesis by secretion of vascular endothelial growth factor (VEGF) and synthesize bone typical extracellular matrix proteins, promoting regeneration. Our group have detected higher levels of VEGF secreted in ASCs spheroids induced to form a hypertrophic cartilage *in vitro*, as the production of typical extracellular matrix proteins of bone *in situ* (manuscript submitted).

strong *in situ* staining for collagen type X, a classic early marker of hypertrophic chondrocytes[60,67], the precursors of endochondral ossification.

In agreement with the intrinsic capacity of ASC/MSC spheroids to form hypertrophic chondrocytes suggested by our preliminary results, Muraglia *et al*[68] reported a transition from chondrogenesis to osteogenesis in human MSC spheroids produced using the pellet technique. Initially, a chondrogenic induction medium was used, composed of human TGF-β1 and dexamethasone. At the end of four weeks, the medium was replaced with osteogenesis inducing factors (β-glycerophosphate and dexamethasone) for an additional three weeks. The authors found crystallization inside the spheroids, together with remodeling from a typical cartilage extracellular matrix to bone. Table 1 summarizes *in vitro* and *in vivo* studies with ASCs spheroids for cartilage and bone engineering.

USE OF SPHEROIDS FOR THE DEVELOPMENTAL ENGINEERING OF CARTILAGE AND BONE

Developmental engineering for bone tissue formation *in vitro* aims to recapitulate the stages of bone development that occur *in vivo*[76,77]. Chondrogenesis is the primordial stage of skeletal development, involving the migration and recruitment of MSCs, the condensation of progenitor cells, and the differentiation and maturation of chondrocytes, which culminate in the formation of cartilage and bone, during endochondral ossification[78,79]. Fell[80] first described one of the early events in chondrogenesis: The aggregation of chondroprogenitor MSCs that leads to pre-

Table 1 *In vitro* and *in vivo* studies with adipose derived stem/stromal cells spheroids for cartilage and bone engineering

Tissue	Spheroid production method	Defect/Animal model	Main outcomes	Ref.
Cartilage	Spontaneous formation in 48-well plate	*In vitro*	Further optimization of chondrogenic induction will be required	[69]
Cartilage	Scaffold	Subchondral bone in Rabbit	The structure and function of regenerated tissue was similar to hyaline cartilage	[70]
Cartilage	Spinner flask	Transplanted subcutaneously in Mice	Spheroid culture is a viable method for chondrogenic differentiation and *in vivo* cartilage formation	[52]
Cartilage	Porous scaffold	Femur trochlea on the femoropatellar groove in Rabbit	Formation of mature cartilage *in vivo*	[71]
Cartilage	Micro-molded non-adhesive hydrogel	*In vitro*	The study confirms that spheroids mimic a stable cartilage tissue	[35]
Bone	Hanging droplet	Muscle pouch in femur in a Rat	Spheroids presented up-regulation of osteogenic markers, extracellular matrix mineralization and, when implanted *in vivo*, greater bone volume	[63]
Bone	Overlay	*In vitro*	Spheroids presented calcium deposits and cells were positive for CD31 (classic endothelial marker)	[72]
Bone	Pellet culture	Osteochondral (femoral trochlear groove) in microminipigs	Spheroids may induce regeneration of cartilage and subchondral bone	[73]
Bone	Agarose chip	Dorsal in Mice	Formation of ectopic bone	[74]
Bone	Elastin-like Polypeptide (ELP) and Polyethyleneimine (PEI) surface	*In vitro*	Spheroids showed superior osteogenic differentiation than monolayer culture. Spheroids produced bone extracellular matrix and presented greater mineralization	[64]
Bone	Centrifugation	*In vitro*	Composite spheroids enhanced expression of osteogenic genes and mineralization after fusion process	[75]
Bone	Non-adhesive surfaces	*In vitro*	Spheroids up-regulated osteogenic markers, showed low mineral production and produced osteocalcin protein	[65]

cartilage condensation. This process depends on cell-cell and cell-matrix interactions, and is associated with intense changes in cytoskeletal architecture[81].

Bone engineering studies rely on mimicking endochondral ossification, the main mechanism of bone regeneration/repair after injury or fractures[82]. Endochondral ossification is tightly coordinated by cellular and molecular mechanisms[77]. MSCs initially condense and differentiate into chondrocytes, forming a hyaline cartilaginous matrix template that is subsequently replaced by vascularized bone tissue[83].

All hypertrophic cartilage-associated molecular events seem to occur in ASC spheroids, suggesting that these cells can be used to faithfully recapitulate endochondral ossification *in vivo*[73]. According to our preliminary results, these main events can also be recapitulated *in vitro* from ASC spheroids induced down the chondrogenic and osteogenic pathways (manuscript submitted). The stage of pre-cartilage condensation is closely linked to an increase in hyaluronidase activity and to the appearance of cell adhesion molecules, mainly cadherins[36,84]. In spheroid formation, N-cadherin expression is directly correlated with successful chondrogenic differentiation, because it mimics the mesenchymal condensation that occurs in embryos[85] by a process of self-assembly[86]. Decorin and extracellular matrix

molecules such as tenascin, TSP-1 and COMP then interact with cell adhesion molecules to activate intracellular signaling pathways and trigger the maturation of chondroprogenitor cells into chondrocytes[84]. Furthermore, induced ASC differentiation upregulates a trio of SOX genes (*SOX9*, *SOX5*, *SOX6*), and this is followed by the downregulation of RUNX2, the master inducer of osteogenesis[87], and ALP, a gene involved in mineralization[88,89]. Although spheroids are capable of recapitulating chondrogenesis steps, in our model spheroid-based chondrogenesis does not progress to bone differentiation as seen in endochondral ossification *in vivo*[35].

During endochondral ossification, mature hypertrophic chondrocytes express classic osteogenic markers, such as RUNX-2, osterix, collagen type I, osteocalcin and osteopontin[82,83,90]. Calcification starts in the cartilage template, when hypertrophic chondrocytes secrete vascular endothelial growth factor, leading to cartilage vascularization and enabling osteoblasts to replace the calcified cartilage by mineralized mature bone[91]. Various studies have attempted to harvest the high angiogenic potential of hypertrophic chondrocytes to improve bone repair, by mimicking the events of hypertrophy *in vitro* to engineer optimized bone-like tissue or to improve angiogenesis and bone repair *in vivo*[31]. Most studies were performed with cells surrounded by biomaterials, and obtained positive results[92-95]. Studies using spheroids as a template for ossification showed that spheroids present an elevated capacity to differentiate into bone *in vitro*[68], and to regenerate this tissue *in vivo*[73,96], which may be linked to their ability to form hypertrophic chondrocytes (Figure 2).

In conclusion, ASC spheroids can be used as a model to mimic the differentiation events of stable or hypertrophic cartilage, depending on inducers and oxygen conditions. Spheroid cells differentiate into chondrocytes mainly due to hypoxia, and are capable of maintaining a stable chondrocyte phenotype. Subsequent differentiation into bone tissue appears to rely on an intermediate state of chondrocyte hypertrophy, which recapitulates endochondral ossification.

SPHEROIDS AS BUILDING-BLOCKS

In the last decade, the major challenge in the field of tissue engineering has been the *in vitro* manufacture of tissues compatible in size to injury sites and with a high density of cells, similar to that observed in native tissues and organs[97]. These requirements were the driving force for the development of "bottom-up" tissue engineering[98], where tissues are created by assembling "building blocks" into higher ordered 3D structures. The building blocks are represented by engineered, scaffold-free, 3D constructs such as spheroids, which are assembled into higher order structures using different technologies, of which the most common is 3D bioprinting[98-100].

The success of "bottom-up" tissue engineering relies on the inherent capacity of building blocks to fuse to each other, resulting in larger tissue constructs[5]. Given the ability of spheroids to recapitulate the main morphogenetic events in tissue formation, including fusion, they represent an ideal choice for building blocks in bottom-up tissue engineering[2]. Improving our understanding of the cellular and molecular mechanisms that underlie spheroid fusion is essential for the biofabrication of complex tissues using spheroids[101].

SPHEROID FUSION

Tissue fusion is a spontaneous process in embryonic development and occurs by cell-to-cell and cell-to-extracellular matrix interactions, involving complex molecular and biophysical processes[102]. When spheroids are used to mimic tissue fusion, the process is controlled by surface tension forces culminating into a single cohesive structure[102,103]. One advantage of spheroid fusion is that the kinetics and morphological changes can be easily quantified using high-throughput technology, mainly by time-lapse brightfield images and fluorescence microscopy[104]. Then, the images obtained can be analyzed with a customized image analysis script[104] running on the free NIH image analysis software ImageJ.

Different studies have investigated the fusion process of spheroids *in vitro*. Fleming *et al*[105] fused uniluminal vascular spheroids *in vitro*, in a process that closely resembles the formation of the descending aorta during embryonic development, *in vivo*. Lehmann *et al*[106] produced 3D cartilage-like single spheroids using dedifferentiated chondrocytes, and generated larger microtissues consisting of several spheroids fused together, as a scaffold-free strategy for reliable treatment of osteoarthritis and cartilage defects due to trauma. These authors observed that fused

spheroids showed increased production of extracellular matrix and higher levels of collagen II compared with single spheroids. Susienka *et al*[104] designed a high-throughput platform to quantify spheroid fusogenicity using two different assays: Initially, a "tack" assay is used to measure the minimum time taken by two spheroids to form a stable microtissue "doublet", while a fusion assay tracks the morphological parameters of fusion. This method is useful to explore the mechanisms involved in spheroid fusion and can be applied to different cell types, to identify differences in fusion processes.

Our preliminary results using the fusogenicity assay described above showed that ASC spheroids, when placed in pairs, start fusing at 24 h, while the whole fusion process is finished by day 7. The cellular and molecular mechanisms that control spheroid fusion remain poorly described. According to our preliminary results, at day 4 of culture, a population of spheroid cells migrates from the spheroid periphery to the region of fusion, at the center of the spheroid. In agreement with these data, Fleming *et al*[105] showed that the fusion of uniluminal vascular spheroids is mediated by the ability of spheroid cells to reposition themselves, maximizing their inter-adhesive interactions and minimizing the free energy of the system as a whole.

In ASC spheroids, we also observed a resistance to fusion directly related to osteogenic differentiation (manuscript in preparation). Similarly, Ahmad *et al*[75] showed that, when subjected to a protocol for mineralization *in vitro*, ASCs spheroids only fused after seven days in culture; in this period, the cells remained viable and stained for Alizarin red O, indicating the presence of calcium deposits.

With regard to cartilage engineering, a study by Lehmann *et al*[106] showed that chondrogenesis increases when spheroids undergo fusion. Fused spheroids presented some similarities to native hyaline cartilage and were highly positive for collagen type II and proteoglycans, which are typical of cartilage extracellular matrix. Our group has shown that fusion is not impaired in ASC spheroids induced to undergo chondrogenesis[35]. Furthermore, in a different spheroid model, using CPCs, we observed that spheroids undergo fusion at day 7[58]; however, the contact area in fused CPC spheroids is reduced compared with that observed in ASC spheroids induced to undergo chondrogenesis.

In conclusion, spheroid fusion is the event that allows bottom-up tissue engineering to form larger tissue constructs. Ours and other research groups have shown that spheroid fusion is a fast, efficient and scalable process. However, further molecular and cellular studies are necessary to understand the mechanisms involved in fusion, in order to produce stable tissue constructs that recapitulate tissue morphogenesis and exhibit the desired functionality.

SPHEROID BIOPRINTING

The 3D bioprinting of tissue constructs is considered one of the latest technologies in tissue engineering and regenerative medicine, promising to facilitate the development of complex tissues and organ constructs[107]. Bioprinting evolved from 3D scaffold printing, a technique developed by Hull[108] in the 80s, and initially applied to improve scaffold properties[109,110].

Currently, 3D bioprinting techniques are an attractive strategy for bottom-up tissue engineering due to the possibility of engineering with precision larger and complex tissue constructs with suitable mechanical properties and desirable biological functions. In 3D bioprinting, biomaterials containing bioactive molecules and encapsulated cells, referred to as the "bioink," are added layer-by-layer to form previously designed patterns[109]. The state-of-the-art is to distribute cells or spheroids and bioactive agents with precision to form a 3D structure, *via* the controlled extrusion activity of a bioprinter[111].

Visconti *et al*[103] discussed the importance of spheroid fusion to form an intra-organ vascular tree by 3D bioprinting. Vascular spheroid fusion resulted in a functional and physiologically relevant 3D structure similar to a blood vessel, showing both vasodilatory and contractile responses[112]. Importantly, the fabrication of a vascular structure is an essential initial step to successfully engineer large tissue constructs due to the need for vascularization in native organs. The biofabrication of larger constructs requires spheroids to be homogeneous in the desired size and shape[113], and our research group has shown that this homogeneity can be obtained by the use of molded non-adherent hydrogel[35].

One interesting strategy, developed by Yu *et al*[114] used a scalable bioink referred to as "tissue strands" in scaffold-free bioprinting, to facilitate the accurate biofabrication of biomimetically developed tissues. The model was based on chondrocyte spheroid fusion to produce the tissue strands, which were then bioprinted into a more complex

cartilage construct without the use of hydrogels. The authors successfully produced bovine articular cartilage tissues with morphological, biochemical and mechanical properties close to those of native cartilage.

In a recent outstanding study, Daly *et al*[115] used inkjet bioprinting to deposit a cell suspension of MSCs and chondrocytes into 3D printed microchambers, to form highly organized arrays of spheroids. The morphological composition and the biomechanical properties of the bioprinted cartilage-like tissue construct were similar to those of native cartilage found *in vivo*.

Despite different efforts and advances in spheroid 3D bioprinting, many challenges must still be overcome to allow this technique to reach its full potential. These challenges include the incorporation of blood vessels and nerve fibers in tissue constructs[116], and the production of large and uniform constructs suitable for future clinical applications[117].

CONCLUSION AND PERSPECTIVES

Recent advances in the developmental engineering area, which aims to recapitulate the cell and molecular stages of embryonic development to form a desired tissue[76,77], have allowed the establishment of spheroid-based *in vitro* models that mimic more closely embryonic processes, including endochondral ossification and mesenchymal condensation, which represent stages of bone and cartilage formation, respectively. Spheroids are ideal building blocks for bottom-up tissue engineering mainly due to their high fusion capacity. Further studies on the spheroid fusion process and the refinement of *in vitro* tissue biofabrication technologies such as 3D bioprinting are now essential for the production of higher order tissues *in vitro*. In conclusion, 3D bioprinting using ASC spheroids as cartilage and bone building blocks is a promising technology for future development of tissue constructs for clinical use, by bottom-up tissue engineering.

ACKNOWLEDGEMENTS

We would like to thank Ana Claudia O Carreira, PhD and Professor Mari Cleide Sogayar, PhD for human recombinant BMP-7 production.

REFERENCES

1 **Achilli TM**, Meyer J, Morgan JR. Advances in the formation, use and understanding of multi-cellular spheroids. *Expert Opin Biol Ther* 2012; **12**: 1347-1360 [PMID: 22784238 DOI: 10.1517/14712598.2012.707181]
2 **Laschke MW**, Menger MD. Life is 3D: Boosting Spheroid Function for Tissue Engineering. *Trends Biotechnol* 2017; **35**: 133-144 [PMID: 27634310 DOI: 10.1016/j.tibtech.2016.08.004]
3 **Forrestal DP**, Klein TJ, Woodruff MA. Challenges in engineering large customized bone constructs. *Biotechnol Bioeng* 2017; **114**: 1129-1139 [PMID: 27858993 DOI: 10.1002/bit.26222]
4 **Guduric V**, Metz C, Siadous R, Bareille R, Levato R, Engel E, Fricain JC, Devillard R, Luzanin O, Catros S. Layer-by-layer bioassembly of cellularized polylactic acid porous membranes for bone tissue engineering. *J Mater Sci Mater Med* 2017; **28**: 78 [PMID: 28386854 DOI: 10.1007/s10856-017-5887-6]
5 **Ovsianikov A**, Khademhosseini A, Mironov V. The Synergy of Scaffold-Based and Scaffold-Free Tissue Engineering Strategies. *Trends Biotechnol* 2018; **36**: 348-357 [PMID: 29475621 DOI: 10.1016/j.tibtech.2018.01.005]
6 **Egger D**, Tripisciano C, Weber V, Dominici M, Kasper C. Dynamic Cultivation of Mesenchymal Stem Cell Aggregates. *Bioengineering (Basel)* 2018; 5 [PMID: 29921755 DOI: 10.3390/bioengineering5020048]
7 **Duguay D**, Foty RA, Steinberg MS. Cadherin-mediated cell adhesion and tissue segregation: qualitative and quantitative determinants. *Dev Biol* 2003; **253**: 309-323 [PMID: 12645933 DOI: 10.1016/S0012-1606(02)00016-7]
8 **Kelm JM**, Fussenegger M. Scaffold-free cell delivery for use in regenerative medicine. *Adv Drug Deliv Rev* 2010; **62**: 753-764 [PMID: 20153387 DOI: 10.1016/j.addr.2010.02.003]
9 **Figtree GA**, Bubb KJ, Tang O, Kizana E, Gentile C. Vascularized cardiac spheroids as novel 3D in vitro models to study cardiac fibrosis. *Cells Tissues Organs* 2017; **204**: 191-198 [DOI: 10.1159/000477436]
10 **Ramanujan VK**. Quantitative imaging of morphometric and metabolic signatures reveals heterogeneity in drug response of three-dimensional mammary tumor spheroids. *Mol Imaging Biol* 2019 [DOI: 10.1007/s11307-019-01324-7]
11 **Sato T**, Anada T, Hamai R, Shiwaku Y, Tsuchiya K, Sakai S, Baba K, Sasaki K, Suzuki O. Culture of hybrid spheroids composed of calcium phosphate materials and mesenchymal stem cells on an oxygen-permeable culture device to predict in vivo bone forming capability. *Acta Biomat* 2019; **19**: 30167-30169 [DOI: 10.1016/j.actbio.2019.03.001]
12 **Bourin P**, Bunnell BA, Casteilla L, Dominici M, Katz AJ, March KL, Redl H, Rubin JP, Yoshimura K, Gimble JM. Stromal cells from the adipose tissue-derived stromal vascular fraction and culture expanded adipose tissue-derived stromal/stem cells: a joint statement of the International Federation for Adipose

Therapeutics and Science (IFATS) and the International Society for Cellular Therapy (ISCT). *Cytotherapy* 2013; **15**: 641-648 [PMID: 23570660 DOI: 10.1016/j.jcyt.2013.02.006]
13 **Halvorsen YC**, Wilkison WO, Gimble JM. Adipose-derived stromal cells--their utility and potential in bone formation. *Int J Obes Relat Metab Disord* 2000; **24** Suppl 4: S41-S44 [PMID: 11126240 DOI: 10.1038/sj.ijo.0801503]
14 **Halvorsen YD**, Franklin D, Bond AL, Hitt DC, Auchter C, Boskey AL, Paschalis EP, Wilkison WO, Gimble JM. Extracellular matrix mineralization and osteoblast gene expression by human adipose tissue-derived stromal cells. *Tissue Eng* 2001; **7**: 729-741 [PMID: 11749730 DOI: 10.1089/107632701753337681]
15 **Dragoo JL**, Choi JY, Lieberman JR, Huang J, Zuk PA, Zhang J, Hedrick MH, Benhaim P. Bone induction by BMP-2 transduced stem cells derived from human fat. *J Orthop Res* 2003; **21**: 622-629 [PMID: 12798061 DOI: 10.1016/S0736-0266(02)00238-3]
16 **Lee SJ**, Kang SW, Do HJ, Han I, Shin DA, Kim JH, Lee SH. Enhancement of bone regeneration by gene delivery of BMP2/Runx2 bicistronic vector into adipose-derived stromal cells. *Biomaterials* 2010; **31**: 5652-5659 [PMID: 20413153 DOI: 10.1016/j.biomaterials.2010.03.019]
17 **Tajima S**, Tobita M, Mizuno H. Current status of bone regeneration using adipose-derived stem cells. *Histol Histopathol* 2018; **33**: 619-627 [PMID: 29094748 DOI: 10.14670/HH-11-942]
18 **Cheng NC**, Estes BT, Young TH, Guilak F. Genipin-crosslinked cartilage-derived matrix as a scaffold for human adipose-derived stem cell chondrogenesis. *Tissue Eng Part A* 2013; **19**: 484-496 [PMID: 23088537 DOI: 10.1089/ten.TEA.2012.0384]
19 **Cheung HK**, Han TT, Marecak DM, Watkins JF, Amsden BG, Flynn LE. Composite hydrogel scaffolds incorporating decellularized adipose tissue for soft tissue engineering with adipose-derived stem cells. *Biomaterials* 2014; **35**: 1914-1923 [PMID: 24331712 DOI: 10.1016/j.biomaterials.2013.11.067]
20 **Calabrese G**, Forte S, Gulino R, Cefalì F, Figallo E, Salvatorelli L, Maniscalchi ET, Angelico G, Parenti R, Gulisano M, Memeo L, Giuffrida R. Combination of Collagen-Based Scaffold and Bioactive Factors Induces Adipose-Derived Mesenchymal Stem Cells Chondrogenic Differentiation *In vitro*. *Front Physiol* 2017; **8**: 50 [PMID: 28210226 DOI: 10.3389/fphys.2017.00050]
21 **Cowan CM**, Shi YY, Aalami OO, Chou YF, Mari C, Thomas R, Quarto N, Contag CH, Wu B, Longaker MT. Adipose-derived adult stromal cells heal critical-size mouse calvarial defects. *Nat Biotechnol* 2004; **22**: 560-567 [PMID: 15077117 DOI: 10.1038/nbt958]
22 **Masuoka K**, Asazuma T, Hattori H, Yoshihara Y, Sato M, Matsumura K, Matsui T, Takase B, Nemoto K, Ishihara M. Tissue engineering of articular cartilage with autologous cultured adipose tissue-derived stromal cells using atelocollagen honeycomb-shaped scaffold with a membrane sealing in rabbits. *J Biomed Mater Res B Appl Biomater* 2006; **79**: 25-34 [PMID: 16506181 DOI: 10.1002/jbm.b.30507]
23 **Dragoo JL**, Carlson G, McCormick F, Khan-Farooqi H, Zhu M, Zuk PA, Benhaim P. Healing full-thickness cartilage defects using adipose-derived stem cells. *Tissue Eng* 2007; **13**: 1615-1621 [PMID: 17518742 DOI: 10.1089/ten.2006.0249]
24 **Mesimäki K**, Lindroos B, Törnwall J, Mauno J, Lindqvist C, Kontio R, Miettinen S, Suuronen R. Novel maxillary reconstruction with ectopic bone formation by GMP adipose stem cells. *Int J Oral Maxillofac Surg* 2009; **38**: 201-209 [PMID: 19168327 DOI: 10.1016/j.ijom.2009.01.001]
25 **Levi B**, James AW, Nelson ER, Vistnes D, Wu B, Lee M, Gupta A, Longaker MT. Human adipose derived stromal cells heal critical size mouse calvarial defects. *PLoS One* 2010; **5**: e11177 [PMID: 20567510 DOI: 10.1371/journal.pone.0011177]
26 **Pak J**, Lee JH, Lee SH. Regenerative repair of damaged meniscus with autologous adipose tissue-derived stem cells. *Biomed Res Int* 2014; **2014**: 436029 [PMID: 24592390 DOI: 10.1155/2014/436029]
27 **Koh YG**, Choi YJ, Kwon SK, Kim YS, Yeo JE. Clinical results and second-look arthroscopic findings after treatment with adipose-derived stem cells for knee osteoarthritis. *Knee Surg Sports Traumatol Arthrosc* 2015; **23**: 1308-1316 [PMID: 24326779 DOI: 10.1007/s00167-013-2807-2]
28 **Paduano F**, Marrelli M, Amantea M, Rengo C, Rengo S, Goldberg M, Spagnuolo G, Tatullo M. Adipose Tissue as a Strategic Source of Mesenchymal Stem Cells in Bone Regeneration: A Topical Review on the Most Promising Craniomaxillofacial Applications. *Int J Mol Sci* 2017; 18 [PMID: 29027958 DOI: 10.3390/ijms18102140]
29 **Khojasteh A**, Kheiri L, Behnia H, Tehranchi A, Nazeman P, Nadjmi N, Soleimani M. Lateral Ramus Cortical Bone Plate in Alveolar Cleft Osteoplasty with Concomitant Use of Buccal Fat Pad Derived Cells and Autogenous Bone: Phase I Clinical Trial. *Biomed Res Int* 2017; **2017**: 6560234 [PMID: 29379800 DOI: 10.1155/2017/6560234]
30 **Spasovski D**, Spasovski V, Baščarević Z, Stojiljković M, Vreća M, Anđelković M, Pavlović S. Intra-articular injection of autologous adipose-derived mesenchymal stem cells in the treatment of knee osteoarthritis. *J Gene Med* 2018; 20 [PMID: 29243283 DOI: 10.1002/jgm.3002]
31 **Baptista LS**, Kronemberger GS, Silva KR, Granjeiro JM. Spheroids of stem cells as endochondral templates for improved bone engineering. *Front Biosci (Landmark Ed)* 2018; **23**: 1969-1986 [PMID: 29772539 DOI: 10.2741/4683]
32 **Saburina IN**, Gorkun AA, Fidarov AF, Kolokol'tsova TD, Zurina IM, Kosheleva NV, Ustinova EE, Repin VS. Induction of Vasculo- and Osteogenesis in Spheroids Formed by Adipose-Derived Stromal Cells. *Bull Exp Biol Med* 2018; **166**: 163-169 [PMID: 30417289 DOI: 10.1007/s10517-018-4306-4]
33 **Ando W**, Tateishi K, Katakai D, Hart DA, Higuchi C, Nakata K, Hashimoto J, Fujie H, Shino K, Yoshikawa H, Nakamura N. In vitro generation of a scaffold-free tissue-engineered construct (TEC) derived from human synovial mesenchymal stem cells: biological and mechanical properties and further chondrogenic potential. *Tissue Eng Part A* 2008; **14**: 2041-2049 [PMID: 18636944 DOI: 10.1089/ten.tea.2008.0015]
34 **Takada E**, Mizuno S. Reproduction of Characteristics of Extracellular Matrices in Specific Longitudinal Depth Zone Cartilage within Spherical Organoids in Response to Changes in Osmotic Pressure. *Int J Mol Sci* 2018; 19 [PMID: 29783650 DOI: 10.3390/ijms19051507]
35 **Côrtes I**, Matsui RAM, Azevedo MS, Beatrici A, Souza KLA, Launay G, Delolme F, Granjeiro JM, Moali C, Baptista LS. A Scaffold- and Serum-Free Method to Mimic Human Stable Cartilage Validated by Secretome. *Tissue Eng Part A* 2019 [PMID: 30734654 DOI: 10.1089/ten.TEA.2018.0311]
36 **Bobick BE**, Chen FH, Le AM, Tuan RS. Regulation of the chondrogenic phenotype in culture. *Birth Defects Res C Embryo Today* 2009; **87**: 351-371 [PMID: 19960542 DOI: 10.1002/bdrc.20167]
37 **Oldberg A**, Antonsson P, Lindblom K, Heinegård D. COMP (cartilage oligomeric matrix protein) is structurally related to the thrombospondins. *J Biol Chem* 1992; **267**: 22346-22350 [PMID: 1429587]
38 **Newton G**, Weremowicz S, Morton CC, Copeland NG, Gilbert DJ, Jenkins NA, Lawler J.

Characterization of human and mouse cartilage oligomeric matrix protein. *Genomics* 1994; **24**: 435-439 [PMID: 7713493 DOI: 10.1006/geno.1994.1649]
39 **Fife RS**, Brandt KD. Identification of a high-molecular-weight (greater than 400 000) protein in hyaline cartilage. *Biochim Biophys Acta* 1984; **802**: 506-514 [PMID: 6095921]
40 **Sheehy EJ**, Vinardell T, Buckley CT, Kelly DJ. Engineering osteochondral constructs through spatial regulation of endochondral ossification. *Acta Biomater* 2013; **9**: 5484-5492 [PMID: 23159563 DOI: 10.1016/j.actbio.2012.11.008]
41 **Sheehy EJ**, Mesallati T, Vinardell T, Kelly DJ. Engineering cartilage or endochondral bone: a comparison of different naturally derived hydrogels. *Acta Biomater* 2015; **13**: 245-253 [PMID: 25463500 DOI: 10.1016/j.actbio.2014.11.031]
42 **Thompson EM**, Matsiko A, Kelly DJ, Gleeson JP, O'Brien FJ. An Endochondral Ossification-Based Approach to Bone Repair: Chondrogenically Primed Mesenchymal Stem Cell-Laden Scaffolds Support Greater Repair of Critical-Sized Cranial Defects Than Osteogenically Stimulated Constructs In Vivo. *Tissue Eng Part A* 2016; **22**: 556-567 [PMID: 26896424 DOI: 10.1089/ten.TEA.2015.0457]
43 **Elbert DL**. Bottom-up tissue engineering. *Curr Opin Biotechnol* 2011; **22**: 674-680 [PMID: 21524904 DOI: 10.1016/j.copbio.2011.04.001]
44 **Beachley V**, Kasyanov V, Nagy-Mehesz A, Norris R, Ozolanta I, Kalejs M, Stradins P, Baptista L, da Silva K, Grainjero J, Wen X, Mironov V. The fusion of tissue spheroids attached to pre-stretched electrospun polyurethane scaffolds. *J Tissue Eng* 2014; **5**: 2041731414556561 [PMID: 25396042 DOI: 10.1177/2041731414556561]
45 **Baer PC**, Griesche N, Luttmann W, Schubert R, Luttmann A, Geiger H. Human adipose-derived mesenchymal stem cells in vitro: evaluation of an optimal expansion medium preserving stemness. *Cytotherapy* 2010; **12**: 96-106 [PMID: 19929458 DOI: 10.3109/14653240903377045]
46 **Park E**, Patel AN. Changes in the expression pattern of mesenchymal and pluripotent markers in human adipose-derived stem cells. *Cell Biol Int* 2010; **34**: 979-984 [PMID: 20446919 DOI: 10.1042/CBI20100124]
47 **Watt FM**, Hogan BL. Out of Eden: stem cells and their niches. *Science* 2000; **287**: 1427-1430 [PMID: 10688781 DOI: 10.1126/science.287.5457.1427]
48 **Chimenti I**, Pagano F, Angelini F, Siciliano C, Mangino G, Picchio V, De Falco E, Peruzzi M, Carnevale R, Ibrahim M, Biondi-Zoccai G, Messina E, Frati G. Human Lung Spheroids as In Vitro Niches of Lung Progenitor Cells with Distinctive Paracrine and Plasticity Properties. *Stem Cells Transl Med* 2017; **6**: 767-777 [PMID: 28297570 DOI: 10.5966/sctm.2015-0374]
49 **Anderer U**, Libera J. In vitro engineering of human autogenous cartilage. *J Bone Miner Res* 2002; **17**: 1420-1429 [PMID: 12162496 DOI: 10.1359/jbmr.2002.17.8.1420]
50 **Markway BD**, Tan GK, Brooke G, Hudson JE, Cooper-White JJ, Doran MR. Enhanced chondrogenic differentiation of human bone marrow-derived mesenchymal stem cells in low oxygen environment micropellet cultures. *Cell Transplant* 2010; **19**: 29-42 [PMID: 19878627 DOI: 10.3727/096368909X478560]
51 **Lennon DP**, Edmison JM, Caplan AI. Cultivation of rat marrow-derived mesenchymal stem cells in reduced oxygen tension: effects on in vitro and in vivo osteochondrogenesis. *J Cell Physiol* 2001; **187**: 345-355 [PMID: 11319758 DOI: 10.1002/jcp.1081]
52 **Yoon HH**, Bhang SH, Shin JY, Shin J, Kim BS. Enhanced cartilage formation via three-dimensional cell engineering of human adipose-derived stem cells. *Tissue Eng Part A* 2012; **18**: 1949-1956 [PMID: 22881427 DOI: 10.1089/ten.TEA.2011.0647]
53 **Occhetta P**, Pigeot S, Rasponi M, Dasen B, Mehrkens A, Ullrich T, Kramer I, Guth-Gundel S, Barbero A, Martin I. Developmentally inspired programming of adult human mesenchymal stromal cells toward stable chondrogenesis. *Proc Natl Acad Sci USA* 2018; **115**: 4625-4630 [PMID: 29666250 DOI: 10.1073/pnas.1720658115]
54 **Yeh HY**, Hsieh FY, Hsu SH. Self-patterning of adipose-derived mesenchymal stem cells and chondrocytes cocultured on hyaluronan-grafted chitosan surface. *Biointerphases* 2016; **11**: 011011 [PMID: 26916660 DOI: 10.1116/1.4942754]
55 **Dikina AD**, Strobel HA, Lai BP, Rolle MW, Alsberg E. Engineered cartilaginous tubes for tracheal tissue replacement via self-assembly and fusion of human mesenchymal stem cell constructs. *Biomaterials* 2015; **52**: 452-462 [PMID: 25818451 DOI: 10.1016/j.biomaterials.2015.01.073]
56 **do Amaral RJ**, Pedrosa Cda S, Kochem MC, Silva KR, Aniceto M, Claudio-da-Silva C, Borojevic R, Baptista LS. Isolation of human nasoseptal chondrogenic cells: a promise for cartilage engineering. *Stem Cell Res* 2012; **8**: 292-299 [PMID: 22099383 DOI: 10.1016/j.scr.2011.09.006]
57 **Baptista LS**, Silva KR, Pedrosa CS, Amaral RJ, Belizário JV, Borojevic R, Granjeiro JM. Bioengineered cartilage in a scaffold-free method by human cartilage-derived progenitor cells: a comparison with human adipose-derived mesenchymal stromal cells. *Artif Organs* 2013; **37**: 1068-1075 [PMID: 23865470 DOI: 10.1111/aor.12121]
58 **Stuart MP**, Matsui RAM, Santos MFS, Côrtes I, Azevedo MS, Silva KR, Beatrici A, Leite PEC, Falagan-Lotsch P, Granjeiro JM, Mironov V, Baptista LS. Successful Low-Cost Scaffold-Free Cartilage Tissue Engineering Using Human Cartilage Progenitor Cell Spheroids Formed by Micromolded Nonadhesive Hydrogel. *Stem Cells Int* 2017; **2017**: 7053465 [PMID: 29527227 DOI: 10.1155/2017/7053465]
59 **Lee JK**, Link JM, Hu JCY, Athanasiou KA. The Self-Assembling Process and Applications in Tissue Engineering. *Cold Spring Harb Perspect Med* 2017; 7 [PMID: 28348174 DOI: 10.1101/cshperspect.a025668]
60 **von der Mark K**, Kirsch T, Nerlich A, Kuss A, Weseloh G, Glückert K, Stöss H. Type X collagen synthesis in human osteoarthritic cartilage. Indication of chondrocyte hypertrophy. *Arthritis Rheum* 1992; **35**: 806-811 [PMID: 1622419 DOI: 10.1002/art.1780350715]
61 **Gelse K**, Klinger P, Koch M, Surmann-Schmitt C, von der Mark K, Swoboda B, Hennig FF, Gusinde J. Thrombospondin-1 prevents excessive ossification in cartilage repair tissue induced by osteogenic protein-1. *Tissue Eng Part A* 2011; **17**: 2101-2112 [PMID: 21513464 DOI: 10.1089/ten.TEA.2010.0691]
62 **Hildebrandt C**, Büth H, Thielecke H. A scaffold-free in vitro model for osteogenesis of human mesenchymal stem cells. *Tissue Cell* 2011; **43**: 91-100 [PMID: 21329953 DOI: 10.1016/j.tice.2010.12.004]
63 **Shen FH**, Werner BC, Liang H, Shang H, Yang N, Li X, Shimer AL, Balian G, Katz AJ. Implications of adipose-derived stromal cells in a 3D culture system for osteogenic differentiation: an in vitro and in vivo investigation. *Spine J* 2013; **13**: 32-43 [PMID: 23384881 DOI: 10.1016/j.spinee.2013.01.002]
64 **Gurumurthy B**, Bierdeman PC, Janorkar AV. Spheroid model for functional osteogenic evaluation of

human adipose derived stem cells. *J Biomed Mater Res A* 2017; **105**: 1230-1236 [PMID: 27943608 DOI: 10.1002/jbm.a.35974]
65 **Rumiński S**, Kalaszczyńska I, Długosz A, Lewandowska-Szumieł M. Osteogenic differentiation of human adipose-derived stem cells in 3D conditions - comparison of spheroids and polystyrene scaffolds. *Eur Cell Mater* 2019; **37**: 382-401 [PMID: 31099888 DOI: 10.22203/eCM.v037a23]
66 **Açil Y**, Springer IN, Broek V, Terheyden H, Jepsen S. Effects of bone morphogenetic protein-7 stimulation on osteoblasts cultured on different biomaterials. *J Cell Biochem* 2002; **86**: 90-98 [PMID: 12112019 DOI: 10.1002/jcb.10197]
67 **Shen G**. The role of type X collagen in facilitating and regulating endochondral ossification of articular cartilage. *Orthod Craniofac Res* 2005; **8**: 11-17 [PMID: 15667640 DOI: 10.1111/j.1601-6343.2004.00308.x]
68 **Muraglia A**, Corsi A, Riminucci M, Mastrogiacomo M, Cancedda R, Bianco P, Quarto R. Formation of a chondro-osseous rudiment in micromass cultures of human bone-marrow stromal cells. *J Cell Sci* 2003; **116**: 2949-2955 [PMID: 12783985 DOI: 10.1242/jcs.00527]
69 **Winter A**, Breit S, Parsch D, Benz K, Steck E, Hauner H, Weber RM, Ewerbeck V, Richter W. Cartilage-like gene expression in differentiated human stem cell spheroids: a comparison of bone marrow-derived and adipose tissue-derived stromal cells. *Arthritis Rheum* 2003; **48**: 418-429 [PMID: 12571852 DOI: 10.1002/art.10767]
70 **Zhang K**, Yan S, Li G, Cui L, Yin J. In-situ birth of MSCs multicellular spheroids in poly(L-glutamic acid)/chitosan scaffold for hyaline-like cartilage regeneration. *Biomaterials* 2015; **71**: 24-34 [PMID: 26318814 DOI: 10.1016/j.biomaterials.2015.08.037]
71 **Zhang K**, Fang H, Qin Y, Zhang L, Yin J. Functionalized Scaffold for in Situ Efficient Gene Transfection of Mesenchymal Stem Cells Spheroids toward Chondrogenesis. *ACS Appl Mater Interfaces* 2018; **10**: 33993-34004 [PMID: 30207161 DOI: 10.1021/acsami.8b12268]
72 **Laschke MW**, Schank TE, Scheuer C, Kleer S, Shadmanov T, Eglin D, Alini M, Menger MD. In vitro osteogenic differentiation of adipose-derived mesenchymal stem cell spheroids impairs their in vivo vascularization capacity inside implanted porous polyurethane scaffolds. *Acta Biomater* 2014; **10**: 4226-4235 [PMID: 24998773 DOI: 10.1016/j.actbio.2014.06.035]
73 **Murata D**, Tokunaga S, Tamura T, Kawaguchi H, Miyoshi N, Fujiki M, Nakayama K, Misumi K. A preliminary study of osteochondral regeneration using a scaffold-free three-dimensional construct of porcine adipose tissue-derived mesenchymal stem cells. *J Orthop Surg Res* 2015; **10**: 35 [PMID: 25890366 DOI: 10.1186/s13018-015-0173-0]
74 **Fennema EM**, Tchang LAH, Yuan H, van Blitterswijk CA, Martin I, Scherberich A, de Boer J. Ectopic bone formation by aggregated mesenchymal stem cells from bone marrow and adipose tissue: A comparative study. *J Tissue Eng Regen Med* 2018; **12**: e150-e158 [PMID: 28485099 DOI: 10.1002/term.2453]
75 **Ahmad T**, Shin HJ, Lee J, Shin YM, Perikamana SKM, Park SY, Jung HS, Shin H. Fabrication of in vitro 3D mineralized tissue by fusion of composite spheroids incorporating biomineral-coated nanofibers and human adipose-derived stem cells. *Acta Biomater* 2018; **74**: 464-477 [PMID: 29803004 DOI: 10.1016/j.actbio.2018.05.035]
76 **Lenas P**, Moos M, Luyten FP. Developmental engineering: a new paradigm for the design and manufacturing of cell-based products. Part II: from genes to networks: tissue engineering from the viewpoint of systems biology and network science. *Tissue Eng Part B Rev* 2009; **15**: 395-422 [PMID: 19589040 DOI: 10.1089/ten.TEB.2009.0461]
77 **Freeman FE**, McNamara LM. Endochondral Priming: A Developmental Engineering Strategy for Bone Tissue Regeneration. *Tissue Eng Part B Rev* 2017; **23**: 128-141 [PMID: 27758156 DOI: 10.1089/ten.TEB.2016.0197]
78 **Colnot C**. Cellular and molecular interactions regulating skeletogenesis. *J Cell Biochem* 2005; **95**: 688-697 [PMID: 15880692 DOI: 10.1002/jcb.20449]
79 **Kim IG**, Ko J, Lee HR, Do SH, Park K. Mesenchymal cells condensation-inducible mesh scaffolds for cartilage tissue engineering. *Biomaterials* 2016; **85**: 18-29 [PMID: 26854388 DOI: 10.1016/j.biomaterials.2016.01.048]
80 **Fell HB**. The histogenesis of cartilage and bone in the long bones of the embryonic fowl. *J Mor* 1925; **40**: 417-459 [DOI: 10.1002/jmor.1050400302]
81 **Goldring MB**, Tsuchimochi K, Ijiri K. The control of chondrogenesis. *J Cell Biochem* 2006; **97**: 33-44 [DOI: 10.1002/jcb.20652]
82 **Wong SA**, Rivera KO, Miclau T, Alsberg E, Marcucio RS, Bahney CS. Microenvironmental Regulation of Chondrocyte Plasticity in Endochondral Repair-A New Frontier for Developmental Engineering. *Front Bioeng Biotechnol* 2018; **6**: 58 [PMID: 29868574 DOI: 10.3389/fbioe.2018.00058]
83 **Valenti MT**, Dalle Carbonare L, Mottes M. Osteogenic Differentiation in Healthy and Pathological Conditions. *Int J Mol Sci* 2016; 18 [PMID: 28035992 DOI: 10.3390/ijms18010041]
84 **DeLise AM**, Fischer L, Tuan RS. Cellular interactions and signaling in cartilage development. *Osteoarthritis Cartilage* 2000; **8**: 309-334 [PMID: 10966838 DOI: 10.1053/joca.1999.0306]
85 **Sart S**, Tsai AC, Li Y, Ma T. Three-dimensional aggregates of mesenchymal stem cells: cellular mechanisms, biological properties, and applications. *Tissue Eng Part B Rev* 2014; **20**: 365-380 [PMID: 24168395 DOI: 10.1089/ten.TEB.2013.0537]
86 **Athanasiou KA**, Eswaramoorthy R, Hadidi P, Hu JC. Self-organization and the self-assembling process in tissue engineering. *Annu Rev Biomed Eng* 2013; **15**: 115-136 [PMID: 23701238 DOI: 10.1146/annurev-bioeng-071812-152423]
87 **Komori T**, Yagi H, Nomura S, Yamaguchi A, Sasaki K, Deguchi K, Shimizu Y, Bronson RT, Gao YH, Inada M, Sato M, Okamoto R, Kitamura Y, Yoshiki S, Kishimoto T. Targeted disruption of Cbfa1 results in a complete lack of bone formation owing to maturational arrest of osteoblasts. *Cell* 1997; **89**: 755-764 [PMID: 9182763 DOI: 10.1016/S0092-8674(00)80258-5]
88 **Torii Y**, Hitomi K, Yamagishi Y, Tsukagoshi N. Demonstration of alkaline phosphatase participation in the mineralization of osteoblasts by antisense RNA approach. *Cell Biol Int* 1996; **20**: 459-464 [PMID: 8931312 DOI: 10.1006/cbir.1996.0060]
89 **Mikami Y**, Tsuda H, Akiyama Y, Honda M, Shimizu N, Suzuki N, Komiyama K. Alkaline phosphatase determines polyphosphate-induced mineralization in a cell-type independent manner. *J Bone Miner Metab* 2016; **34**: 627-637 [PMID: 26475372 DOI: 10.1007/s00774-015-0719-6]
90 **Hu DP**, Ferro F, Yang F, Taylor AJ, Chang W, Miclau T, Marcucio RS, Bahney CS. Cartilage to bone transformation during fracture healing is coordinated by the invading vasculature and induction of the core

pluripotency genes. *Development* 2017; **144**: 221-234 [PMID: 28096214 DOI: 10.1242/dev.130807]
91 **Klumpers DD**, Mooney DJ, Smit TH. From Skeletal Development to Tissue Engineering: Lessons from the Micromass Assay. *Tissue Eng Part B Rev* 2015; **21**: 427-437 [PMID: 25946390 DOI: 10.1089/ten.TEB.2014.0704]
92 **Matsiko A**, Thompson EM, Lloyd-Griffith C, Cunniffe GM, Vinardell T, Gleeson JP, Kelly DJ, O'Brien FJ. An endochondral ossification approach to early stage bone repair: Use of tissue-engineered hypertrophic cartilage constructs as primordial templates for weight-bearing bone repair. *J Tissue Eng Regen Med* 2018; **12**: e2147-e2150 [PMID: 29327428 DOI: 10.1002/term.2638]
93 **Daly AC**, Pitacco P, Nulty J, Cunniffe GM, Kelly DJ. 3D printed microchannel networks to direct vascularisation during endochondral bone repair. *Biomaterials* 2018; **162**: 34-46 [PMID: 29432987 DOI: 10.1016/j.biomaterials.2018.01.057]
94 **Critchley S**, Cunniffe G, O'Reilly A, Diaz-Payno P, Schipani R, McAlinden A, Withers D, Shin J, Alsberg E, Kelly DJ. Regeneration of Osteochondral Defects Using Developmentally Inspired Cartilaginous Templates. *Tissue Eng Part A* 2019; **25**: 159-171 [PMID: 30358516 DOI: 10.1089/ten.TEA.2018.0046]
95 **Stüdle C**, Vallmajó-Martín Q, Haumer A, Guerrero J, Centola M, Mehrkens A, Schaefer DJ, Ehrbar M, Barbero A, Martin I. Spatially confined induction of endochondral ossification by functionalized hydrogels for ectopic engineering of osteochondral tissues. *Biomaterials* 2018; **171**: 219-229 [PMID: 29705655 DOI: 10.1016/j.biomaterials.2018.04.025]
96 **Ishihara K**, Nakayama K, Akieda S, Matsuda S, Iwamoto Y. Simultaneous regeneration of full-thickness cartilage and subchondral bone defects in vivo using a three-dimensional scaffold-free autologous construct derived from high-density bone marrow-derived mesenchymal stem cells. *J Orthop Surg Res* 2014; **9**: 98 [PMID: 25312099 DOI: 10.1186/s13018-014-0098-z]
97 **Khademhosseini A**, Langer R, Borenstein J, Vacanti JP. Microscale technologies for tissue engineering and biology. *Proc Natl Acad Sci USA* 2006; **103**: 2480-2487 [PMID: 16477028 DOI: 10.1073/pnas.0507681102]
98 **Nichol JW**, Khademhosseini A. Modular Tissue Engineering: Engineering Biological Tissues from the Bottom Up. *Soft Matter* 2009; **5**: 1312-1319 [PMID: 20179781 DOI: 10.1039/b814285h]
99 **Guven S**, Chen P, Inci F, Tasoglu S, Erkmen B, Demirci U. Multiscale assembly for tissue engineering and regenerative medicine. *Trends Biotechnol* 2015; **33**: 269-279 [PMID: 25796488 DOI: 10.1016/j.tibtech.2015.02.003]
100 **Dinh ND**, Luo R, Christine MTA, Lin WN, Shih WC, Goh JC, Chen CH. Effective Light Directed Assembly of Building Blocks with Microscale Control. *Small* 2017; 13 [PMID: 28481437 DOI: 10.1002/smll.201700684]
101 **Olsen TR**, Mattix B, Casco M, Herbst A, Williams C, Tarasidis A, Simionescu D, Visconti RP, Alexis F. Manipulation of cellular spheroid composition and the effects on vascular tissue fusion. *Acta Biomater* 2015; **13**: 188-198 [PMID: 25463485 DOI: 10.1016/j.actbio.2014.11.024]
102 **Yang X**, Mironov V, Wang Q. Modeling fusion of cellular aggregates in biofabrication using phase field theories. *J Theor Biol* 2012; **303**: 110-118 [PMID: 22763135 DOI: 10.1016/j.jtbi.2012.03.003]
103 **Visconti RP**, Kasyanov V, Gentile C, Zhang J, Markwald RR, Mironov V. Towards organ printing: engineering an intra-organ branched vascular tree. *Expert Opin Biol Ther* 2010; **10**: 409-420 [PMID: 20132061 DOI: 10.1517/14712590903563352]
104 **Susienka MJ**, Wilks BT, Morgan JR. Quantifying the kinetics and morphological changes of the fusion of spheroid building blocks. *Biofabrication* 2016; **8**: 045003 [PMID: 27721222 DOI: 10.1088/1758-5090/8/4/045003]
105 **Fleming PA**, Argraves WS, Gentile C, Neagu A, Forgacs G, Drake CJ. Fusion of uniluminal vascular spheroids: a model for assembly of blood vessels. *Dev Dyn* 2010; **239**: 398-406 [PMID: 19918756 DOI: 10.1002/dvdy.22161]
106 **Lehmann M**, Martin F, Mannigel K, Kaltschmidt K, Sack U, Anderer U. Three-dimensional scaffold-free fusion culture: the way to enhance chondrogenesis of in vitro propagated human articular chondrocytes. *Eur J Histochem* 2013; **57**: e31 [PMID: 24441184 DOI: 10.4081/ejh.2013.e31]
107 **Gopinathan J**, Noh I. Recent trends in bioinks for 3D printing. *Biomater Res* 2018; **22**: 11 [PMID: 29636985 DOI: 10.1186/s40824-018-0122-1]
108 **Hull CW,** inventor; 3D Systems Inc., assignee. Apparatus for production of three-dimensional objects by stereolithography. United States patent US 4575330A. 1986 March 11
109 **Zhang YS**, Oklu R, Dokmeci MR, Khademhosseini A. Three-Dimensional Bioprinting Strategies for Tissue Engineering. *Cold Spring Harb Perspect Med* 2018; 8 [PMID: 28289247 DOI: 10.1101/cshperspect.a025718]
110 **Derakhshanfar S**, Mbeleck R, Xu K, Zhang X, Zhong W, Xing M. 3D bioprinting for biomedical devices and tissue engineering: A review of recent trends and advances. *Bioact Mater* 2018; **3**: 144-156 [PMID: 29744452 DOI: 10.1016/j.bioactmat.2017.11.008]
111 **Baptista LS**, Kronemberger GS, Côrtes I, Charelli LE, Matsui RAM, Palhares TN, Sohier J, Rossi AM, Granjeiro JM. Adult Stem Cells Spheroids to Optimize Cell Colonization in Scaffolds for Cartilage and Bone Tissue Engineering. *Int J Mol Sci* 2018; 19 [PMID: 29693604 DOI: 10.3390/ijms19051285]
112 **Gentile C**, Fleming PA, Mironov V, Argraves KM, Argraves WS, Drake CJ. VEGF-mediated fusion in the generation of uniluminal vascular spheroids. *Dev Dyn* 2008; **237**: 2918-2925 [PMID: 18816835 DOI: 10.1002/dvdy.21720]
113 **Mehesz AN**, Brown J, Hajdu Z, Beaver W, da Silva JV, Visconti RP, Markwald RR, Mironov V. Scalable robotic biofabrication of tissue spheroids. *Biofabrication* 2011; **3**: 025002 [PMID: 21562365 DOI: 10.1088/1758-5082/3/2/025002]
114 **Yu Y**, Moncal KK, Li J, Peng W, Rivero I, Martin JA, Ozbolat IT. Three-dimensional bioprinting using self-assembling scalable scaffold-free "tissue strands" as a new bioink. *Sci Rep* 2016; **6**: 28714 [PMID: 27346373 DOI: 10.1038/srep28714]
115 **Daly AC**, Kelly DJ. Biofabrication of spatially organised tissues by directing the growth of cellular spheroids within 3D printed polymeric microchambers. *Biomaterials* 2019; **197**: 194-206 [PMID: 30660995 DOI: 10.1016/j.biomaterials.2018.12.028]
116 **Huang Y**, Zhang XF, Gao G, Yonezawa T, Cui X. 3D bioprinting and the current applications in tissue engineering. *Biotechnol J* 2017; 12 [PMID: 28675678 DOI: 10.1002/biot.201600734]
117 **Park SH**, Jung CS, Min BH. Advances in three-dimensional bioprinting for hard tissue engineering. *Tissue Eng Regen Med* 2016; **13**: 622-635 [PMID: 30603444 DOI: 10.1007/s13770-016-0145-4]

World Journal of Stem Cells

Submit a Manuscript: https://www.f6publishing.com

World J Stem Cells 2020 February 26; 12(2): 123-138

DOI: 10.4252/wjsc.v12.i2.123

ISSN 1948-0210 (online)

ORIGINAL ARTICLE

Basic Study

Clonal isolation of endothelial colony-forming cells from early gestation chorionic villi of human placenta for fetal tissue regeneration

Kewa Gao, Siqi He, Priyadarsini Kumar, Diana Farmer, Jianda Zhou, Aijun Wang

ORCID number: Kewa Gao (0000-0002-8781-890X); Siqi He (0000-0002-3601-1938); Priyadarsini Kumar (0000-0001-6800-9632); Diana Farmer (0000-0002-3530-5993); Jianda Zhou (0000-0002-3766-6573); Aijun Wang (0000-0002-2985-3627).

Author contributions: This study was designed and supervised by Wang A, Zhou J and Farmer D; experiments were performed by Gao K, He S and Kumar P; data analysis was conducted by Gao K and Wang A; funding was obtained by Farmer D and Wang A; the manuscript was written and revised by Gao K, He S, Kumar P, Farmer D, Zhou J and Wang A.

Supported by the Shriners Hospital for Children Postdoctoral Research Fellowship award, No. 84704-NCA-19; UC Davis School of Medicine Dean's Fellowship award and funding from the NIH, No. 5R01NS100761-02 and No.R03HD091601-01; the California Institute of Regenerative Medicine, No. PC1-08103 and No. CLIN1-11404; Shriners Hospitals for Children, No. 85120-NCA-16, No. 85119-NCA-18, No. 85108-NCA-19 and No. 87200-NCA-19; March of Dimes Foundation, No. 5FY1682.

Institutional review board statement: The study was submitted to the UCD Institutional Review Board (IRB) and determined to be exempt from review.

Conflict-of-interest statement:

Kewa Gao, Siqi He, Jianda Zhou, Department of Burns and Plastic Surgery, The Third Xiangya Hospital of Central South University, Changsha 410013, Hunan Province, China

Kewa Gao, Siqi He, Priyadarsini Kumar, Diana Farmer, Aijun Wang, Surgical Bioengineering Laboratory, Department of Surgery, University of California Davis, Sacramento, CA 95817, United States

Kewa Gao, Siqi He, Priyadarsini Kumar, Diana Farmer, Aijun Wang, Institute for Pediatric Regenerative Medicine, Shriners Hospitals for Children, Sacramento, CA 95817, United States

Aijun Wang, Department of Biomedical Engineering, University of California Davis, Davis, CA 95817, United States

Corresponding author: Aijun Wang, PhD, Associate Professor, Surgical Bioengineering Laboratory, Department of Surgery, University of California, Davis School of Medicine, 4625 2nd Ave., Room 3005, Sacramento, CA 95817, United States. aawang@ucdavis.edu

Abstract

BACKGROUND

Endothelial colony-forming cells (ECFCs) have been implicated in the process of vascularization, which includes vasculogenesis and angiogenesis. Vasculogenesis is a *de novo* formation of blood vessels, and is an essential physiological process that occurs during embryonic development and tissue regeneration. Angiogenesis is the growth of new capillaries from pre-existing blood vessels, which is observed both prenatally and postnatally. The placenta is an organ composed of a variety of fetal-derived cells, including ECFCs, and therefore has significant potential as a source of fetal ECFCs for tissue engineering.

AIM

To investigate the possibility of isolating clonal ECFCs from human early gestation chorionic villi (CV-ECFCs) of the placenta, and assess their potential for tissue engineering.

METHODS

The early gestation chorionic villus tissue was dissociated by enzyme digestion. Cells expressing CD31 were selected using magnetic-activated cell sorting, and plated in endothelial-specific growth medium. After 2-3 wks in culture, colonies displaying cobblestone-like morphology were manually picked using cloning cylinders. We characterized CV-ECFCs by flow cytometry, immunophenotyping,

Authors of this manuscript have no conflicts of interest to disclose.

Data sharing statement: We agree to share the research methods and data in this study to public.

Manuscript source: Invited manuscript

Received: July 5, 2019
Peer-review started: July 17, 2019
First decision: August 23, 2019
Revised: December 3, 2019
Accepted: December 23, 2019
Article in press: December 23, 2019
Published online: February 26, 2020

P-Reviewer: Huang YC
S-Editor: Wang YQ
L-Editor: Filipodia
E-Editor: Liu MY

tube formation assay, and Dil-Ac-LDL uptake assay. Viral transduction of CV-ECFCs was performed using a Luciferase/tdTomato-containing lentiviral vector, and transduction efficiency was tested by fluorescent microscopy and flow cytometry. Compatibility of CV-ECFCs with a delivery vehicle was determined using an FDA approved, small intestinal submucosa extracellular matrix scaffold.

RESULTS

After four passages in 6-8 wks of culture, we obtained a total number of 1.8×10^7 CV-ECFCs using 100 mg of early gestational chorionic villus tissue. Immunophenotypic analyses by flow cytometry demonstrated that CV-ECFCs highly expressed the endothelial markers CD31, CD144, CD146, CD105, CD309, only partially expressed CD34, and did not express CD45 and CD90. CV-ECFCs were capable of acetylated low-density lipoprotein uptake and tube formation, similar to cord blood-derived ECFCs (CB-ECFCs). CV-ECFCs can be transduced with a Luciferase/tdTomato-containing lentiviral vector at a transduction efficiency of 85.1%. Seeding CV-ECFCs on a small intestinal submucosa extracellular matrix scaffold confirmed that CV-ECFCs were compatible with the biomaterial scaffold.

CONCLUSION

In summary, we established a magnetic sorting-assisted clonal isolation approach to derive CV-ECFCs. A substantial number of CV-ECFCs can be obtained within a short time frame, representing a promising novel source of ECFCs for fetal treatments.

Key words: Placenta; Endothelial colony forming cells; Chorionic villi; Angiogenesis; Tissue engineering

Core tip: We established a magnetic sorting-assisted clonal isolation protocol to derive chorionic villus endothelial colony-forming cells (CV-ECFCs) from early gestation placentas. Using our protocol, a substantial number of CV-ECFCs can be obtained from chorionic villus sampling specimens within a short time frame, making it feasible for autologous fetal treatment. CV-ECFCs are comparable to umbilical cord blood-derived ECFCs in terms of surface marker expression, tube formation capability, transducibility, and compatibility with biomaterial delivery vehicles. CV-ECFCs represent a novel autologous source of cells for fetal or postnatal treatment of congenital anomalies or defects.

Citation: Gao K, He S, Kumar P, Farmer D, Zhou J, Wang A. Clonal isolation of endothelial colony-forming cells from early gestation chorionic villi of human placenta for fetal tissue regeneration. *World J Stem Cells* 2020; 12(2): 123-138
URL: https://www.wjgnet.com/1948-0210/full/v12/i2/123.htm
DOI: https://dx.doi.org/10.4252/wjsc.v12.i2.123

INTRODUCTION

Over the past three decades, fetal medicine, especially fetal surgery, has been substantially developed for the treatment of congenital disorders. These include structural defects, such as spina bifida, congenital diaphragmatic hernia, sacrococcygeal teratoma, cardiac malformations[1-3], and genetic disorders, such as hemophilia[4,5], Duchenne muscular dystrophy[6] and cystic fibrosis[7,8]. For the past several years, our group has been exploring and establishing stem cell-based regenerative fetal treatments combined with tissue engineering for a variety of congenital disorders. For instance, we have successfully isolated placental mesenchymal stem/stromal cells (PMSCs) from the chorionic villus of early gestation placentas, and developed a PMSC-based fetal treatment for spina bifida (SB)[3,4,9-12]. Using the surgically-created fetal ovine SB model, we showed that augmenting *in utero* surgical repair of SB defects with PMSCs can rescue neurons and cure SB-

associated motor function deficits at birth[3,9-11]. However, consistent with numerous other cases in which therapeutic effects were observed using MSCs, the transplanted PMSCs did not persist following transplantation, nor contribute to tissue regeneration by integration[3,13-17]. Rather, the PMSCs rescued neurons *via* paracrine mechanisms. In the aforementioned studies, small intestinal submucosa extracellular matrix (SIS-ECM) was the biomaterial scaffold used to deliver the stem cells *in vivo*[9,18,19]. Porcine small intestinal submucosa (SIS) scaffold is a Food and Drug Administration-approved natural ECM, which serves as a suitable provisional matrix for tissue regeneration. Based on our previous application of SIS-ECM, we believe it can be useful as a scaffold for delivering various types of stem cells to different affected tissues.

In another recent study of hemophilia A, we showed that when co-transplanting PMSCs with cord blood-derived endothelial colony-forming cells (CB-ECFCs), PMSCs integrated into the host environment and formed stable, long-term engraftment[20]. This observation suggests that ECFCs play a critical role in facilitating the long-term survival and engraftment of PMSCs[20].

The potential of ECFCs is also noted in vascularization, including vasculogenesis and angiogenesis. Vasculogenesis is the *de novo* formation of blood vessels, and is an essential physiological process that occurs during embryonic development and tissue regeneration. Angiogenesis is the growth of new capillaries from pre-existing blood vessels, which is observed both prenatally and postnatally[21]. ECFCs are highly proliferative endothelial progenitor cells that can differentiate into mature endothelial cells[22], and facilitate the functional formation of angiogenesis and thus vascularization. Therefore, cell therapies using ECFCs isolated from various tissue sources, such as bone marrow[23], adipose tissue[24], peripheral blood[25] and cord blood[20,26], have been sought as a therapeutic method to improve vascularization for various disorders[27]. Vascularization is vital to the development, maintenance, and regeneration of tissues. Angiogenesis, one vascularization process in which new blood vessels are formed from preexisting ones, plays a crucial role in embryonic and fetal development[21,28]. A defect in angiogenesis can lead to a variety of diseases, such as heart and brain ischemia, neurodegeneration, hypertension, osteoporosis, respiratory distress, and preeclampsia, to name a few[29]. Therefore, improving angiogenesis can ameliorate these aforementioned disorders by substantially increasing the supply of nutrients and oxygen to the affected tissues, and thus subsequently promoting tissue regeneration and functional repair[30-32]. Furthermore, the proliferative capacity of ECFCs, as well as their ability to integrate into the circulatory system, has allowed them to also be used as a delivery method of mutant genes to treat genetic vascular diseases[20,33]. Overall, the potential of ECFCs is greatly noted, and they may be ideal for treating the various disorders listed above, both adult and congenital. For example, an ideal long-term treatment strategy for congenital genetic diseases, such as hemophilia, is to apply appropriate stem cells during the first trimester of gestation, and treat the fetus prior to the development of a fetal immune system[4,34].

The placenta is a highly vascularized organ that plays a pivotal role in supporting and regulating fetal development with active vascularization beginning at an early gestational age[35]. During the first trimester of gestation, the placenta rapidly develops from the trophectoderm. The developmental process includes the formation of the villus tree and the extensive vasculature necessary to support the developing fetus. Hence, the early gestation placenta may pose a source from which we can reliably obtain a variety of progenitor cells such as ECFCs, in addition to the PMSCs that we have already established[35-37].

Several methods have been established to isolate ECFCs from term placentas. Patel *et al*[38] isolated large numbers of ECFCs by flow cytometry enrichment of $CD45^{-}CD34^{+}CD31^{Lo}$ cells from term placentas, and found that placenta-derived ECFCs possessed angiogenic qualities similar to CB-ECFCs. Solomon and colleagues obtained ECFCs from the micro- and macrovascular tissues of human term placentas using CD31 magnetic bead sorting and colony isolation[39]. Thus far, a protocol for isolating ECFCs from early gestational preterm placentas has not been well-established, and the feasibility of using these ECFCs as an autologous source for fetal treatment has not been explored. In this study, we established a method for isolating ECFCs from early gestation placentas, and characterized their phenotype and angiogenic functions.

MATERIALS AND METHODS

Isolation of single cells from the chorionic villus of early gestation human placenta by enzymatic dissociation

Discarded human early gestation (GA 12-16 wk) placentas were collected from the University of California, Davis, Medical Center. The study was submitted to the University of California, Davis, Institutional Review Board, and was determined to be exempt from review. The chorionic villi of the placenta were dissected into small pieces and washed three times with 1X phosphate-buffered saline (PBS) solution containing 100 IU/mL of penicillin and 100 μg/mL of streptomycin. Chorionic villus tissue (100 mg) was placed in a 100 mm dish and digested with 10 mL of enzyme solution containing 1 mg/mL collagenase Type I (Gibco), 0.1% trypsin (Invitrogen), and 0.2 mg/mL DNase (Invitrogen) by incubating at 37 °C, 5% CO_2 for 20 min. The cell suspension was collected, neutralized with a medium containing 10% fetal bovine serum (FBS), and placed on ice. Fresh enzyme solution was added to the remaining tissue in the petri dish and incubated for an additional 20 min. The collection of cells and enzyme digestion was repeated until the whole tissue was completely dissociated. The cell suspensions were pooled, filtered through 70 μm nylon mesh, and incubated with red blood cell lysate buffer for 5 min at room temperature.

Sorting CD31-positive cells by magnetic beads and culture

Cells that were obtained by enzyme dissociation, as described above, were labeled with magnetic bead antibodies, and sorted according to the manufacturer's protocol (MACS cell separation system; Miltenyi Biotec). Briefly, cells were first labeled with PE-mouse anti-human CD31 antibody and then bound to anti-PE microbeads (MiltenyiBiotec). Labeled cells were passed through a separation column under the magnetic field, and CD31-positive cells were collected and seeded on a rat-tail collagen Type I (BD Biosciences Discovery)-coated tissue culture treated dish at a low seeding density (2000-4000 cells/cm^2). Cells were cultured in Endothelial Cell Growth Medium MV-2 media (ECGM-MV2, PromoCell) with the addition of 250 ng/mL TGF-β inhibitor SB431542 (Stemcell Technologies) and 10 ng/mL vascular endothelial growth factor (VEGF; R&D Systems). Cells were fed every day for the first 7 d and every 2 d until the appearance of cell colonies.

Isolation of cell clones using the cloning cylinder

Once a cell colony with a cobblestone-like morphology appeared and grew to about 20 cells, it was hand-picked using a cloning cylinder. The rim of a sterile cloning cylinder (Millipore/Sigma) was coated with sterile vacuum grease and placed onto the location of the target clone marked under the microscope. Trypsin-EDTA was used to detach the cells within the cloning cylinder. All cells obtained from each of the selected colonies was seeded into one well of a 24-well plate (Corning). After about 2-3 wks of culture and upon reaching about 90% confluency, the cells were passaged into a 6-well tissue culture treated dish. In addition, 5000 cells from each colony were seeded into one well of a 96-well plate for CD31 and VE-Cadherin staining to confirm the ECFC phenotype. The monoclonal cells that displayed cobblestone-like morphology and co-expressed CD31 and VE-Cadherin underwent further expansion. CV-ECFCs were frozen at passage five and subsequently used for all experiments.

Cord blood-derived ECFCs isolation and culture

Cord blood was collected from discarded term placentas obtained from the University of California Medical Center. CB-ECFCs were isolated as previously described[20]. They were cultured in ECGM-MV2 media (PromeCell). CB-ECFCs between passages 4-6 were used in this study.

Flow cytometry

Flow cytometry was used to characterize the cellular composition of the chorionic villus of human early gestation placental tissue, and the surface markers of isolated and expanded CV-ECFCs. The Attune NxT Flow Cytometer (ThermoFisher Scientific) was used for performing flow cytometry, and FlowJo software (FlowJo LLC) was used for data analyses. All antibodies were obtained from BD Biosciences. For characterization of early gestation placenta cellular composition, single cells obtained from enzymatic dissociation of placental villi were fractionated into tubes containing approximately 5 x 10^5 cells per sample and stained with PE-CD31 (555446), APC-CD13 (561698), APC-CD90 (561971), APC-CD34 (560940), APC-CD45 (560973), APC-CD105 (562408), APC-CD117 (561118), and Alexa Fluor 647-CD146 (563619). For phenotypic characterization of CV-ECFCs, cells were stained with PE-CD31 (555446), PE-CD34 (555446), PE-CD144 (560410), PE-CD90 (561972), PE-CD45 (555483), APC-CD105 (562408), Alexa Fluor 647-CD146 (563619), and Alexa Fluor 647-CD309 (560495). PE-Ms IgG1 κ (555749), APC-Ms IgG1 κ (550854), and Alexa Fluor 647-Ms IgG1 κ (557783) were used as isotype controls, and anti-mouse Igκ CompBeads were used to generate compensation controls. The LIVE/DEAD™ Fixable Near-IR Dead Cell Stain Kit (ThermoFisher Scientific) was used to exclude interference from the non-specific

staining of dead cells. CV-ECFCs were transduced using an established protocol[20]. Transduction efficiency was assessed by tdTomato expression quantified by flow cytometry.

Immunohistochemistry and immunocytochemistry staining

Chorionic villus tissue was dissected from human early gestation placentas, fixed with 10% formalin for 24 h, protected by 30% sucrose dehydration until the tissue specimen settled to the bottom of the tube, and then embedded in O.C.T compound (Sakura Finetek). Serial sections were made at 6 μm thickness using a Cryostat (Leica CM3050S) and mounted onto microscope slides (Matsunami Glass). O.C.T compound was washed off by water. Tissue sections were permeabilized by incubating the tissues with PBS containing 0.5% Triton X-100 for 10 min. Tissue sections were then incubated with PBS containing 5% bovine serum albumin (BSA) for 1 h at room temperature to block non-specific binding sites. Samples were incubated with primary antibody diluted in PBS containing 1% BSA at 4 °C overnight. The dilutions of primary antibodies were: Mouse anti-human CD146 (BD Biosciences) 1:50, mouse anti-human NG2 (BD Biosciences) 1:50, mouse anti-human CD34 (Dako) 1:25, rabbit anti-human von Willebrand factor (vWF) (Dako) 1:200. Tissue sections were then stained with the respective secondary antibodies: donkey anti-rabbit, conjugated with Alexa647 (ThermoFisher Scientific) and donkey anti-mouse, conjugated with Alexa647 (ThermoFisher Scientific), diluted 1:500 with 1% BSA in PBS, and incubated for 1 h at room temperature. The slides were then counterstained with 1:5000 dilution of DAPI for 5 min, mounted with Prolong Diamond Antifade Mountant (Invitrogen), and imaged with a Zeiss Observer Z1 microscope. For CV-ECFC immunocytochemical characterization, cells were seeded in 96-well plates and fixed with 10% formalin. Cells were stained using rabbit anti-VE-Cadherin (Cell Signaling) at 1:400 dilution or mouse anti-CD31 antibodies (Dako) at 1:40 dilution and imaged, as described above.

Acetylated low-density lipoprotein uptake

The CV-ECFCs were cultured in 0.5% BSA for 24 h and then incubated with 10 μg/mL Dil-Ac-LDL (Alfa Aesar) in serum-free culture medium at 37 °C for 5 h. Cells were then washed three times with PBS, fixed with 10% formalin for 15 min, and stained with DAPI (1:5000 in water) to label nuclei. The cells were imaged using a Zeiss Observer Z1 microscope.

Tube formation assay

Twenty-four-well culture dishes were coated with 300 μL Matrigel (BD Biosciences) per well and allowed to gel for 60 min at 37 °C. CV-ECFCs (100,000) were seeded onto the Matrigel-coated wells and incubated at 37 °C, 5% CO_2. Phase contrast images were acquired 12 h after seeding using a Zeiss Observer Z1 microscope. Tube formation was quantified using the angiogenesis analyzer in ImageJ software for total junction numbers and total branch lengths.

Genetical modification and viral transduction of CV-ECFCs

CV-ECFCs could serve as a promising autologous cell source for the treatment of genetic diseases. To test if CV-ECFCs can be genetically modified, we transduced CV-ECFCs using lentiviral vectors for proof-of-concept evaluations. All lentiviral constructs were generated at the Institute for Regenerative Cures (IRC) Vector Core, University of California, Davis. CV-ECFCs were transduced in a transduction medium composed of DMEM high glucose, 10% FBS and 8 μg/mL protamine sulfate (MP Biomedicals) with pCCLc-MNDU3-LUC-PGK-Tomato-WPRE for quantitative analysis at a multiplicity of infection (MOI) of 10 for 6 h. After 6 h, the transduction medium was discarded, and cells were cultured in ECGM-MV2 medium for 72 h. A fluorescence microscope (Zeiss Observer Z1) was used to observe tdTomato expression, and flow cytometry was used to detect transduction efficiency.

Cytocompatibility of CV-ECFCs with biomaterial scaffolds

CV-ECFCs represent a promising new cell source for various fetal or adult tissue engineering applications. To test the cytocompatibility of CV-ECFCs with biomaterial scaffolds, we used a clinical grade SIS-ECM scaffold as a representative scaffold to be tested *in vitro*. Punch-outs (6 mm) of the SIS-ECM scaffold (Biodesign® Dural graft, Cook Biotech, West Lafayette, IN) were incubated in the culture medium overnight. A quantity of 2×10^5 transduced CV-ECFCs were suspended in 10 μL culture medium, seeded onto the pre-equilibrated SIS-ECM scaffold, and cultured at 37 °C, 5% CO_2 for 4 h to allow cells to attach. Then, the culture medium was subsequently added to cover the CV-ECFC/SIS scaffold composite, and incubated at 37 °C, 5% CO_2 for 24 h. A fluorescence microscope (Zeiss Observer Z1) was then used to observe cell morphology on the scaffold.

Statistical analysis

All data analysis was performed using PRISM 7 software (GraphPad Software Inc.). Descriptive statistical data are reported as mean ± SD.

RESULTS

Cellular composition characterization of the human early gestation placenta chorionic villus

The placenta is composed of a variety of progenitor cells, and undergoes rapid development during the early gestational period of pregnancy. Hence, it serves as a unique source for obtaining progenitor cells that could be utilized for tissue engineering purposes. We first analyzed the cellular composition of early gestation placenta villi. The typical endothelial cell markers CD31, CD34 and vWF were used to characterize the endothelial cells present in the chorionic villus tissue (gestation age of 14 wk 5 d). Results confirmed that these endothelial cell markers were broadly distributed throughout the chorionic villus tissues (Figure 1A, the first three panels). CD146 is a marker expressed on the endothelium in capillaries and perivascular cells around the venules. We found that CD146-positive cells were widely present in placental villi tissues (Figure 1A, the 4th panel). Flow cytometry quantitative analysis was used to characterize the cell phenotypes derived from the enzymatic dissociation of placental tissue. We found that during early gestation (12-16 wk), placental chorionic villus tissues had 52.3% ± 24.1% CD45-positive cells , 43.9% ± 10.39% CD13-positive cells, 23.98% ± 14.28% CD90-positive cells, 24.5% ± 5.47% CD105-positive cells, 23.83% ± 13.66% CD31-positive cells, 14.79% ± 7.65% CD34-positive cells, 9.57% ± 2.5% CD146-positive cells, and 7.35% ± 10.79% CD117-positive cells (Figure 1B and C). Since CD31 is an established, specific endothelial cell marker, it was selected for the magnetic sorting strategy of CV-ECFCs from chorionic villi. We also analyzed the co-expression of CD31 and other markers on the isolated cells derived from early gestation placental chorionic villus tissues. We found that 12.56% ± 4.24% of CD31-positive cells were also CD45 positive, and most likely of the non-adherent hematopoietic lineage. A subpopulation of CD31-positive cells (4.22% ± 1.53%) were also positive for CD34, a marker of immature endothelial progenitor cells. This subpopulation will most likely be able to grow into colonies with high proliferative potential. A subpopulation of CD31-positive cells (1.34% ± 0.67%) were also positive for CD90, and CD90 is generally considered as an MSC marker (Figure 1D). Although the cells that simultaneously expressed CD31 and CD90 account for only a small fraction of all cells, their higher proliferative capacity overtook the expansion of CD31-sorted CV-ECFCs. Hence, manual cloning was necessary to obtain pure populations of CV-ECFCs.

Clonal isolation of CV-ECFCs by magnetic beads sorting

By enzymatically dissociating tissues, we obtained $1.22 \times 10^6 \pm 0.32 \times 10^6$ single cells from 100 mg of chorionic villus tissue (n = 5). Single cells were then subjected to magnetic bead sorting and manual cloning. After 4-6 passages and confirmation of surface markers, an ECFC cell line with proliferative potential was obtained. A brief illustration of this process is shown in Figure 2A. The CD31-positive cells were added to ECGM-MV2 containing TGF-β inhibitor and VEGF. Cell colonies grown from single cells appeared 5-10 d after being cultured, and they presented with multiple morphologies (Figure 2B). CV-ECFC colonies exhibited a cobblestone-like morphology, whereas MSC clones exhibited a spindle-shaped morphology. There were also colonies that exhibited non-uniform morphologies. Cell colonies that displayed a cobblestone-like morphology were chosen using a cloning cylinder, seeded, and cultured in a 24-well plate. In order to get a uniform population and increased cell number for subsequent characterization by immunocytochemistry, cells underwent two additional passages. Those cell lines that co-expressed CD31 and CD144 were expanded for subsequent experiments (Figure 2C). After a total of four passages within 6-8 wk of culture, a total number of 1.8×10^7 CV-ECFCs per 100 mg of chorionic villus tissue was obtained.

Flow cytometry analysis of CV-ECFC morphology

The immunophenotypic profile of CV-ECFCs was analyzed by flow cytometry. These cells were positive for well-established ECFC surface markers, including CD31 (99.55% ± 0.49%), CD144 (98.95% ± 0.64%), CD146 (98.3% ± 1.98%), CD105 (97.7% ± 1.56%), CD309 (39.6% ± 0.99%), and low expression of CD34 (23.2% ± 12.87%). They were negative for hematopoietic and MSC surface markers CD45 (1.87% ± 2.18%) and CD90 (2.95% ± 4.02%) (n = 3) (Figure 3). The expression levels of various surface

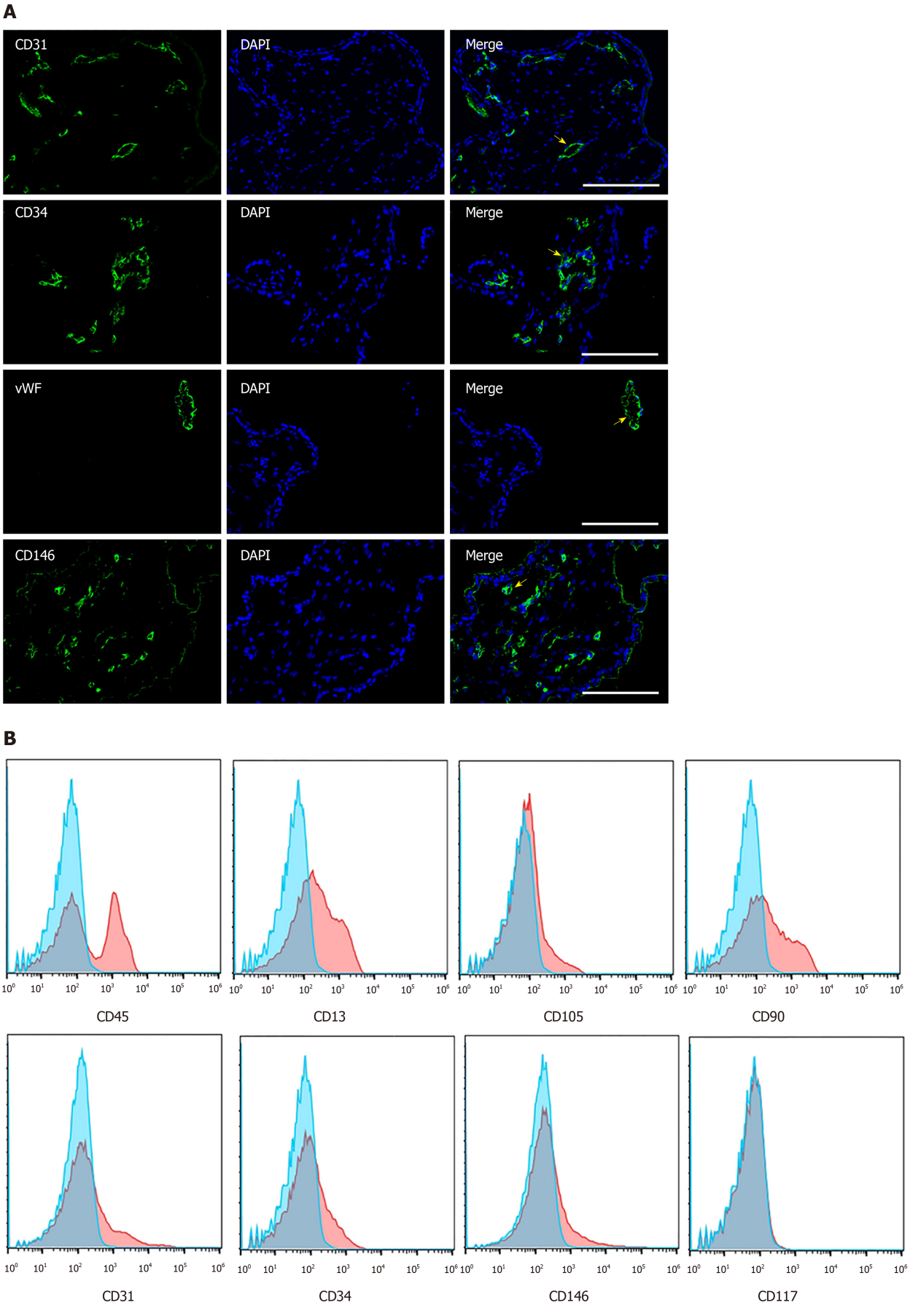
A
CD31
DAPI
Merge
CD34
DAPI
Merge
vWF
DAPI
Merge
CD146
DAPI
Merge
B
CD45
CD13
CD105
CD90
CD31
CD34
CD146
CD117

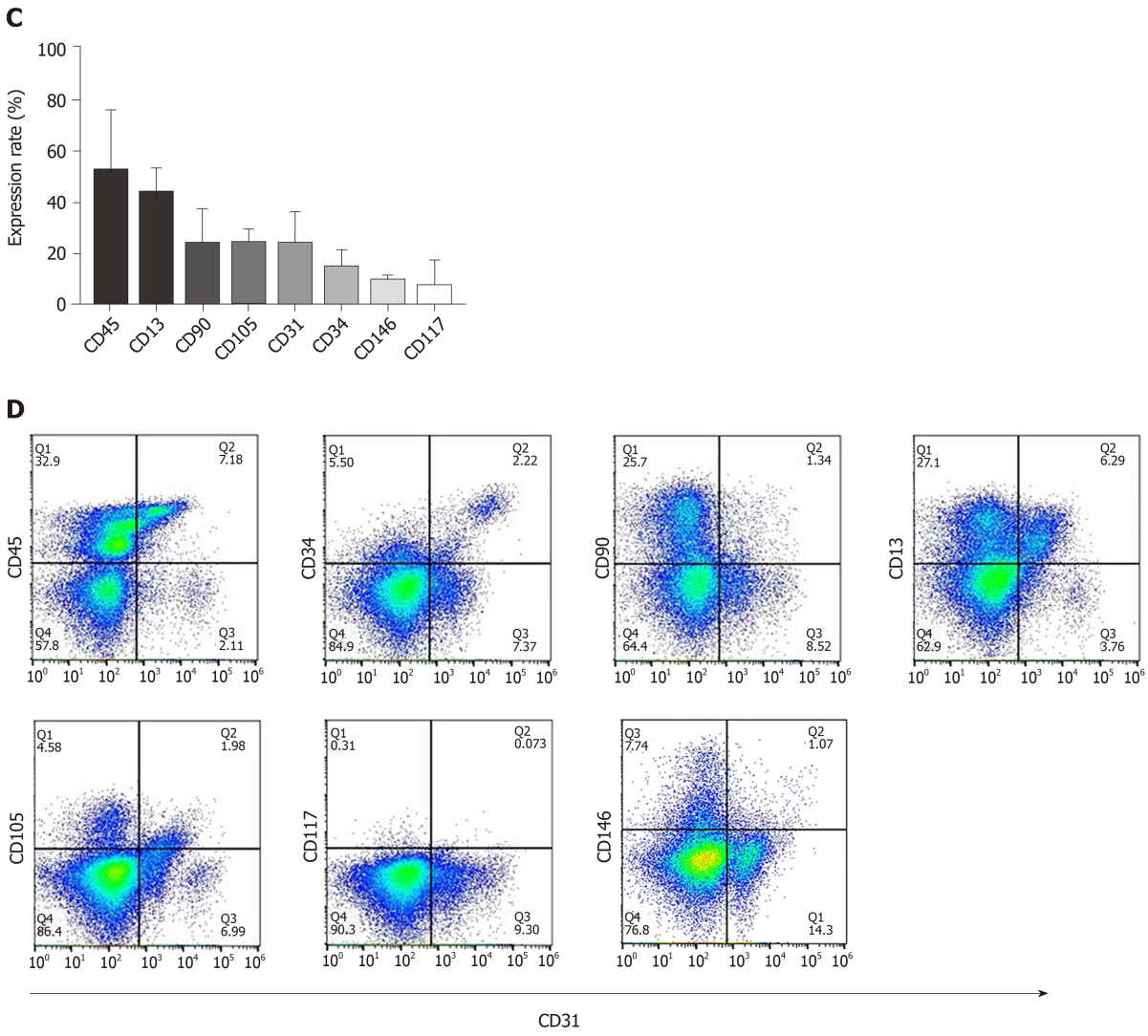

Figure 1 Characterization and cellular composition of the human early gestation placenta. Cellular composition of the human early gestation placenta chorionic villi was characterized. A: Immunofluorescence staining of CD31, CD34, von Willebrand factor and CD146 showed positive cells, depicted with arrows, located in chorionic villi and organized into blood vessel structures; B, C: Flow cytometry analysis of the surface markers of single cells derived by enzymatic dissociation of the placental chorionic villi; each marker's expression is quantitively presented (data were expressed as mean ± SD, *n* = 3); D: Flow cytometry analysis of the co-expression of typical endothelial cell marker CD31 and other surface markers. Scale bar = 100 μm.

markers were similar to CB-ECFCs, as previously published[20], except for the expression level of CD34 of CV-ECFCs, which was higher than that of CB-ECFCs (2.16% ± 1.06%).

CV-ECFCs are functionally comparable to CB-ECFCs

Tube formation and Dil-Ac-LDL uptake experiments are commonly used to identify endothelial cells from a functional perspective. Like CB-ECFCs, CV-ECFCs formed a similar tubular structure on the surface of Matrigel, which can persist for more than 48 h and then disintegrate. The capacity of *in vitro* angiogenesis of CV-ECFCs and CB-ECFCs showed no significant difference in quantity by the angiogenesis analyzer in ImageJ (Figure 4A). These CV-ECFCs showed a comparable ability of Dil-Ac-LDL uptake to CB-ECFCs (Figure 4B).

To explore the possibility of CV-ECFCs expressing exogenous proteins, and their potential for treating genetic defects, the transduction rate of these cells was explored. CV-ECFCs were transduced with a tdTomato-expressing lentiviral vector, and the transduction rate reached 85.1% at an MOI of 10 by flow cytometry analysis of transduced and non-transduced cells (Figure 5A). We tested the compatibility of CV-ECFCs with SIS biomaterial scaffold for future potential tissue engineering. CV-ECFCs adhered well to the surface of the SIS scaffold, and displayed normal morphology, similar to CB-ECFCs. These results show that CV-ECFCs can be delivered to a defective site *via* a SIS-ECM scaffold or other similar collagen-based scaffolds (Figure 5B).

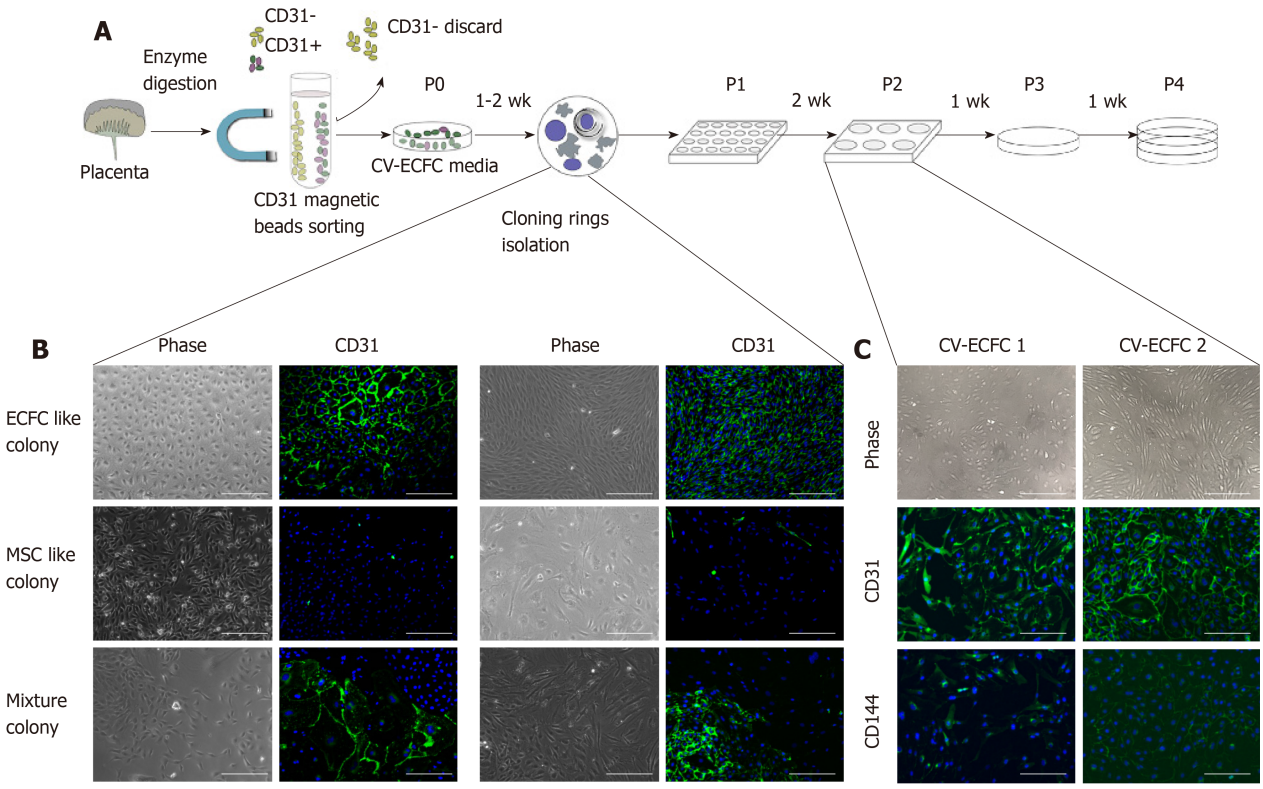

Figure 2 Isolation procedure of endothelial colony-forming cells from placental chorionic villi. A: Depiction of the isolation of chorionic villus endothelial colony-forming cells from chorionic-villus cells by enzymatic dissociation of chorionic villus tissue, followed by CD31 magnetic bead sorting and subsequent manual clonal isolation and expansion; B: Morphology of the colonies formed by CD31$^+$-sorted cells. CD31 was expressed only by colonies that had a cobblestone-like morphology and not by ones that displayed spindle shaped morphology. Two representative colonies are shown for each morphology; C: Immunofluorescence staining of isolated colonies for expression of CD31 and CD144. Scale bar = 100 μm.

DISCUSSION

The placenta is a highly vascularized organ, and the vascularization process begins at an early gestational age[35]. This study confirmed that endothelial cells account for about 20%-40% of total placental cells present during early gestation. We showed that endothelial cells are present in the chorionic villi and likely involved in the formation and development of blood vessels. Proliferative ECFCs are rare in placental cell populations, which makes the isolation of viable ECFCs technically challenging, especially since the number of available cells from clinical chorionic villus sampling (CVS) specimens is limited[40,41]. Flow cytometry sorting is one method that has been used to isolate subpopulations from mixed cells and tissues. However, the viability of flow cytometry-sorted cells is predominantly low, making it unfeasible to obtain large numbers of cells from limited amounts of tissue[41] for any *in utero* autologous fetal therapy. Hence, to isolate a viable and expandable purified population of endothelial progenitor cells (CV-ECFCs), we first utilized CD31 magnetic bead sorting, which resulted in two distinct populations of cells with high proliferative potential. One population had an endothelial progenitor cobble-stone like morphology and co-expressed CD31 and CD34, and are therefore most likely CV-ECFCs. The second population had a mesenchymal spindle shape morphology, and unlike PMSCs that are CD31-negative, these cells co-expressed CD31 and CD90. These cells had a higher proliferative capacity compared to CV-ECFCs, and when co-existing with CV-ECFCs, they outnumber CV-ECFCs. This observation was consistent with the findings of Rapp *et al*[42], where they isolated and cultured ECFCs from term placentas. The recent study showed the presence of bipotent progenitor cells in term placenta, where the CD31^{Lo} population differentiated into both endothelial and mesenchymal colonies[40]. Hence, CD31/CD90-double positive cells, with the mesenchymal phenotype in our isolation method, could be these bipotential progenitor cells. In addition, according to our previous study, PMSCs could transform into the mesenchymal phenotype and undergo growth arrest when they were co-cultured[20]. Studies have reported that TGF-β can promote the endothelial-to-mesenchymal transition process to make endothelial cells gain a mesenchymal phenotype and induce growth arrest[43,44]. Therefore, we added TGF-β inhibitor to the ECGM-MV2 medium to maintain the

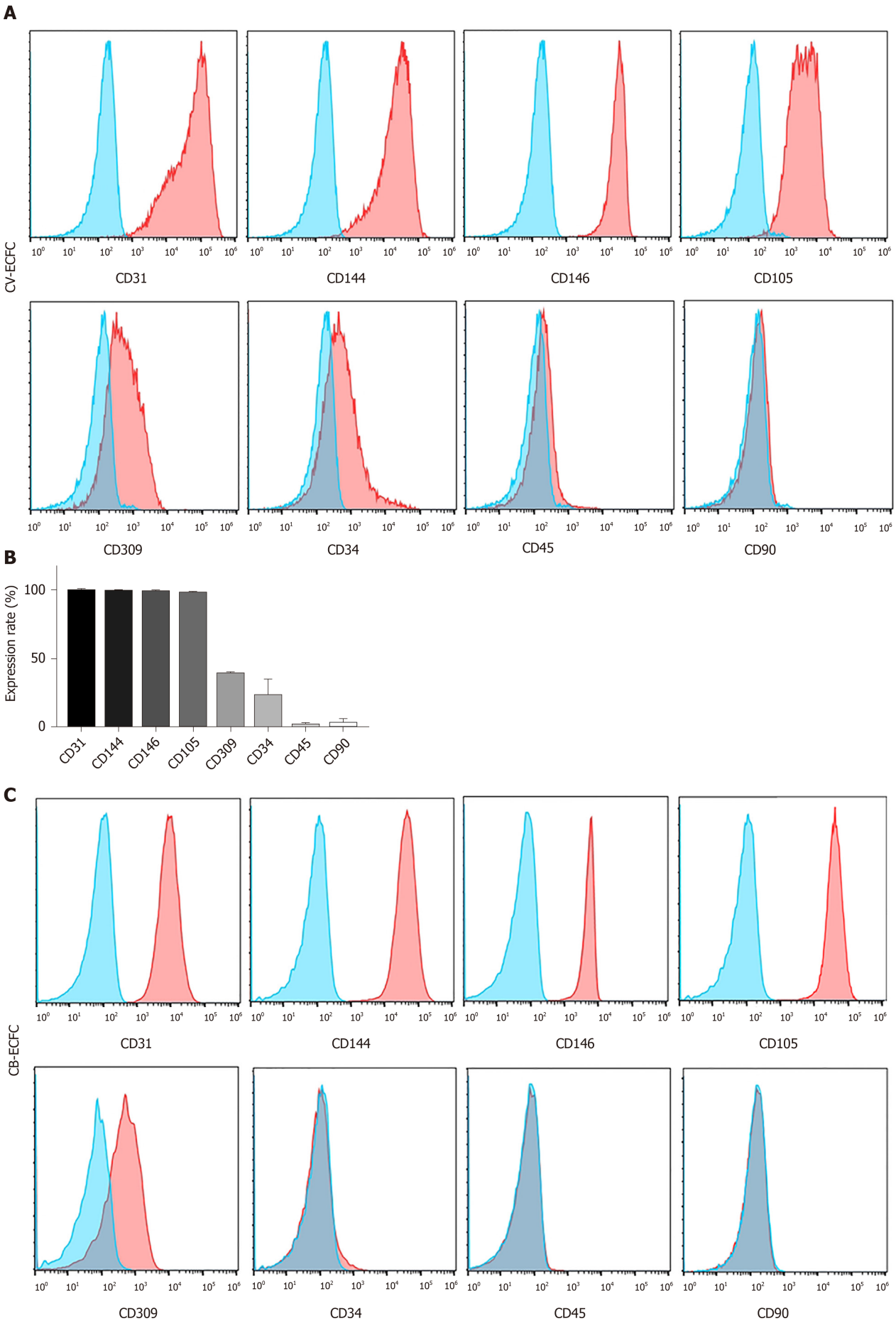
A
CV-ECFC
CD31
CD144
CD146
CD105
CD309
CD34
CD45
CD90
B
Expression rate (%)
100
50
0
CD31
CD144
CD146
CD105
CD309
CD34
CD45
CD90
C
CB-ECFC
CD31
CD144
CD146
CD105
CD309
CD34
CD45
CD90

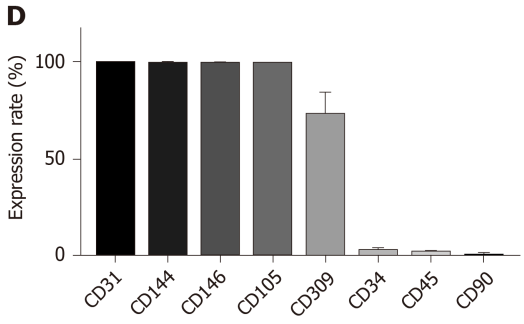

Figure 3 Chorionic villi-derived endothelial colony-forming cells express typical endothelial surface markers, similar to cord blood-derived endothelial colony-forming cells. A: Flow cytometry immunophenotypic analyses demonstrate that chorionic villus endothelial colony-forming cells were positive for the endothelial markers CD31, CD144, CD146, CD105, CD309, low expression of CD34, and were negative for the hematopoietic and MSC markers CD45 and CD90, respectively; B: Quantification of the markers; C and D: Flow cytometry immunophenotypic analysis of the surface marker of cord blood-derived endothelial colony-forming cells. Data are expressed as mean ± SD, $n = 3$.

endothelial cell phenotype. Due to the above reasoning, in order to separate these two cell populations, we picked colonies manually based on their morphology. The expanded cells were further characterized for surface expression of endothelial markers, leading to a pure ECFC cell line that was obtained within 8 wk of culture.

One key element of developing well-vascularized, viable regenerative therapeutics is the incorporation of autologous or allogeneic endothelial cells or endothelial progenitor cells derived from various tissue sources to the therapeutic modality or construct. This strategy has been widely used in treating vasculogenesis and/or angiogenesis-related diseases and conditions such as heart failure, acute kidney injury, stroke and wound healing[45-48]. CB-ECFCs are a good source of postnatal treatments, but cannot be used as an autologous cell source for fetal treatments. In this study, we developed a protocol to derive CV-ECFCs from early gestation placentas that could potentially be used as an autologous source of cells for fetal treatment. Our approach allows one to obtain CV-ECFCs from small amounts of tissue (about 100 mg), which is similar to the size of clinical CVS specimens. This method can also be applicable to large-scale expansion and banking of CV-ECFCs from large or whole placental tissue. CV-ECFCs are similar to CB-ECFCs with respect to cell phenotype, *in vitro* tube-forming capability, transducibility, and compatibility with biomaterial scaffolds. Compared with CB-ECFCs, the CV-ECFCs we isolated express higher levels of the stem cell marker CD34, which likely correlates with a more primitive function and therapeutic capacity. Finally, in combination with the current fetal surgery techniques, these cells hold promise as a novel autologous and/or allogeneic regenerative treatment for congenital anomalies or defects. Further *in vivo* functional evaluation of these cells is warranted.

In summary, we established a CD31 magnetic sorting-assisted approach to isolate clonal CV-ECFCs from human early gestation placentas that hold promise to be used as an autologous cell source for fetal treatment of congenital anomalies or defects.

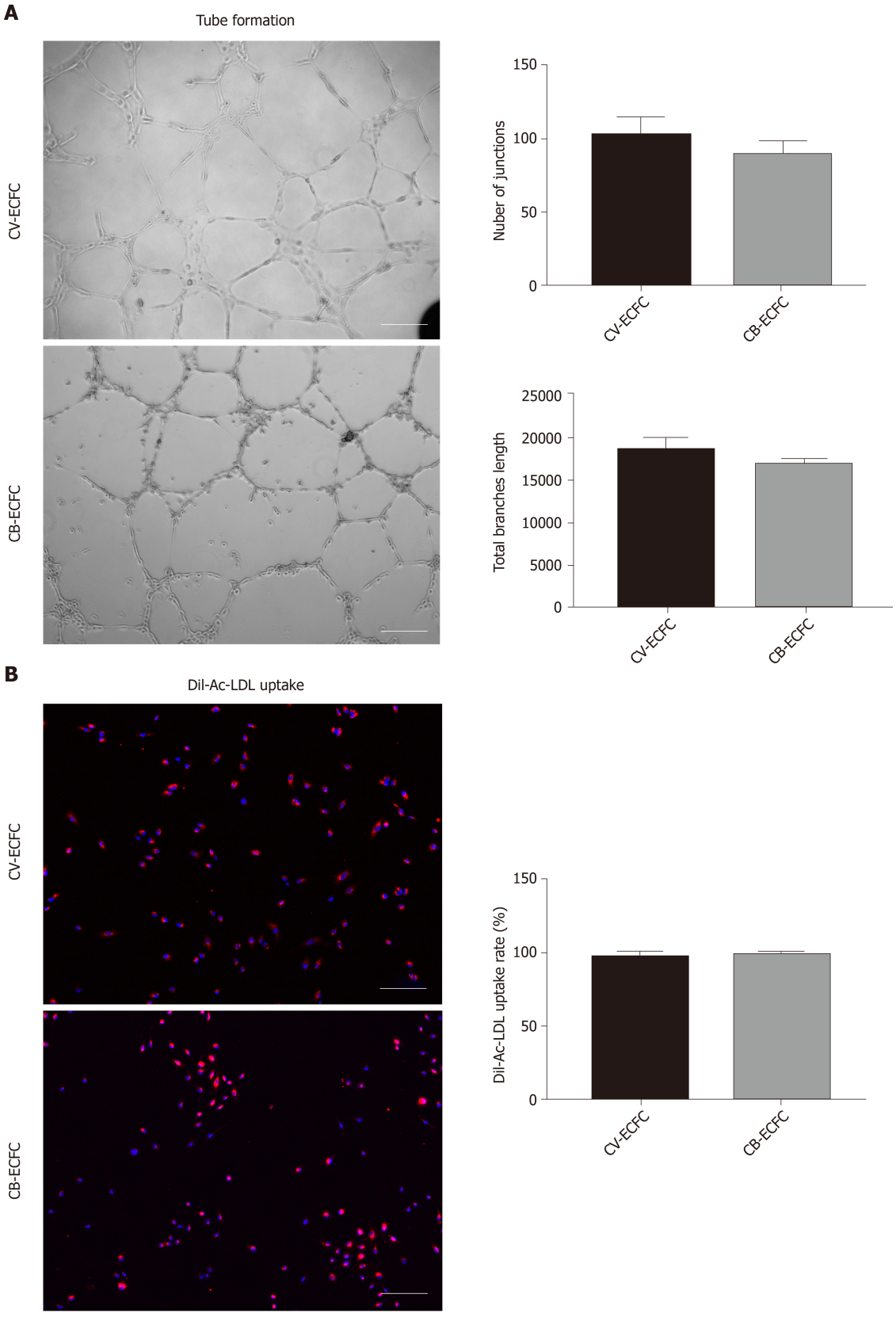

Figure 4 Chorionic villus endothelial colony-forming cells have endothelial functions. A: Representative phase-contrast images of chorionic villus endothelial colony-forming cells (CV-ECFCs), cord blood-derived ECFCs (CB-ECFCs) tube formation assay, and quantification of junction numbers and total branch lengths. There is no difference between CV-ECFCs and CB-ECFCs; B: Representative images for DiI-Ac-LDL uptake by CV-ECFCs and CB-ECFCs. There is no difference in their respective uptake rates. Data are expressed as mean ± SD, n = 3, Scale bar = 100 μm.

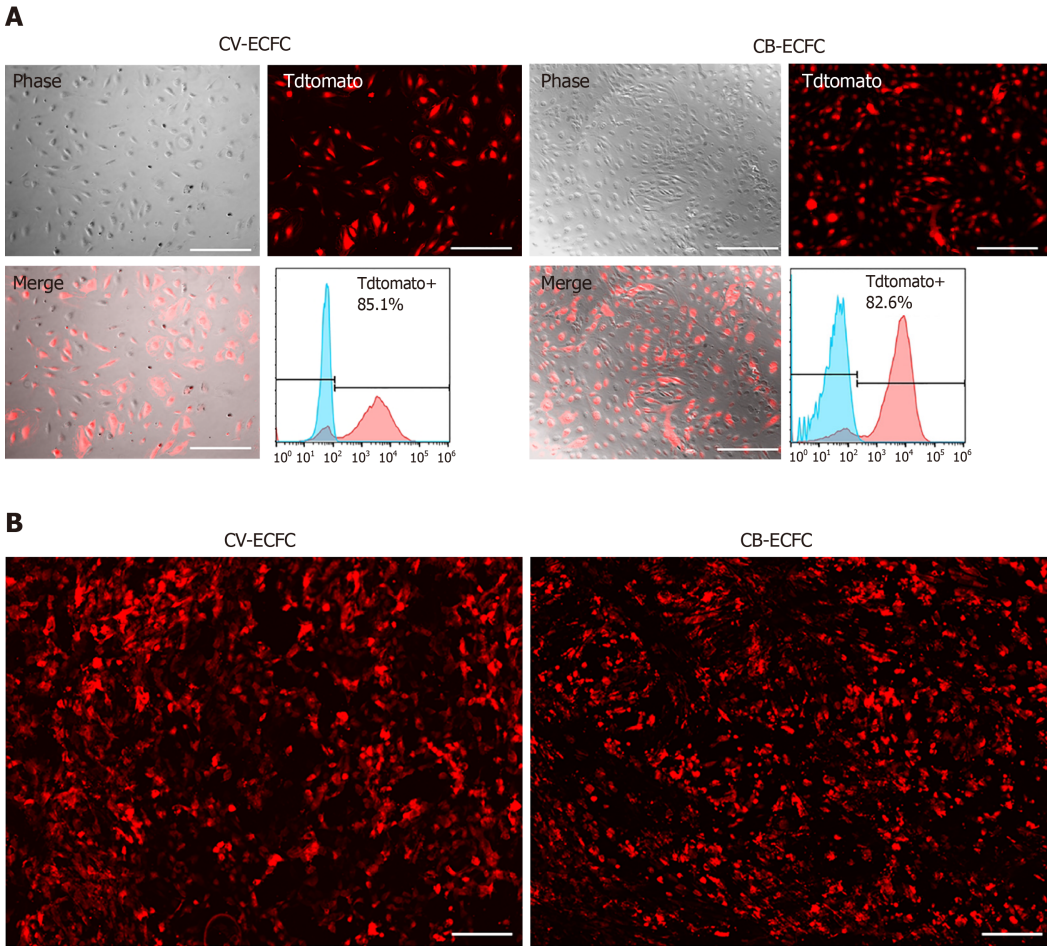

Figure 5 Chorionic villus endothelial colony-forming cells can be transduced by lentiviral vector and are compatible with a small intestinal submucosa scaffold. A: Representative images of chorionic villus endothelial colony-forming cells (CV-ECFCs) and cord blood-derived ECFCs (CB-ECFCs) transduced with a pCCLc-MNDU3-LUC-PGK-Tomato-WPRE lentiviral vector. Flow cytometric analysis showed a transduction rate of 85.1% and 82.8%, respectively; B: tdTomato lentiviral vector-transduced CV-ECFCs (left panel) and CB-ECFCs (right panel) seeded onto a small intestinal submucosa extracellular matrix scaffold, showing adherence. Scale bar = 100 μm.

ARTICLE HIGHLIGHTS

Research background

Fetal medicine and fetal surgery have been substantially developed for the treatment of congenital defects. Stem cell transplantation is an important means of tissue reconstruction and repair of genetic defects. Endothelial colony-forming cells (ECFCs) represent a promising cell candidate for their unique role in facilitating the formation of angiogenesis and vascularization.

Research motivation

ECFCs isolated from the chorionic villus tissue of early gestation placentas can serve as a source of cells for prenatal autologous fetal cell transplantation, as well as provide a basis for studying the development, physiological function, congenital disease, and fetal treatment of the developing fetus and placenta.

Research objectives

The objective of this study is to establish an isolation protocol to obtain ECFCs from the chorionic villus of human early gestation placentas, as well as to investigate the characterization of these cells and their potential applications in gene delivery and tissue engineering.

Research methods

Dissected chorionic villus tissues were enzymatically digested to obtain single cells. Then, magnetic bead sorting, monoclonal culture and colony isolation were performed to obtain chorionic villi-derived ECFCs (CV-ECFCs). Immunohistochemical identification, flow cytometry, Matrigel tube formation assays, LDL uptake assays and lentiviral transduction were carried out to characterize the morphology, phenotype and function of the purified and expanded CV-ECFCs.

Research results

Using the established isolation protocol, we were able to obtain 1.8×10^7 pure CV-ECFCs from a single cell colony culture within 6-8 wks. CV-ECFCs showed typical endothelial phenotypes and functions. CV-ECFCs have demonstrated the ability to be transduced with lentiviruses, and function as carriers for gene therapy. They also possess good biocompatibility with biomaterial delivery vehicles, such as small intestinal submucosa extracellular matrix for potential tissue engineering applications.

Research conclusions

This study shows that ECFCs are present in early gestation placental chorionic villi, and can be isolated and expanded to a significant number in a short period of time. These CV-ECFCs possess typical endothelial cell phenotypes and functions, and hold the potential of being used in gene therapy and tissue engineering applications.

Research perspectives

CV-ECFCs isolated from early gestation placentas provide a new source of ECFCs for the fetal treatment of congenital disorders. Combined with existing *in utero* treatment technologies, this cell therapy could be widely applied toward a variety of diseases and conditions. In future research, we will further explore the *in vivo* applications of these cells in various animal models. Investigating the phenotype and functions of CV-ECFCs will also facilitate our understanding of the development, cellular composition, and function of the developing placenta and its interaction with the developing fetus.

ACKNOWLEDGEMENTS

The authors thank Cook Biotech Inc. for generously providing us with the ECM material. We acknowledge Alexandra Maria Iavorovschi for the help with manuscript editing.

REFERENCES

1 **Deprest JA**, Flake AW, Gratacos E, Ville Y, Hecher K, Nicolaides K, Johnson MP, Luks FI, Adzick NS, Harrison MR. The making of fetal surgery. *Prenat Diagn* 2010; **30**: 653-667 [PMID: 20572114 DOI: 10.1002/pd.2571]
2 **Harrison MR**. The University of California at San Francisco Fetal Treatment Center: a personal perspective. *Fetal Diagn Ther* 2004; **19**: 513-524 [PMID: 15539877 DOI: 10.1159/000080165]
3 **Wang A**, Brown EG, Lankford L, Keller BA, Pivetti CD, Sitkin NA, Beattie MS, Bresnahan JC, Farmer DL. Placental mesenchymal stromal cells rescue ambulation in ovine myelomeningocele. *Stem Cells Transl Med* 2015; **4**: 659-669 [PMID: 25911465 DOI: 10.5966/sctm.2014-0296]
4 **Kumar P**, Gao K, Wang C, Pivetti C, Lankford L, Farmer D, Wang A. In Utero Transplantation of Placenta-Derived Mesenchymal Stromal Cells for Potential Fetal Treatment of Hemophilia A. *Cell Transplant* 2018; **27**: 130-139 [PMID: 29562772 DOI: 10.1177/0963689717728937]
5 **Porada CD**, Rodman C, Ignacio G, Atala A, Almeida-Porada G. Hemophilia A: an ideal disease to correct in utero. *Front Pharmacol* 2014; **5**: 276 [PMID: 25566073 DOI: 10.3389/fphar.2014.00276]
6 **Koppanati BM**, Li J, Reay DP, Wang B, Daood M, Zheng H, Xiao X, Watchko JF, Clemens PR. Improvement of the mdx mouse dystrophic phenotype by systemic in utero AAV8 delivery of a minidystrophin gene. *Gene Ther* 2010; **17**: 1355-1362 [PMID: 20535217 DOI: 10.1038/gt.2010.84]
7 **Keswani SG**, Balaji S, Le L, Leung A, Katz AB, Lim FY, Habli M, Jones HN, Wilson JM, Crombleholme TM. Pseudotyped AAV vector-mediated gene transfer in a human fetal trachea xenograft model: implications for in utero gene therapy for cystic fibrosis. *PLoS One* 2012; **7**: e43633 [PMID: 22937069 DOI: 10.1371/journal.pone.0043633]
8 **Conese M**, Ascenzioni F, Boyd AC, Coutelle C, De Fino I, De Smedt S, Rejman J, Rosenecker J, Schindelhauer D, Scholte BJ. Gene and cell therapy for cystic fibrosis: from bench to bedside. *J Cyst Fibros* 2011; **10** Suppl 2: S114-S128 [PMID: 21658631 DOI: 10.1016/S1569-1993(11)60017-9]
9 **Kabagambe S**, Keller B, Becker J, Goodman L, Pivetti C, Lankford L, Chung K, Lee C, Chen YJ, Kumar P, Vanover M, Wang A, Farmer D. Placental mesenchymal stromal cells seeded on clinical grade extracellular matrix improve ambulation in ovine myelomeningocele. *J Pediatr Surg* 2017 [PMID: 29122293 DOI: 10.1016/j.jpedsurg.2017.10.032]
10 **Vanover M**, Pivetti C, Lankford L, Kumar P, Galganski L, Kabagambe S, Keller B, Becker J, Chen YJ, Chung K, Lee C, Paxton Z, Deal B, Goodman L, Anderson J, Jensen G, Wang A, Farmer D. High density placental mesenchymal stromal cells provide neuronal preservation and improve motor function following in utero treatment of ovine myelomeningocele. *J Pediatr Surg* 2019; **54**: 75-79 [PMID: 30529115 DOI: 10.1016/j.jpedsurg.2018.10.032]
11 **Chen YJ**, Chung K, Pivetti C, Lankford L, Kabagambe SK, Vanover M, Becker J, Lee C, Tsang J, Wang A, Farmer DL. Fetal surgical repair with placenta-derived mesenchymal stromal cell engineered patch in a rodent model of myelomeningocele. *J Pediatr Surg* 2017 [PMID: 29096888 DOI: 10.1016/j.jpedsurg.2017.10.040]
12 **Lankford L**, Selby T, Becker J, Ryzhuk V, Long C, Farmer D, Wang A. Early gestation chorionic villi-derived stromal cells for fetal tissue engineering. *World J Stem Cells* 2015; **7**: 195-207 [PMID: 25621120 DOI: 10.4252/wjsc.v7.i1.195]
13 **Pittenger M**. Sleuthing the source of regeneration by MSCs. *Cell Stem Cell* 2009; **5**: 8-10 [PMID: 19570508 DOI: 10.1016/j.stem.2009.06.013]
14 **Caplan AI**, Correa D. The MSC: an injury drugstore. *Cell Stem Cell* 2011; **9**: 11-15 [PMID: 21726829 DOI: 10.1016/j.stem.2011.06.008]
15 **Cheng ZJ**, He XJ. Anti-inflammatory effect of stem cells against spinal cord injury via regulating

macrophage polarization. *J Neurorestoratology* 2017; **5**: 31-38 [DOI: 10.2147/JN.S115696]
16 **Shi Zj**, Huang HY, Feng SQ. Stem cell-based therapies to treat spinal cord injury: A review. *J Neurorestoratology* 2017; **5**: 125-131 [DOI: 10.2147/JN.S139677]
17 **Zhang ZR**, Wang FY, Song MJ. The cell repair research of spinal cord injury: A review of cell transplantation to treat spinal cord injury. *J Neurorestoratology* 2019; **7**: 55-62 [DOI: 10.26599/JNR.2019.9040011]
18 **Denost Q**, Adam JP, Pontallier A, Montembault A, Bareille R, Siadous R, Delmond S, Rullier E, David L, Bordenave L. Colorectal tissue engineering: A comparative study between porcine small intestinal submucosa (SIS) and chitosan hydrogel patches. *Surgery* 2015; **158**: 1714-1723 [PMID: 26275832 DOI: 10.1016/j.surg.2015.06.040]
19 **Lankford L**, Chen YJ, Saenz Z, Kumar P, Long C, Farmer D, Wang A. Manufacture and preparation of human placenta-derived mesenchymal stromal cells for local tissue delivery. *Cytotherapy* 2017; **19**: 680-688 [PMID: 28438482 DOI: 10.1016/j.jcyt.2017.03.003]
20 **Gao K**, Kumar P, Cortez-Toledo E, Hao D, Reynaga L, Rose M, Wang C, Farmer D, Nolta J, Zhou J, Zhou P, Wang A. Potential long-term treatment of hemophilia A by neonatal co-transplantation of cord blood-derived endothelial colony-forming cells and placental mesenchymal stromal cells. *Stem Cell Res Ther* 2019; **10**: 34 [PMID: 30670078 DOI: 10.1186/s13287-019-1138-8]
21 **Zygmunt M**, Herr F, Münstedt K, Lang U, Liang OD. Angiogenesis and vasculogenesis in pregnancy. *Eur J Obstet Gynecol Reprod Biol* 2003; **110** Suppl 1: S10-S18 [PMID: 12965086 DOI: 10.1016/S0301-2115(03)00168-4]
22 **Medina RJ**, Barber CL, Sabatier F, Dignat-George F, Melero-Martin JM, Khosrotehrani K, Ohneda O, Randi AM, Chan JKY, Yamaguchi T, Van Hinsbergh VWM, Yoder MC, Stitt AW. Endothelial Progenitors: A Consensus Statement on Nomenclature. *Stem Cells Transl Med* 2017; **6**: 1316-1320 [PMID: 28296182 DOI: 10.1002/sctm.16-0360]
23 **Yu S**, Li Z, Zhang W, Du Z, Liu K, Yang D, Gong S. Isolation and characterization of endothelial colony-forming cells from mononuclear cells of rat bone marrow. *Exp Cell Res* 2018; **370**: 116-126 [PMID: 29908162 DOI: 10.1016/j.yexcr.2018.06.013]
24 **Szöke K**, Reinisch A, Østrup E, Reinholt FP, Brinchmann JE. Autologous cell sources in therapeutic vasculogenesis: In vitro and in vivo comparison of endothelial colony-forming cells from peripheral blood and endothelial cells isolated from adipose tissue. *Cytotherapy* 2016; **18**: 242-252 [PMID: 26669908 DOI: 10.1016/j.jcyt.2015.10.009]
25 **Kolbe M**, Dohle E, Katerla D, Kirkpatrick CJ, Fuchs S. Enrichment of outgrowth endothelial cells in high and low colony-forming cultures from peripheral blood progenitors. *Tissue Eng Part C Methods* 2010; **16**: 877-886 [PMID: 19891540 DOI: 10.1089/ten.TEC.2009.0492]
26 **Zhang H**, Tao Y, Ren S, Liu H, Zhou H, Hu J, Tang Y, Zhang B, Chen H. Isolation and characterization of human umbilical cord-derived endothelial colony-forming cells. *Exp Ther Med* 2017; **14**: 4160-4166 [PMID: 29067104 DOI: 10.3892/etm.2017.5035]
27 **Shafiee A**, Patel J, Lee JS, Hutmacher DW, Fisk NM, Khosrotehrani K. Mesenchymal stem/stromal cells enhance engraftment, vasculogenic and pro-angiogenic activities of endothelial colony forming cells in immunocompetent hosts. *Sci Rep* 2017; **7**: 13558 [PMID: 29051567 DOI: 10.1038/s41598-017-13971-3]
28 **Drake CJ**. Embryonic and adult vasculogenesis. *Birth Defects Res C Embryo Today* 2003; **69**: 73-82 [PMID: 12768659 DOI: 10.1002/bdrc.10003]
29 **Tahergorabi Z**, Khazaei M. A review on angiogenesis and its assays. *Iran J Basic Med Sci* 2012; **15**: 1110-1126 [PMID: 23653839]
30 **Hao D**, Xiao W, Liu R, Kumar P, Li Y, Zhou P, Guo F, Farmer DL, Lam KS, Wang F, Wang A. Discovery and Characterization of a Potent and Specific Peptide Ligand Targeting Endothelial Progenitor Cells and Endothelial Cells for Tissue Regeneration. *ACS Chem Biol* 2017; **12**: 1075-1086 [PMID: 28195700 DOI: 10.1021/acschembio.7b00118]
31 **Novosel EC**, Kleinhans C, Kluger PJ. Vascularization is the key challenge in tissue engineering. *Adv Drug Deliv Rev* 2011; **63**: 300-311 [PMID: 21396416 DOI: 10.1016/j.addr.2011.03.004]
32 **Böttcher-Haberzeth S**, Biedermann T, Reichmann E. Tissue engineering of skin. *Burns* 2010; **36**: 450-460 [PMID: 20022702 DOI: 10.1016/j.burns.2009.08.016]
33 **Lin Y**, Chang L, Solovey A, Healey JF, Lollar P, Hebbel RP. Use of blood outgrowth endothelial cells for gene therapy for hemophilia A. *Blood* 2002; **99**: 457-462 [PMID: 11781225 DOI: 10.1182/blood.v99.2.457]
34 **Almeida-Porada G**, Atala A, Porada CD. In utero stem cell transplantation and gene therapy: rationale, history, and recent advances toward clinical application. *Mol Ther Methods Clin Dev* 2016; **5**: 16020 [PMID: 27069953 DOI: 10.1038/mtm.2016.20]
35 **Robin C**, Bollerot K, Mendes S, Haak E, Crisan M, Cerisoli F, Lauw I, Kaimakis P, Jorna R, Vermeulen M, Kayser M, van der Linden R, Imanirad P, Verstegen M, Nawaz-Yousaf H, Papazian N, Steegers E, Cupedo T, Dzierzak E. Human placenta is a potent hematopoietic niche containing hematopoietic stem and progenitor cells throughout development. *Cell Stem Cell* 2009; **5**: 385-395 [PMID: 19796619 DOI: 10.1016/j.stem.2009.08.020]
36 **Crisan M**, Yap S, Casteilla L, Chen CW, Corselli M, Park TS, Andriolo G, Sun B, Zheng B, Zhang L, Norotte C, Teng PN, Traas J, Schugar R, Deasy BM, Badylak S, Buhring HJ, Giacobino JP, Lazzari L, Huard J, Péault B. A perivascular origin for mesenchymal stem cells in multiple human organs. *Cell Stem Cell* 2008; **3**: 301-313 [PMID: 18786417 DOI: 10.1016/j.stem.2008.07.003]
37 **Parolini O**, Alviano F, Bagnara GP, Bilic G, Bühring HJ, Evangelista M, Hennerbichler S, Liu B, Magatti M, Mao N, Miki T, Marongiu F, Nakajima H, Nikaido T, Portmann-Lanz CB, Sankar V, Soncini M, Stadler G, Surbek D, Takahashi TA, Redl H, Sakuragawa N, Wolbank S, Zeisberger S, Zisch A, Strom SC. Concise review: isolation and characterization of cells from human term placenta: outcome of the first international Workshop on Placenta Derived Stem Cells. *Stem Cells* 2008; **26**: 300-311 [PMID: 17975221 DOI: 10.1634/stemcells.2007-0594]
38 **Patel J**, Seppanen E, Chong MS, Yeo JS, Teo EY, Chan JK, Fisk NM, Khosrotehrani K. Prospective surface marker-based isolation and expansion of fetal endothelial colony-forming cells from human term placenta. *Stem Cells Transl Med* 2013; **2**: 839-847 [PMID: 24106336 DOI: 10.5966/sctm.2013-0092]
39 **Solomon I**, O'Reilly M, Ionescu L, Alphonse RS, Rajabali S, Zhong S, Vadivel A, Shelley WC, Yoder MC, Thébaud B. Functional Differences Between Placental Micro- and Macrovascular Endothelial Colony-Forming Cells. *Stem Cells Transl Med* 2016; **5**: 291-300 [PMID: 26819255 DOI: 10.5966/sctm.2014-0162]
40 **Shafiee A**, Patel J, Hutmacher DW, Fisk NM, Khosrotehrani K. Meso-Endothelial Bipotent Progenitors

from Human Placenta Display Distinct Molecular and Cellular Identity. *Stem Cell Reports* 2018; **10**: 890-904 [PMID: 29478891 DOI: 10.1016/j.stemcr.2018.01.011]

41 **Gumina DL**, Su EJ. Endothelial Progenitor Cells of the Human Placenta and Fetoplacental Circulation: A Potential Link to Fetal, Neonatal, and Long-term Health. *Front Pediatr* 2017; **5**: 41 [PMID: 28361046 DOI: 10.3389/fped.2017.00041]

42 **Rapp BM**, Saadatzedeh MR, Ofstein RH, Bhavsar JR, Tempel ZS, Moreno O, Morone P, Booth DA, Traktuev DO, Dalsing MC, Ingram DA, Yoder MC, March KL, Murphy MP. Resident Endothelial Progenitor Cells From Human Placenta Have Greater Vasculogenic Potential Than Circulating Endothelial Progenitor Cells From Umbilical Cord Blood. *Cell Med* 2012; **2**: 85-96 [PMID: 27004134 DOI: 10.3727/215517911X617888]

43 **Cooley BC**, Nevado J, Mellad J, Yang D, St Hilaire C, Negro A, Fang F, Chen G, San H, Walts AD, Schwartzbeck RL, Taylor B, Lanzer JD, Wragg A, Elagha A, Beltran LE, Berry C, Feil R, Virmani R, Ladich E, Kovacic JC, Boehm M. TGF-β signaling mediates endothelial-to-mesenchymal transition (EndMT) during vein graft remodeling. *Sci Transl Med* 2014; **6**: 227ra34 [PMID: 24622514 DOI: 10.1126/scitranslmed.3006927]

44 **Heldin CH**, Landström M, Moustakas A. Mechanism of TGF-beta signaling to growth arrest, apoptosis, and epithelial-mesenchymal transition. *Curr Opin Cell Biol* 2009; **21**: 166-176 [PMID: 19237272 DOI: 10.1016/j.ceb.2009.01.021]

45 **Kim JY**, Song SH, Kim KL, Ko JJ, Im JE, Yie SW, Ahn YK, Kim DK, Suh W. Human cord blood-derived endothelial progenitor cells and their conditioned media exhibit therapeutic equivalence for diabetic wound healing. *Cell Transplant* 2010; **19**: 1635-1644 [PMID: 20659357 DOI: 10.3727/096368910X516637]

46 **Yerebakan C**, Sandica E, Prietz S, Klopsch C, Ugurlucan M, Kaminski A, Abdija S, Lorenzen B, Boltze J, Nitzsche B, Egger D, Barten M, Furlani D, Ma N, Vollmar B, Liebold A, Steinhoff G. Autologous umbilical cord blood mononuclear cell transplantation preserves right ventricular function in a novel model of chronic right ventricular volume overload. *Cell Transplant* 2009; **18**: 855-868 [PMID: 19500473 DOI: 10.3727/096368909X471170]

47 **Burger D**, Viñas JL, Akbari S, Dehak H, Knoll W, Gutsol A, Carter A, Touyz RM, Allan DS, Burns KD. Human endothelial colony-forming cells protect against acute kidney injury: role of exosomes. *Am J Pathol* 2015; **185**: 2309-2323 [PMID: 26073035 DOI: 10.1016/j.ajpath.2015.04.010]

48 **Li YF**, Ren LN, Guo G, Cannella LA, Chernaya V, Samuel S, Liu SX, Wang H, Yang XF. Endothelial progenitor cells in ischemic stroke: an exploration from hypothesis to therapy. *J Hematol Oncol* 2015; **8**: 33 [PMID: 25888494 DOI: 10.1186/s13045-015-0130-8]

World Journal of Stem Cells

Submit a Manuscript: https://www.f6publishing.com

World J Stem Cells 2020 February 26; 12(2): 139-151

DOI: 10.4252/wjsc.v12.i2.139

ISSN 1948-0210 (online)

ORIGINAL ARTICLE

Basic Study

Comparison between the therapeutic effects of differentiated and undifferentiated Wharton's jelly mesenchymal stem cells in rats with streptozotocin-induced diabetes

Chen-Yuan Hsiao, Tien-Hua Chen, Ben-Shian Huang, Po-Han Chen, Cheng-Hsi Su, Jia-Fwu Shyu, Pei-Jiun Tsai

ORCID number: Chen-Yuan Hsiao (0000-0001-7334-526X); Tien-Hua Chen (0000-0002-4622-2421); Ben-Shian Huang (0000-0003-2838-6315); Po-Han Chen (0000-0003-3893-1639); Cheng-Hsi Su (0000-0001-8629-1651); Jia-Fwu Shyu (0000-0002-1594-4675); Pei-Jiun Tsai (0000-0003-0177-4713).

Author contributions: All authors participated in various aspects of the study and to the development of the report; Chen PH, Shyu JF, and Tsai PJ designed and performed all of the *in vitro* experiments; Hsiao CY, Chen TH, Huang BS, Su CH, and Tsai PJ designed and performed all of the animal experiments; Hsiao CY, Chen TH, Shyu JF, and Tsai PJ analyzed the statistical work and wrote the manuscript; Shyu JF and Tsai PJ contributed equally to this work; All authors reviewed and approved the manuscript.

Supported by Taipei Veterans General Hospital, No. V106B-024; Yen Tjing Ling Medical Foundation, No. CI-106-20; Cheng Hsin General Hospital, No. CY10716; Taiwan Ministry of Science and Technology, No. MOST 105-2314-B-010-010-MY3 and No. MOST 106-2314-B-010-009.

Institutional review board statement: The study was reviewed and approved by the Taipei Veterans General Hospital Institutional Review Board (2018-02-008BC).

Chen-Yuan Hsiao, Graduate Institute of Medical Sciences, National Defense Medical Center, Taipei 114, Taiwan

Chen-Yuan Hsiao, Department of Surgery, Landseed International Hospital, Taoyuan 324, Taiwan

Tien-Hua Chen, Po-Han Chen, Pei-Jiun Tsai, Institute of Anatomy and Cell Biology, School of Medicine, National Yang Ming University, Taipei 112, Taiwan

Tien-Hua Chen, Pei-Jiun Tsai, Trauma Center, Department of Surgery, Veterans General Hospital, Taipei 112, Taiwan

Tien-Hua Chen, Division of General Surgery, Department of Surgery, Veterans General Hospital, Taipei 112, Taiwan

Ben-Shian Huang, Department of Obstetrics and Gynecology, Veterans General Hospital, Taipei 112, Taiwan

Cheng-Hsi Su, Department of Surgery, Cheng Hsin General Hospital, Taipei 112, Taiwan

Jia-Fwu Shyu, Department of Biology and Anatomy, National Defense Medical Center, Taipei 114, Taiwan

Pei-Jiun Tsai, Department of Critical Care Medicine, Veterans General Hospital, Taipei 112, Taiwan

Corresponding author: Pei-Jiun Tsai, MD, PhD, Assistant Professor, Institute of Anatomy and Cell Biology, School of Medicine, National Yang Ming University, 201 Shih-Pai Road Section 2, Taipei 112, Taiwan. pjtsai@vghtpe.gov.tw

Abstract

BACKGROUND

Despite the availability of current therapies, including oral antidiabetic drugs and insulin, for controlling the symptoms caused by high blood glucose, it is difficult to cure diabetes mellitus, especially type 1 diabetes mellitus.

AIM

Cell therapies using mesenchymal stem cells (MSCs) may be a promising option. However, the therapeutic mechanisms by which MSCs exert their effects, such as

Institutional animal care and use committee statement: All procedures involving animals were reviewed and approved by the Institutional Animal Care and Use Committee of the Taipei Veterans General Hospital (IACUC protocol number: 2017-055).

Informed consent statement: All study participants, or their legal guardian, provided informed written consent prior to study enrollment.

Conflict-of-interest statement: There is no conflict of interest associated with any of the senior author or other coauthors contributed their efforts in this manuscript. All the Authors have no conflict of interest related to the manuscript.

Data sharing statement: Technical appendix, statistical code, and dataset available from the corresponding author at (pjtsai@vghtpe.gov.tw). No additional data are available.

ARRIVE guidelines statement: The authors have read the ARRIVE guidelines, and the manuscript was prepared and revised according to the ARRIVE guidelines.

Manuscript source: Unsolicited manuscript

Received: August 27, 2019
Peer-review started: August 27, 2019
First decision: October 19, 2019
Revised: December 27, 2019
Accepted: January 6, 2020
Article in press: January 6, 2020
Published online: February 26, 2020

P-Reviewer: Elhamid SA, Koch T, Nagahara H
S-Editor: Zhang L
L-Editor: Filipodia
E-Editor: Qi LL

whether they can differentiate into insulin-producing cells (IPCs) before transplantation, are uncertain.

METHODS
In this study, we used three types of differentiation media over 10 d to generate IPCs from human Wharton's jelly MSCs (hWJ-MSCs). We further transplanted the undifferentiated hWJ-MSCs and differentiated IPCs derived from them into the portal vein of rats with streptozotocin-induced diabetes, and recorded the physiological and pathological changes.

RESULTS
Using fluorescent staining and C-peptide enzyme-linked immunoassay, we were able to successfully induce the differentiation of hWJ-MSCs into IPCs. Transplantation of both IPCs derived from hWJ-MSCs and undifferentiated hWJ-MSCs had the therapeutic effect of ameliorating blood glucose levels and improving intraperitoneal glucose tolerance tests. The transplanted IPCs homed to the pancreas and functionally survived for at least 8 wk after transplantation, whereas the undifferentiated hWJ-MSCs were able to improve the insulitis and ameliorate the serum inflammatory cytokine in streptozotocin-induced diabetic rats.

CONCLUSION
Differentiated IPCs can significantly improve blood glucose levels in diabetic rats due to the continuous secretion of insulin by transplanted cells that survive in the islets of diabetic rats. Transplantation of undifferentiated hWJ-MSCs can significantly improve insulitis and re-balance the inflammatory condition in diabetic rats with only a slight improvement in blood glucose levels.

Key words: Human Wharton's jelly mesenchymal stem cell; Insulin-producing cells; Diabetes mellitus; Differentiation; Regeneration therapy; Anti-inflammatory

Core tip: The therapeutic mechanism of differentiated and undifferentiated human Wharton's jelly mesenchymal stem cells in streptozotocin-induced diabetic rats may differ. Differentiated insulin-producing cells can significantly improve blood glucose levels due to continuously secretion insulin by the transplanted cells that survive in the islets of diabetic rats. Transplantation of undifferentiated human Wharton's jelly mesenchymal stem cells can significantly improve insulitis and re-balance the inflammatory condition with only a slight improvement in blood glucose levels. The results of this study will provide basic and essential information for future application of cell regenerative therapy in diabetic patients.

Citation: Hsiao CY, Chen TH, Huang BS, Chen PH, Su CH, Shyu JF, Tsai PJ. Comparison between the therapeutic effects of differentiated and undifferentiated Wharton's jelly mesenchymal stem cells in rats with streptozotocin-induced diabetes. *World J Stem Cells* 2020; 12(2): 139-151
URL: https://www.wjgnet.com/1948-0210/full/v12/i2/139.htm
DOI: https://dx.doi.org/10.4252/wjsc.v12.i2.139

INTRODUCTION

Diabetes mellitus (DM) is a chronic metabolic disease in which the primary disturbance is an inappropriately high blood glucose level. DM is caused by insufficient insulin secretion or by varying degrees of insulin resistance in tissues. The former is called type 1 diabetes, and the latter is type 2 diabetes. Type 1 diabetes is also known as juvenile-onset DM or insulin-dependent DM and usually develops in childhood or adolescence. Patients with type 1 DM have traditionally been treated with long-term insulin injections to maintain normal blood glucose levels. Insulin injection therapy can only temporarily lower blood glucose levels, and cannot alleviate DM complications such as nephropathy, neuropathy, and retinopathy.

Currently, clinicians have the ability to offer other diabetes treatments, such as islet transplantation or cadaveric whole pancreas transplantation. A shortage of donors, high perioperative risks, and the long-term postoperative need for immunosuppressants are some of the major concerns and challenges of these treatments[1]. Researchers are currently moving towards finding more appropriate and effective medical technologies, such as cell therapy, to cure diabetes.

Stem cells, which are the source of cell therapy, are undifferentiated cells that have the ability of self-renewal and differentiation. There are wide differences between stem cells in what they can achieve, depending on their specific microenvironment. Human mesenchymal stem cells (hMSCs) are a type of multipotent stem cell that can differentiate into mesodermal (*e.g.*, osteocytes, adipocytes and chondrocytes), ectodermal (neurocytes), and endodermal (hepatocytes) lineages[2]. hMSCs were first identified in the bone marrow and subsequently isolated from various tissues including adipose tissue, amniotic fluid, dental tissues, umbilical cord blood, and Wharton's jelly. hMSCs are believed to have immunomodulatory features, which make them an effective tool in the treatment of chronic diseases[3]. Human Wharton's jelly mesenchymal stem cells (hWJ-MSCs), which can be easily obtained from the connective tissue of the umbilical cord, are a type of multipotent MSC that are not prone to spontaneous differentiation when cultured *in vitro*[4]. Compared with embryonic stem cells, the use of hWJ-MSCs does not have ethical concerns. Additionally, these cells are less likely to cause rejection after transplantation and will not cause teratomas *in vivo*[5,6]. Our research team has well studied the characteristics, recognition, and function of hWJ-MSCs and published an article in Stem Cells in 2004[5]. In addition to their ability to improve cardiac function in animal models of acute myocardial infarction[7], treat carbon tetrachloride-induced liver failure in rats[8], reverse pulmonary fibrosis in a bleomycin-induced pulmonary fibrosis rat model[9], and ameliorate mouse spinocerebellar ataxia type 1[10], our research team found that hWJ-MSCs can also restore the hypoglycemic state in diabetic animals[11-13]. However, the therapeutic effects and mechanism of action of hWJ-MSCs, such as whether they differentiate into insulin-producing cells (IPCs) before transplantation, remains unknown. We hypothesized that IPCs differentiated from hWJ-MSCs have a more efficient and curative effect than undifferentiated WJ-MSCs in streptozotocin (STZ)-induced diabetic rats. We first generated IPCs from hWJ-MSCs by using three successive types of differentiation media over 10 d. Subsequently, we transplanted the undifferentiated hWJ-MSCs and differentiated IPCs derived from them into the portal vein of the STZ-induced diabetic rats, and recorded the physiological and pathological changes.

MATERIALS AND METHODS

WJ-MSC culture

All procedures were approved by the Institutional Review Board. The isolation of hWJ-MSCs was conducted as described by Wang *et al*[5]. Briefly, with the written informed consent of the parents, fresh human umbilical cords were obtained after birth and stored in Hank's balanced salt solution (Biological Industries, Beit HaEmek, Israel) prior to tissue processing to obtain MSCs. After the blood vessels were removed, the mesenchymal tissue was scraped off Wharton's jelly and centrifuged at 250 g for 5 min. After centrifugation, the pellets were resuspended in 15 mL serum-free Dulbecco's modified Eagle's medium (DMEM; Gibco, Grand Island, NY, United States) containing 0.2 g/mL collagenase and incubated for 16 h at 37°C. Next, the cells were washed, resuspended in DMEM containing 2.5% trypsin, and incubated for 30 min at 37°C with agitation. Finally, the cells were washed again and cultured in DMEM supplemented with 10% fetal bovine serum (Sigma St. Louis, MO, United States) and glucose (4.5 g/L) in 5% CO_2 in a 37°C incubator.

Differentiation of WJ-MSCs into IPCs

The differentiation protocol followed the steps described in our published article[11]. Briefly, at the fourth passage, after reaching 70% confluence, MSCs were induced to differentiate into IPCs. Differentiation was divided into three stages. Undifferentiated WJ-MSCs were detached by HyQTase, diluted with SFM-A, and centrifuged. Cells were counted for initial seeding density and when they reached 10^6 cells/cm^2, they were resuspended in SFM-A and seeded on ultralow attachment tissue culture plates (Corning, Fisher Scientific International, Hampton, NH, United States). SFM-A contained DMEM/F12 (1:1) (Gibco, Grand Island, NY, United States) with 17.5 mM glucose, 1% fatty acid free BSA Cohn fraction V (Sigma-Aldrich), 1% penicillin/streptomycin/amphoteric B (PSA; Biological Industries), 1X insulin-

transferrin-selenium-X (ITS-X; 5 mg/L insulin, 5 mg/L transferrin, 5 mg/L selenium), 4 nM activin A, 1 mM sodium butyrate, and 50 μM 2-mercaptoethanol. The cells were cultured in this medium for 2 d. On the third day, the culture medium was changed to SFM-B, which contains DMEM/F12 (1:1) with 17.5 mM glucose, 1% BSA, 1% PSA, ITS-X, and 0.3 mM taurine. On the fifth day, the cell culture was replaced by SFM-C, which contained DMEM/F12 (1:1) with 17.5 mM glucose, 1.5% BSA, ITS-X, 1% PSA, 3 mM taurine, 100 nM glucagon-like peptide-1 (amide fragment 7–36; Sigma Aldrich), 1 mM nicotinamide, and 1X nonessential amino acids. For the next 5 d, the culture medium was exchanged with fresh SFM-C every 2 d.

Immunofluorescence staining of IPCs and undifferentiated MSCs

The target cells were seeded in 12-well cell culture plates with a circular coverslip on each well. After 20 min of fixation in 4% paraformaldehyde, primary antibodies were added in 1 × PBS supplemented with 10% goat serum and 0.1% TRITON X-100, and incubated overnight at 4°C. The next day, 0.5% Fluorescein AffiniPure Donkey Anti-Rabbit IgG (H+L) in 1 × PBS supplemented with 10% goat serum and 0.1% TRITON X-100 was added for 90 min. The coverslips were then lifted and flipped onto a slide mounted with FluoroQuest tm Mounting medium with DAPI (AAT Bioquest, Sunnyvale, CA, United States). A confocal microscope was used to check the results of the immunofluorescence staining.

Measuring C-peptide and insulin secretion of the cells by ELISA

The media were collected from IPCs and undifferentiated MSCs and stored at -20°C. The C-peptide concentration was determined using the C-peptide ELISA kit (Mercodia, Uppsala, Sweden). Insulin concentration was determined using the insulin ELISA kit (Mercodia).

Establishing the diabetic rat model and cell transplantation

The animal study was approved by the Institutional Animal Care and USE Committee of Taipei Veterans General Hospital (No: 2017-055). Hyperglycemia was induced in male Sprague-Dawley rats of a closed colony (body weight 250-300 g) through intraperitoneal injection of 30 mg/kg of STZ on three consecutive days. Blood glucose levels were determined using the Roche ACCU-CHEK glucose meter (Roche Diagnostics, Indianapolis, IN, United States) from tapped tail vein blood. Stable hyperglycemia (blood glucose levels ranging between 380 and 480 mg/dL) developed 1 wk later. The diabetic rats were anesthetized with pentobarbital (40 mg/kg, intraperitoneal injection). After midline laparotomy, the portal vein was identified. Subsequently, 5×10^6 differentiated IPCs or 5×10^6 undifferentiated MSCs suspended in 1 mL heparinized saline were injected into the portal vein, followed by 2 mL normal saline (NS) to push the grafts into the portal vein. The control group underwent the same procedure, but was only injected with NS. Body weight and blood sugar levels were recorded before and after cell transplantation. Blood was collected from a tail vein and blood sugar levels were measured with a blood glucose meter (Roche, Basel, Switzerland).

Intraperitoneal glucose tolerance test

The diabetic rats were fasted for 6 to 8 h, after which 10% glucose (2 g glucose/kg of body weight) were administered intraperitoneally. Blood samples were obtained from the tail vein and analyzed for glucose levels using the Roche ACCU-CHEK glucose meter (Roche Diagnostics).

Immunofluorescence, immunohistochemical analyses, and hematoxylin and eosin staining of the pancreas in rats

The diabetic rats were sacrificed 8 wk after transplantation. The pancreas was removed and embedded in optimal cutting temperature compound (Sakura Finetek United States Inc, Torrance, CA, United States) in liquid nitrogen. The cryosections (5 μm) were washed twice with PBS. The sections were mounted with mounting medium (Vector Laboratories, Burlingame, CA, United States). After applying the primary and secondary antibodies, immunofluorescence staining was checked by fluorescence microscopy using appropriate filters and immunohistochemistry staining was checked under the optical microscope.

Assessment of insulitis

Pancreatic tissue obtained from the rats 8 wk after transplantation was fixed in formalin, embedded in paraffin, serial sectioned at 5 μm thickness, stained with hematoxylin and eosin, and examined for inflammation. The degree of insulitis in the pancreas was evaluated by scoring 100 pancreas serial sections/rat in a blinded fashion using the following criteria: 0, normal islet; 1, peri-insulitis (mononuclear cell

infiltration < 25% of the islet); 2, intra-insulitis (mononuclear cell infiltration 25%–50% of the islet); 3, severe insulitis (mononuclear cell infiltration > 50% of the islet); as previously described[12,14]. Investigators were blinded to the identity of the section.

Statistical analysis

Statistical analysis was carried out using SPSS 14.0 software program (Statistics Package for Social Sciences, SPSS Inc. Chicago, Illinois, United States). The data in this article are expressed as the mean ± standard deviation (SD). Statistical analyses used the parametric independent *t*-test and nonparametric Mann-Whitney *U* test (two independent samples). A *P* value of less than or equal to 0.05 was considered statistically significant.

RESULTS

Differentiation of hWJ-MSCs into IPCs

As in our previous study, we successfully differentiated hWJ-MSCs into IPCs by our three-stage protocol in 10 d[8]. Figure 1A shows the spindle-shaped hWJ-MSCs before differentiation, and Figure 1B shows the islet-like clusters after differentiation. The islet-like clusters stained positive with dithizone, which labels insulin-secreting cells (Figure 1C). Anti-insulin antibodies (green) revealed that insulin was expressed in the islet-like clusters that were co-stained with anti-human nuclear antibodies (red) by immunofluorescence staining (Figure 1D-G). We confirmed that the islet-like clusters were insulin-producing cells both by inverted microscopy and by confocal microscopy.

Comparison of serum C-peptide concentration and insulin concentration between undifferentiated hWJ-MSCs and IPCs in response to glucose stimulation

The concentration of C-peptide and insulin in the culture media from undifferentiated hWJ-MSCs and IPCs was measured using the insulin ELISA kit and C-peptide ELISA kit. Differentiated IPCs secreted large amounts of C-peptide and insulin, whereas undifferentiated hWJ-MSCs secreted them in lower amounts. Importantly, the differentiated IPCs secreted more C-peptide (high glucose *vs* low glucose = 30.79 ± 2.5 *vs* 6.1 ± 1.0 pmol/L, $P < 0.001$) and insulin (29.8 ± 2.8 *vs* 9.7 ± 1.7 mU/L, $P < 0.001$) in response to the higher glucose levels in the environment (Figure 2).

Comparison of the physiological changes between STZ-treated diabetic rats treated with undifferentiated hWJ-MSCs and IPCs

The blood sugar rose to more than 400 mg/dL after three doses of intraperitoneal STZ (30 mg/kg) administration. Compared to the NS treatment group, the rats that received IPC treatment showed significantly decreased blood glucose levels 7 d after the transplantation (NS *vs* IPC = 435.6 ± 32.0 *vs* 250.3 ± 27.0 mg/dL, $P < 0.001$). Although hyperglycemia diminished gradually from the second week to the eighth week (NS *vs* IPC = 511.6 ± 43.5 *vs* 349.1 ± 39.4 mg/dL, $P = 0.018$) after IPC transplantation, the blood glucose level was still significantly lower every week than that in the NS treatment group. In the rats from the undifferentiated hWJ-MSCs group, the decrease in blood glucose levels after transplantation was lower than that in the IPC treatment group (1 wk: NS *vs* MSC = 435.6 ± 32.0 *vs* 361.6 ± 30.7 mg/dL, $P < 0.001$; MSC *vs* IPC = 361.6 ± 30.7 *vs* 250.3 ± 27.0 mg/dL, $P < 0.001$. 8 wk: NS *vs* MSC = 511.6 ± 43.5 *vs* 439.6 ± 32.8 mg/dL, $P = 0.026$; MSC *vs* IPC = 439.6 ± 32.8 *vs* 349.1 ± 39.4 mg/dL, $P = 0.001$), and showed a relative stability until the fifth week (Figure 3A).

The insulin content of the blood samples collected from the tail vein of rats was measured every 2 wk using the insulin ELISA kit, which not only detected human insulin but also rat insulin. The serum insulin level in the rats from the IPC group was higher than that in the animals from the NS treatment group (192.2 ± 25.9 *vs* 53.7 ± 14.2 mU/L, $P < 0.001$), and was stable for 8 wk (92.2 ± 18.2 *vs* 50.7 ± 9.3 mU/L, $P < 0.001$) after transplantation. It is worth noting that the serum insulin level in rats from the IPC group decreased progressively between weeks 1 and 8. Compared to the undifferentiated hWJ-MSCs group, the insulin level of rats in the IPC group was significantly higher only at the first week after transplantation (192.2 ± 25.9 *vs* 112.6 ± 15.6 mU/L, $P < 0.001$). When the undifferentiated hWJ-MSC group and NS group were compared, we found that the insulin level of the animals in the former group was also significantly higher (1 wk: 112.6 ± 15.6 *vs* 53.7 ± 14.2 mU/L, $P = 0.001$) until the eighth week after transplantation (99.1 ± 14.4 *vs* 50.7 ± 9.3 mU/L, $P < 0.001$), although the weekly decline in serum insulin levels was not volatile (Figure 3B). We also measured the serum C-peptide level using the ELISA kit, which could detect human C-peptide levels. The changes in serum C-peptide levels in the IPC treatment

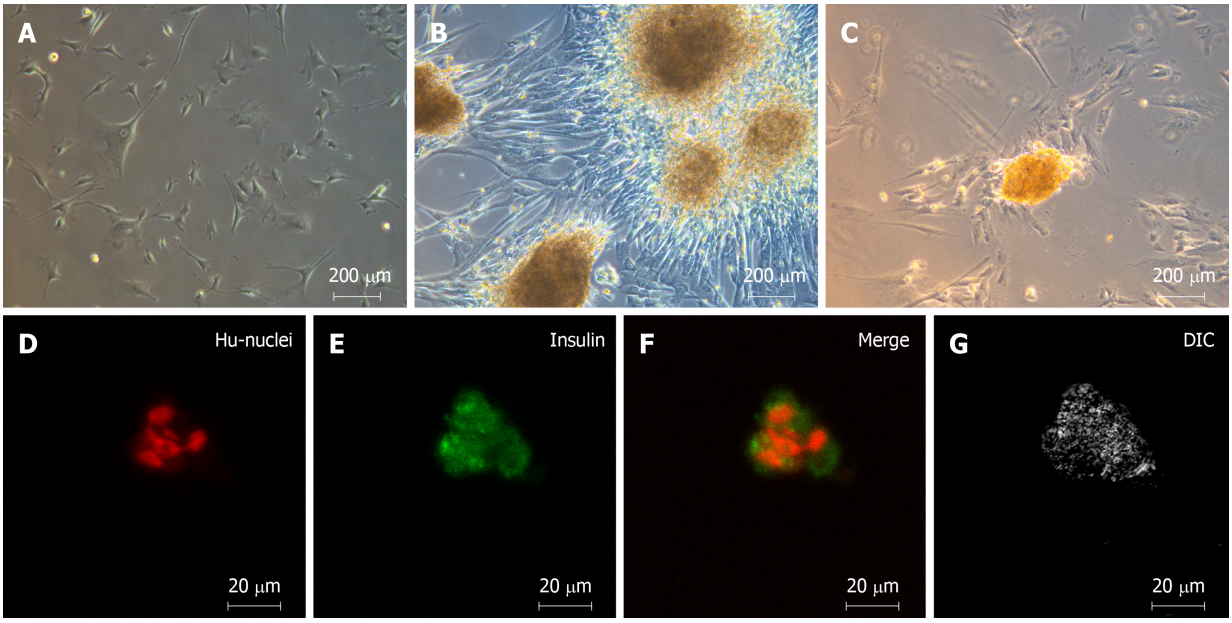

Figure 1 Morphology of undifferentiated human Wharton's jelly mesenchymal stem cells and islet-like clusters differentiated from human Wharton's jelly mesenchymal stem cells. A: Undifferentiated spindle-shaped human Wharton's jelly mesenchymal stem cells (20 ×); B: Islet-like clusters after differentiation (20 ×); C: Dithizone-positive cells, which represent insulin-secreting cells (20 ×); D-G: Immunofluorescence staining with anti-insulin antibodies (green) and anti-human-nuclei antibodies (red) (40 ×).

group was consistent with the changes seen for insulin (1 wk: 64.5 ± 23.9 *vs* 26.4 ± 0.7 pmol/L, $P = 0.001$). However, the serum C-peptide level of rats in the undifferentiated hWJ-MSC treatment group had a smaller change than the one seen in the NS group (1 wk: 28.4 ± 1.2 *vs* 26.4 ± 0.7 pmol/L, $P = 0.002$), a finding that was more consistent with the results of blood glucose changes (Figure 3B).

The intra-peritoneal glucose tolerance test (IPGTT) was performed 1 and 8 wk after transplantation to estimate the kinetics of glucose metabolism. Diabetic rats receiving IPC treatment had significantly better glucose metabolism than those from the NS treatment group, at wk 1 or 8. However, the IPGTT curve in the IPC treatment group was flatter at wk 8 than at wk 1, a change that may have been related to the gradual death of transplanted IPCs over time. Diabetic rats receiving undifferentiated hWJ-MSC treatment also had some ability to improve their glucose metabolism, but this was not statistically significant (Figure 3C). The area under the curve was calculated from the IPGTT graph curve and provided a quantitative analysis of the ability to metabolize glucose. The greater the area under the curve, the worse the ability to metabolize glucose. We found that rats in the IPC treatment group had a significantly better capacity to metabolize glucose than the other two groups in the first week (IPC *vs* NS: $P = 0.002$; IPC *vs* MSC: $P = 0.03$), but improvement in the ability to metabolize glucose decreased in the eighth week (Figure 3C).

Furthermore, we checked the serum cytokine level of diabetic rats in the eighth week after transplantation by the enzyme-linked immunosorbent assay. The inflammatory response was observed by serum levels of interferon gamma (IFN-γ) and interleukin 1 beta (IL-1β) (Figure 4A and B), while serum IL-4 and transforming growth factor beta (TGF-β) level were observed for anti-inflammatory response (Figure 4C and D). Serum IFN-γ (23.0 ± 1.6 *vs* 68.9 ± 5.5 pg/mL, $P < 0.001$) and IL-1β (7.8 ± 0.8 *vs* 15.7 ± 1.7 pg/mL, $P < 0.001$) levels were significantly decreased in the undifferentiated hWJ-MSC treatment group compared with the NS treatment group. Serum IL-4 and TGF-β levels increased in both the differentiated IPC and undifferentiated hWJ-MSC treatment group with a much more significant change in the undifferentiated hWJ-MSC treatment group. (IL4:MSC *vs* NS = 322.6 ± 42.0 *vs* 149.2 ± 12.7 pg/mL, $P < 0.001$; TGF-β:MSC *vs* NS = 97.1 ± 10.1 *vs* 57.2 ± 4.5 pg/mL, $P < 0.001$).

Comparison of the pathological changes between treatment with undifferentiated hWJ-MSCs and IPCs in STZ-induced diabetic rats

The rats were sacrificed 8 wk after transplantation and the pancreas was used for further pathological examinations. We found that the cells co-localized with strong red (human nucleus) and strong green (human insulin) fluorescence in the pancreas of IPC-treated rats by confocal microscopy. These cells were the differentiated human

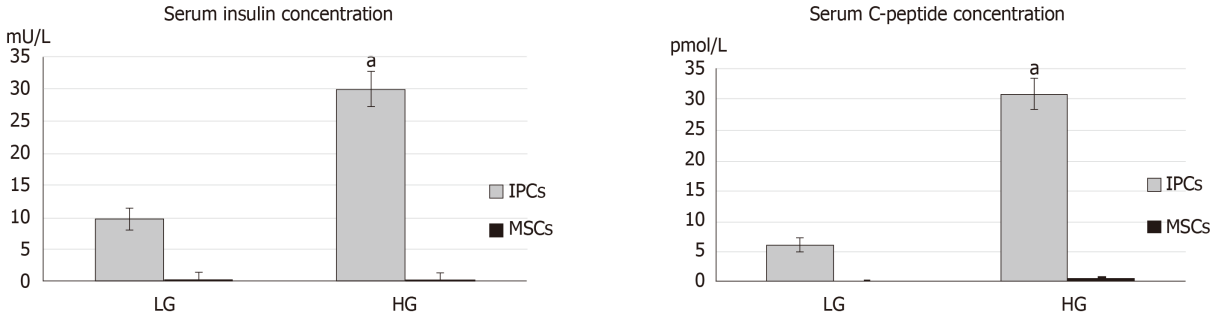

Figure 2 Comparison of serum C-peptide concentration and insulin concentration between undifferentiated human Wharton's jelly mesenchymal stem cells and insulin-producing cells in response to glucose stimulation. Differentiated insulin-producing cells (IPCs) secreted significant amounts of C-peptide and insulin, whereas undifferentiated human Wharton's jelly mesenchymal stem cells (MSCs) secreted lower amounts. $^{a}P < 0.05$ when comparing the concentration of C-peptide and insulin by differentiated insulin-producing cells in response to the higher glucose (HG) and lower glucose (LG) environments.

IPCs that we transplanted *via* the portal vein and subsequently traveled to and survived in the pancreas. In the pancreas of undifferentiated hWJ-MSC treatment group, we found cells that only had red (human nucleus) fluorescence without green fluorescence as well as a few cells with red (human nucleus) fluorescence and very weak green fluorescence. These meant that the undifferentiated hWJ-MSCs transplanted *via* the portal vein could also travel to and survive in the pancreas, and a few of them could be differentiated into IPCs in rat pancreatic tissues (Figure 5).

In addition, we used DAB and FastRed immunohistochemistry staining and optical microscopy to examine sections of the pancreas. The presence of insulin could be identified by the brown color, and the human nuclei would appear red. No red-stained cells could be seen on pancreatic sections in animals from the NS treatment group, but a few brown cells were present (Figure 6A and B). In pancreatic sections of animals from the undifferentiated hWJ-MSC treatment group, we saw some red-stained cells and some separately brown-stained cells as well as a few cells that were double-stained red and brown. (Figure 6C and D). We could easily find cells double-stained red and brown in the islets of the rats from the IPC treatment group, which indicated that the transplanted IPCs could functionally survive in the pancreas (Figure 6E and F).

Finally, we performed systemic samplings of pancreatic sections with hematoxylin and eosin to score for the presence and the degree of insulitis. The percentage of islets free from lymphocyte infiltration was about 7% in the NS treatment group, but 38% in the hWJ-MSC treatment group ($P = 0.004$). Only 18% of the islets from hWJ-MSC-treated rats had severe insulitis compared with 43% of NS-treated animals ($P = 0.003$, Figure 6G).

DISCUSSION

Oral anti-hyperglycemic drugs and subcutaneous insulin injections are used to clinically control hyperglycemia. Pancreas or islet cell transplantation are other options for patients with type 1 diabetes. However, a shortage of donors and an annual decline in the incidence of insulin-dependent diabetes are the Achille's heel of these therapeutic approaches. To date, no efficient therapies exist to cure type 1 diabetes mellitus. Recent research efforts have revealed that transplanting derivatives of stem cells can reduce the symptoms of diabetes[15]. The derivatives of stem cells are insulin-secreting cells that are induced by different environments. In a previous study, we found that insulin-secreting cells that are induced by hWJ-MSCs cells can treat the hyperglycemic state in diabetic rats[8]. However, the mechanism for this is not clear. The aim of this study was to investigate and compare the therapeutic effects of undifferentiated human hWJ-MSCs and IPCs differentiated from the hWJ-MSCs in diabetic rats.

Some findings from the literature indicated that MSCs could differentiate *in vitro*, prior to transplantation, into cells with specific functions. These studies claimed that cells differentiated in this manner would be able to better target the treatment of specific diseases[16,17]. Other investigators believe that undifferentiated MSCs can home to sites of injury and repair the damage after transplantation, and also differentiate into functional cells in specific microenvironments[17,18]. Consistent with the literature, our study showed that undifferentiated hWJ-MSCs could indeed exist in the pancreas of STZ-induced diabetic rats and reduce the insulitis. Even though the transplantation

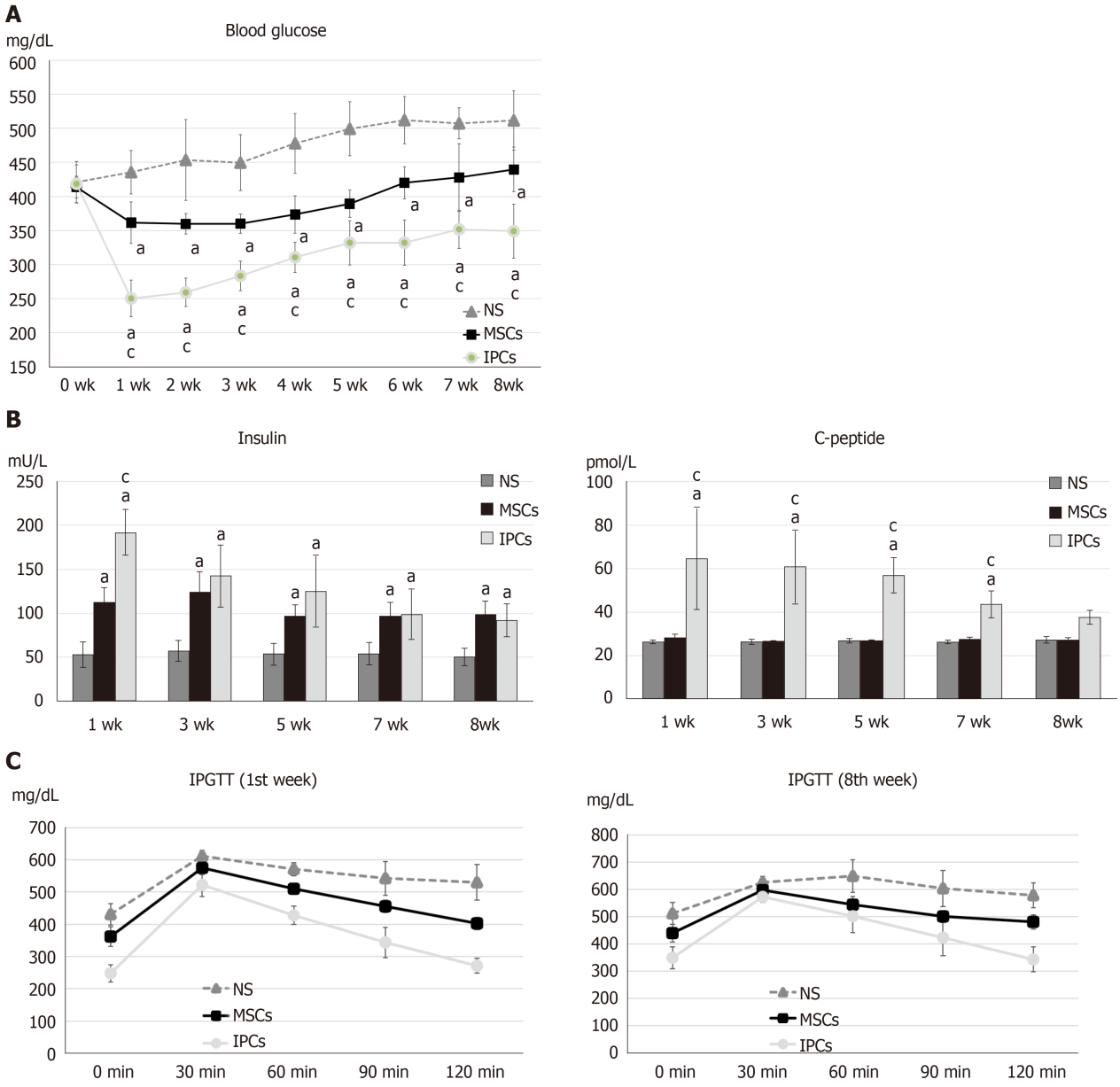

Figure 3 Comparison of differences in blood glucose, serum insulin, serum C-peptide, and intraperitoneal glucose tolerance test results between streptozotocin-induced diabetic rats treated with undifferentiated human Wharton's jelly mesenchymal stem cells and insulin-producing cells. A: $^{a}P < 0.05$, compared to the normal saline (NS) treatment group, the rats in the two treatment groups had significantly decreased blood glucose levels; $^{c}P < 0.05$, blood glucose levels in rats in the insulin-producing cell (IPC) group were significantly lower than in rats from the undifferentiated human Wharton's jelly mesenchymal stem cell (hWJ-MSC) group; B: $^{a}P < 0.05$, compared to the NS treatment group, the rats in other two treatment groups had significantly higher serum insulin levels; $^{c}P < 0.05$, serum insulin levels in rats from the IPC group were significantly higher than those in rats from the undifferentiated hWJ-MSC group; $^{a}P < 0.05$, compared to the NS treatment group, rats in the IPC treatment group had significantly higher serum C-peptide levels; $^{c}P < 0.05$, serum C-peptide level blood glucose level of rats from the IPC group was significantly higher than those in rats from the undifferentiated hWJ-MSC group; C: IPC and MSC treatment led to better improvement in the intraperitoneal glucose tolerance test (IPGTT) result than NS treatment in both the first and eighth weeks.

of undifferentiated hWJ-MSCs was able to only slightly ameliorate the hyperglycemia, these cells were more stable during the entire observation period. By comparison, the transplantation of IPCs differentiated *in vitro* from undifferentiated hWJ-MSCs exposed to three differentiation media, containing different growth factors, was able to dramatically rescue the hyperglycemia in the first week, but the effects declined gradually afterwards.

In addition to measuring blood glucose, we also measured serum insulin and C-peptide levels. The proinsulin secreted by the pancreatic islets would be cleaved into two parts, functional insulin and the by-product C-peptide, both of which are released into the blood in an equimolar ratio. Clinically, serum C-peptide would not be attacked by the anti-insulin antibodies, nor would it be affected by the additional insulin supplementation. Thus, the serum level of C-peptide, which has no physiological functions, was used to more accurately assess the proportion of

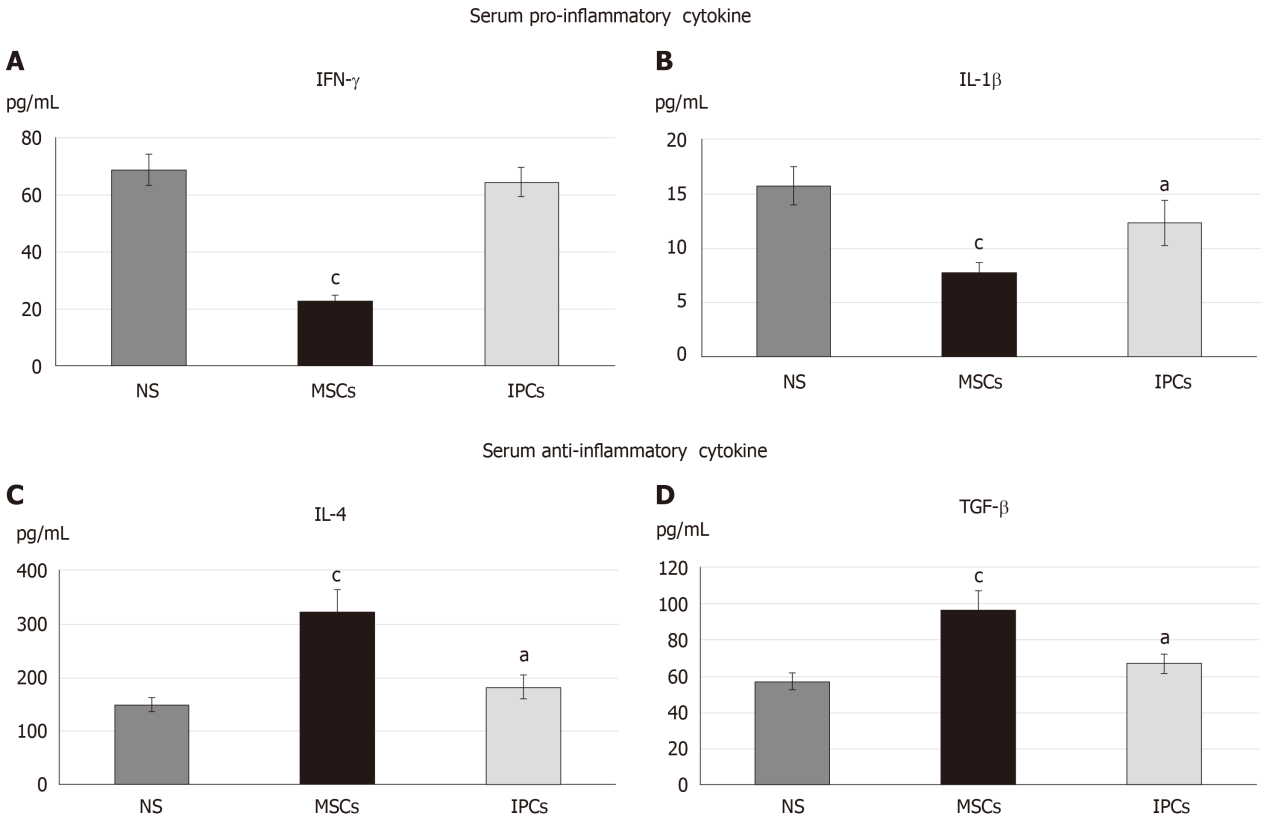

Figure 4 Comparison of the serum cytokine profile in the different treatment groups of diabetic rats. [a]*P* < 0.05, *P* < 0.05 when compared with the serum concentration of the normal saline (NS) group. [c]*P* < 0.05, *P* < 0.05 when comparing the serum concentration between the mesenchymal stem cell (MSC) group and insulin-producing cell (IPC) group. NS: Normal saline treatment group; MSCs: Undifferentiated Wharton's jelly mesenchymal stem cells treatment group; IPCs: Insulin-producing cells treatment group.

remaining islets that had the ability to secrete insulin. In our study, we used the insulin ELISA kit to determine serum insulin levels. However, the commercial insulin ELISA kit cannot clearly distinguish between human and rat insulin. The level of serum insulin that we measured was the total insulin that was secreted by both the transplanted human IPCs and original rat islets. On the other hand, the commercial C-peptide ELISA kit that we used was specific for human C-peptide. Thus, the level of serum C-peptide that we measured represented only the C-peptide released by the transplanted human IPCs.

Both the serum C-peptide levels and insulin levels in rats from the IPC transplantation group were significantly higher than those in the other two groups and gradually declined afterwards. The IPGTT also significantly improved in the IPC transplantation group. This demonstrated that the transplanted human IPCs indeed had secreted insulin *in vivo* and directly contributed to reducing the hyperglycemia. However, because the IPCs are not stem cells, their survival would inevitably decline over time. The above result was compatible with that obtained from measuring blood glucose levels. With respect to the undifferentiated hWJ-MSCs group, we found that the serum C-peptide level was similar to the one from the NS treatment group, but the serum insulin level was slightly higher. This indicated that the transplanted undifferentiated hWJ-MSCs could improve the ability of the injured rat islets to secrete insulin, as opposed to secreting much insulin. The improvement was quantitatively less pronounced but more stable than in the IPC treatment group throughout the entire observation period. These data were also compatible with the changes in blood glucose levels.

Further, we checked the serum cytokine level of diabetic rats in the eighth week after transplantation by enzyme-linked immunosorbent assay. The serum proinflammatory cytokine, including IFN-γ and IL-1β, were significant decreased in the undifferentiated hWJ-MSCs treatment group than NS treatment group. The serum anti-inflammatory cytokine, including IL-4 and TGF-β, presented significant increase in both the undifferentiated hWJ-MSCs treatment group and differentiated IPCs treatment group in comparison with the NS treatment group. Both undifferentiated hWJ-MSCs and differentiated IPCs treatment could have the anti-inflammatory effect while the undifferentiated MSCs treatment could also dramatically diminish the

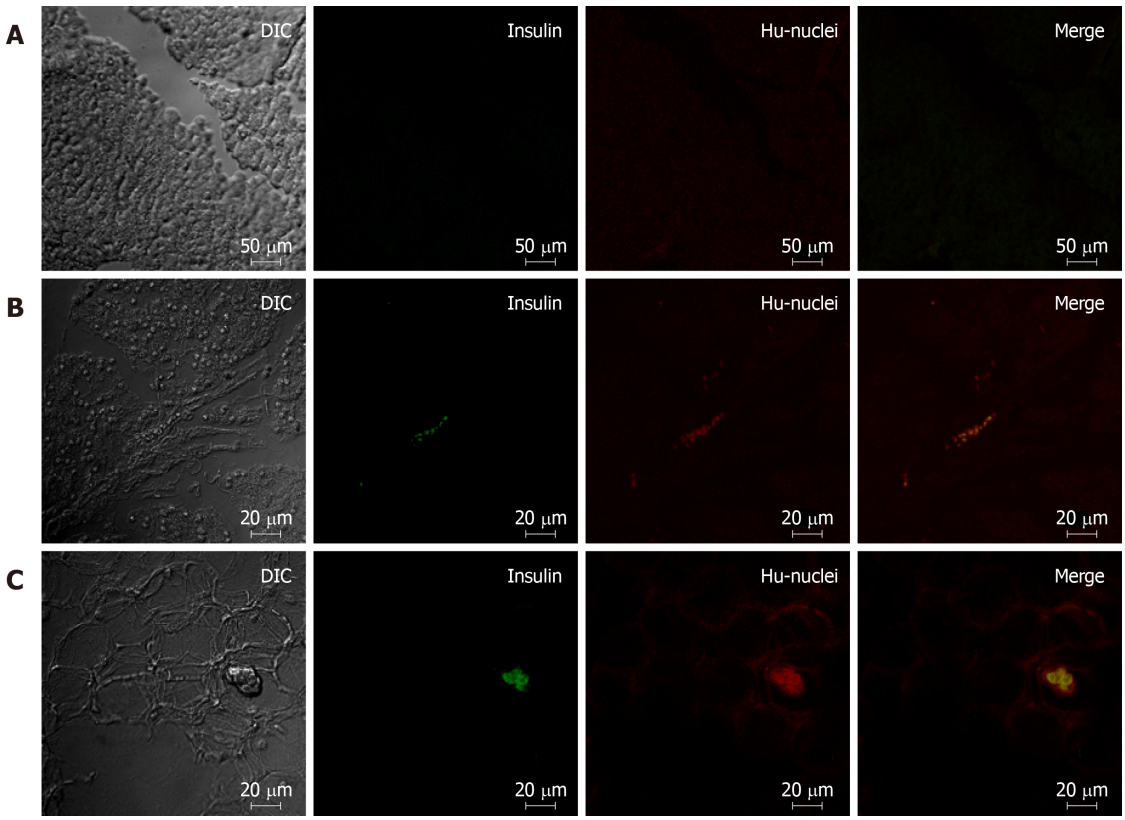

Figure 5 Comparison of pancreatic immunofluorescence staining in the different treatment groups of diabetic rats. A: Pancreas of rats from the saline treatment group (20 ×); B: Pancreas of rats from the mesenchymal stem cell treatment group (10 ×); C: Pancreas of rats from the insulin-producing cell treatment group (10 ×). Red: Human cell nucleus; green: human insulin.

inflammatory response in STZ-induced diabetic rats. The function of restoration of immune balance was more prominent in the undifferentiated hWJ-MSCs treatment group.

In contrast with the rats from the transplanted differentiated IPC group, the insulitis was significantly improved in the rats transplanted with undifferentiated hWJ-MSCs. However, to our disappointment, this great pathological improvement resulted in smaller improvements in the actual blood glucose levels and glucose metabolism in the animals. This could be explained by the fact that the islets did not have sufficient time to return to their normal working environment from a very severe infiltration stage due to the insufficient observation time after treatment or the insufficient transplantation dosage. Another potential explanation could be that the insulin produced by the rat pancreatic β cells failed to achieve a substantial hypoglycemic effect.

Overall, cell therapy has the ability to mitigate the hyperglycemia of diabetic rats to a certain degree. However, more *in vivo* studies are needed to develop methods to improve the survival of cells and to effectively extend the period of euglycemia after treatment. In future research studies exploring the treatment of diabetes with cell therapies, administering higher numbers of cells or increasing the frequency of their administration, and the simultaneous application of differentiated and undifferentiated hWJ-MSCs, should be considered to achieve better therapeutic effects. It is expected that the results of these experiments will provide a better basis for the future treatment of diabetes.

In conclusion, transplantation of differentiated IPCs can significantly reduce blood glucose levels and improve glucose metabolism in diabetic rats. The therapeutic mechanism of this intervention may reside in the continuous secretion of insulin by transplanted cells that survive in the pancreatic islets of the rats. Meanwhile, the transplantation of undifferentiated hWJ-MSCs can significantly improve islet infiltration and restore immune balance in diabetic rats, with less pronounced improvements in the blood glucose levels.

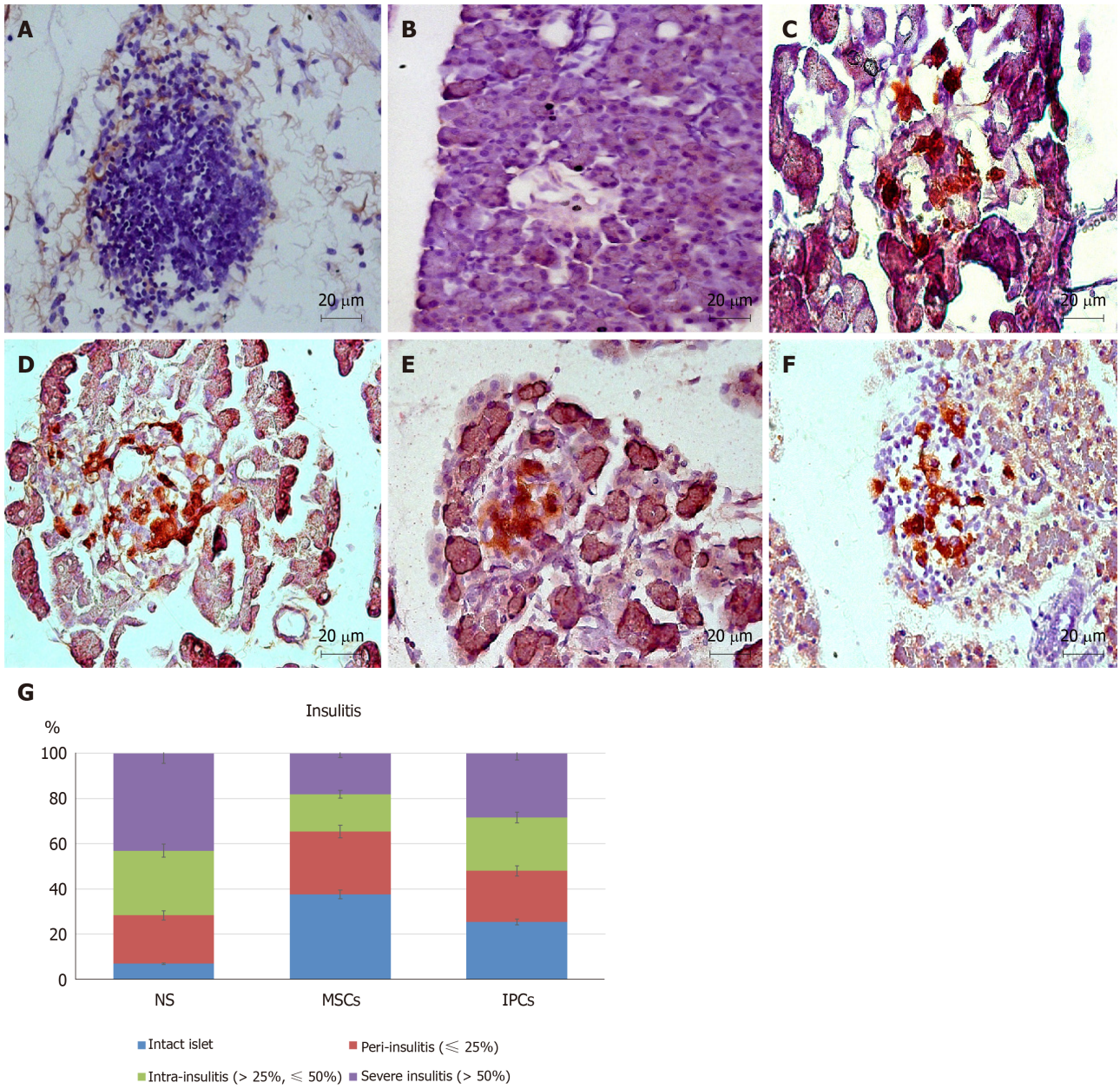

Figure 6 Comparison of pancreatic immunohistochemistry staining in the different treatment groups of diabetic rats. A, B: Pancreas of rats from the normal saline (NS) treatment group (40 ×); C, D: Pancreas of rats from the mesenchymal stem cell (MSC) treatment group (40 ×); E, F: Pancreas of rats from the insulin-producing cell (IPC) treatment group (40 ×); G: Intact islets: 0% lymphocyte infiltration, peri-insulitis: < 25% lymphocyte infiltration, intra-insulitis: 25%-50% lymphocyte infiltration, severe insulitis: > 50% lymphocyte infiltration. The percentage of islets free from lymphocyte infiltration was about 7% in rats from the NS treatment group but was 38% in rats from the MSC treatment group ($^aP < 0.05$). Only 18% of the islets from MSC-treated rats showed severe insulitis compared with 43% of rats from the NS treatment group ($^aP < 0.05$). NS: normal saline treatment group; MSCs: Undifferentiated Wharton's jelly-MSCs treatment group; IPCs: Insulin-producing cells treatment group; Red: Human cell nucleus; Brown: Human insulin.

ARTICLE HIGHLIGHTS

Research background

Despite the availability of current therapies, including oral antidiabetic drugs and insulin, to control the symptoms caused by high blood glucose, it is difficult to cure diabetes mellitus, especially type 1 diabetes mellitus.

Research motivation

Both islet transplantation and cadaveric whole pancreas transplantation are the treatment choice for diabetes. However, shortage of donors, high perioperative risks, and the long-term postoperative need of immunosuppressants are some of the major concerns and challenges for these treatments. More appropriate and effective medical technologies to cure diabetes are needed. Cell therapies using mesenchymal stem cells (MSCs) may be a promising option.

Research objectives
In this study, we tried to figure out the therapeutic mechanisms by which MSCs exert their effects for diabetic rats.

Research methods
We used three types of differentiation media over 10 d to generate insulin-producing cells (IPCs) from human Wharton's jelly MSCs (hWJ-MSCs). We further transplanted the undifferentiated hWJ-MSCs and differentiated IPCs derived from them into the portal vein of rats with streptozotocin-induced diabetes and recorded the physiological and pathological changes.

Research results
Using fluorescent staining and C-peptide ELISA, we have shown that we were able to successfully induce the differentiation of hWJ-MSCs into IPCs. Transplantation of both IPCs derived from hWJ-MSCs and undifferentiated hWJ-MSCs had the therapeutic effect of ameliorating blood glucose levels and improving intraperitoneal glucose tolerance tests. The transplanted IPCs homed to the pancreas and functionally survived for at least 8 wk after transplantation, whereas the undifferentiated hWJ-MSCs were able to improve the insulitis and ameliorate the serum inflammatory cytokine in streptozotocin-induced diabetic rats.

Research conclusions
The therapeutic mechanism of differentiated and undifferentiated human hWJ-MSCs in streptozotocin-induced diabetic rats may be different. Differentiated IPCs can significantly improve blood glucose levels due to continuously secretion insulin by the transplanted cells that survived in the islets of diabetic rats. Transplantation of undifferentiated hWJ-MSCs can significantly improve insulitis and re-balance the inflammatory condition with only a slight improvement in blood glucose levels.

Research perspectives
The results of this study will provide basic and essential information for future application of cell regenerative therapy in diabetic patients.

REFERENCES

1 **Fioretto P**, Kim Y, Mauer M. Diabetic nephropathy as a model of reversibility of established renal lesions. *Curr Opin Nephrol Hypertens* 1998; **7**: 489-494 [PMID: 9818194 DOI: 10.1186/s13287-016-0465-2]
2 **Mangi AA**, Noiseux N, Kong D, He H, Rezvani M, Ingwall JS, Dzau VJ. Mesenchymal stem cells modified with Akt prevent remodeling and restore performance of infarcted hearts. *Nat Med* 2003; **9**: 1195-1201 [PMID: 12910262 DOI: 10.1038/nm912]
3 **Ullah I**, Subbarao RB, Rho GJ. Human mesenchymal stem cells - current trends and future prospective. *Biosci Rep* 2015; 35 [PMID: 25797907 DOI: 10.1042/BSR20150025]
4 **Karahuseyinoglu S**, Cinar O, Kilic E, Kara F, Akay GG, Demiralp DO, Tukun A, Uckan D, Can A. Biology of stem cells in human umbilical cord stroma: in situ and in vitro surveys. *Stem Cells* 2007; **25**: 319-331 [PMID: 17053211 DOI: 10.1634/stemcells.2006-0286]
5 **Wang HS**, Hung SC, Peng ST, Huang CC, Wei HM, Guo YJ, Fu YS, Lai MC, Chen CC. Mesenchymal stem cells in the Wharton's jelly of the human umbilical cord. *Stem Cells* 2004; **22**: 1330-1337 [PMID: 15579650 DOI: 10.1634/stemcells.2004-0013]
6 **Casiraghi F**, Perico N, Remuzzi G. Mesenchymal stromal cells for tolerance induction in organ transplantation. *Hum Immunol* 2018; **79**: 304-313 [PMID: 29288697 DOI: 10.1016/j.humimm.2017.12.008]
7 **Hsiao CY**, Tsai JP, Chu PC, Liu SI, Pan CH, Chen CP, Su CH, Weng ZC, Chen TH, Shyu JF, Chang HH, Wang HS. Transplantation of Wharton's jelly mesenchymal stem cells to improve cardiac function in myocardial infarction rats. *J Biomedical Sci* 2016; **5**: 1 [DOI: 10.4172/2254-609X.100020]
8 **Kao SY**, Shyu JF, Wang HS, Hsiao CY, Su CH, Chen TH, Weng ZC, Tsai PJ. Transplantation of Hepatocyte-like Cells Derived from Umbilical Cord Stromal Mesenchymal Stem Cells to Treat Acute Liver Failure Rat. *J Biomedical Sci* 2016; **4**: 1 [DOI: 10.4172/2254-609X.10002]
9 **Chu KA**, Wang SY, Yeh CC, Fu TW, Fu YY, Ko TL, Chiu MM, Chen TH, Tsai PJ, Fu YS. Reversal of bleomycin-induced rat pulmonary fibrosis by a xenograft of human umbilical mesenchymal stem cells from Wharton's jelly. *Theranostics* 2019; **9**: 6646-6664 [PMID: 31588241 DOI: 10.7150/thno.33741]
10 **Tsai PJ**, Yeh CC, Huang WJ, Min MY, Huang TH, Ko TL, Huang PY, Chen TH, Hsu SPC, Soong BW, Fu YS. Xenografting of human umbilical mesenchymal stem cells from Wharton's jelly ameliorates mouse spinocerebellar ataxia type 1. *Transl Neurodegener* 2019; **8**: 29 [PMID: 31508229 DOI: 10.1186/s40035-019-0166-8]
11 **Tsai PJ**, Wang HS, Shyr YM, Weng ZC, Tai LC, Shyu JF, Chen TH. Transplantation of insulin-producing cells from umbilical cord mesenchymal stem cells for the treatment of streptozotocin-induced diabetic rats. *J Biomed Sci* 2012; **19**: 47 [PMID: 22545626 DOI: 10.1186/1423-0127-19-47]
12 **Tsai PJ**, Wang HS, Lin GJ, Chou SC, Chu TH, Chuan WT, Lu YJ, Weng ZC, Su CH, Hsieh PS, Sytwu HK, Lin CH, Chen TH, Shyu JF. Undifferentiated Wharton's Jelly Mesenchymal Stem Cell Transplantation Induces Insulin-Producing Cell Differentiation and Suppression of T-Cell-Mediated Autoimmunity in Nonobese Diabetic Mice. *Cell Transplant* 2015; **24**: 1555-1570 [PMID: 25198179 DOI: 10.3727/096368914X683016]
13 **Wang HS**, Shyu JF, Shen WS, Hsu HC, Chi TC, Chen CP, Huang SW, Shyr YM, Tang KT, Chen TH. Transplantation of insulin-producing cells derived from umbilical cord stromal mesenchymal stem cells to treat NOD mice. *Cell Transplant* 2011; **20**: 455-466 [PMID: 20719086 DOI: 10.3727/096368910X522270]
14 **Verdaguer J**, Schmidt D, Amrani A, Anderson B, Averill N, Santamaria P. Spontaneous autoimmune diabetes in monoclonal T cell nonobese diabetic mice. *J Exp Med* 1997; **186**: 1663-1676 [PMID: 9362527

DOI: 10.1084/jem.186.10.1663]
15 **Bai L**, Meredith G, Tuch BE. Glucagon-like peptide-1 enhances production of insulin in insulin-producing cells derived from mouse embryonic stem cells. *J Endocrinol* 2005; **186**: 343-352 [PMID: 16079260 DOI: 10.1677/joe.1.06078]
16 **Thulé PM**, Liu JM. Regulated hepatic insulin gene therapy of STZ-diabetic rats. *Gene Ther* 2000; **7**: 1744-1752 [PMID: 11083496 DOI: 10.1038/sj.gt.3301297]
17 **Krabbe C**, Zimmer J, Meyer M. Neural transdifferentiation of mesenchymal stem cells--a critical review. *APMIS* 2005; **113**: 831-844 [PMID: 16480453 DOI: 10.1111/j.1600-0463.2005.apm_3061.x]
18 **Phinney DG**, Prockop DJ. Concise review: mesenchymal stem/multipotent stromal cells: the state of transdifferentiation and modes of tissue repair--current views. *Stem Cells* 2007; **25**: 2896-2902 [PMID: 17901396 DOI: 10.1634/stemcells.2007-0637]

World Journal of Stem Cells

Submit a Manuscript: https://www.f6publishing.com

World J Stem Cells 2020 February 26; 12(2): 152-167

DOI: 10.4252/wjsc.v12.i2.152

ISSN 1948-0210 (online)

ORIGINAL ARTICLE

Basic Study

C-C chemokine receptor type 2-overexpressing exosomes alleviated experimental post-stroke cognitive impairment by enhancing microglia/macrophage M2 polarization

Huai-Chun Yang, Min Zhang, Rui Wu, Hai-Qing Zheng, Li-Ying Zhang, Jing Luo, Li-Li Li, Xi-Quan Hu

ORCID number: Huai-Chun Yang (0000-0001-8977-5280); Min Zhang (0000-0002-9618-3731); Rui Wu (0000-0001-6236-5548); Hai-Qing Zheng (0000-0002-6200-2074); Li-Ying Zhang (0000-0001-5939-2991); Jing Luo (0000-0002-3072-7345); Li-Li Li (0000-0002-4928-1144); Xi-Quan Hu (0000-0003-2769-8624).

Author contributions: Hu XH, Yang HC, and Zhang M conceived and designed the experiments. Yang HC and Zhang M performed the experiments. Yang HC, Zhang M and Wu R acquired, analyzed and interpreted the data. Hu XH, Yang HC, and Zhang M wrote the manuscript. All authors have read and revised the final manuscript and approved it for publication.

Supported by the National Natural Science Foundation of China, No. 81871847 and No. 81672261.

Institutional review board statement: The study was reviewed and approved by the Institutional Animal Ethics Committee of Life Sciences School, Sun Yat-sen University.

Institutional animal care and use committee statement: Animal studies were reviewed and approved by the Institutional Animal Ethics Committee of Life Sciences School, Sun Yat-sen University.

Conflict-of-interest statement: The authors declare no conflicts of interest.

Huai-Chun Yang, Rui Wu, Hai-Qing Zheng, Li-Ying Zhang, Jing Luo, Li-Li Li, Xi-Quan Hu, Department of Rehabilitation Medicine, the Third Affiliated Hospital, Sun Yat-sen University, Guangzhou 510000, Guangdong Province, China

Min Zhang, Department of Andrology, the First Affiliated Hospital, Sun Yat-sen University, Guangzhou 510000, Guangdong Province, China

Corresponding author: Xi-Quan Hu, MD, PhD, Chief Physician, Professor, Department of Rehabilitation Medicine, the Third Affiliated Hospital, Sun Yat-sen University, No. 600 Tianhe Road, Guangzhou 510000, Guangdong Province, China. sysu_hu@163.com

Abstract

BACKGROUND

Human-derived mesenchymal stromal cells have been shown to improve cognitive function following experimental stroke. The activity of exosomes has been verified to be comparable to the therapeutic effects of mesenchymal stromal cells. However, the effects of exosomes derived from human umbilical cord mesenchymal stem cells (HUC-MSCs) (Exo^{Ctrl}) on post-stroke cognitive impairment (PSCI) have rarely been reported. Moreover, whether exosomes derived from C-C chemokine receptor type 2 (CCR2)-overexpressing HUC-MSCs (Exo^{CCR2}) can enhance the therapeutic effects on PSCI and the possible underlying mechanisms have not been studied.

AIM

To investigate the effects of Exo^{Ctrl} on PSCI and whether Exo^{CCR2} can enhance therapeutic effects on PSCI.

METHODS

Transmission electron microscopy, qNano® particles analyzer, and Western blotting were employed to determine the morphology and CCR2 expression of Exo^{Ctrl} or Exo^{CCR2}. ELISA was used to study the binding capacity of exosomes to CC chemokine ligand 2 (CCL2) *in vivo*. After the intravenous injection of Exo^{Ctrl} or Exo^{CCR2} into experimental rats, the effect of Exo^{Ctrl} and Exo^{CCR2} on PSCI was assessed by Morris water maze. Remyelination and oligodendrogenesis were analyzed by Western blotting and immunofluorescence microscopy. QRT-PCR and immunofluorescence microscopy were conducted to compare the microglia/macrophage polarization. The infiltration and activation of hematogenous macrophages were analyzed by Western blotting and transwell

Data sharing statement: The data used to support the findings of this study are available from the corresponding author upon request.

ARRIVE guidelines statement: The manuscript has been prepared and revised according to the ARRIVE guidelines.

Manuscript source: Invited manuscript

Received: October 22, 2019
Peer-review started: October 22, 2019
First decision: November 18, 2019
Revised: December 27, 2019
Accepted: January 19, 2020
Article in press: January 19, 2020
Published online: February 26, 2020

P-Reviewer: Fatkhudinov T, Oltra E
S-Editor: Dou Y
L-Editor: A
E-Editor: Qi LL

migration analysis.

RESULTS

CCR2-overexpressing HUC-MSCs loaded the CCR2 receptor into their exosomes. The morphology and diameter distribution between Exo^{Ctrl} and Exo^{CCR2} showed no significant difference. Exo^{CCR2} bound significantly to CCL2 but Exo^{Ctrl} showed little CCL2 binding. Although both Exo^{CCR2} and Exo^{Ctrl} showed beneficial effects on PSCI, oligodendrogenesis, remyelination, and microglia/macrophage polarization, Exo^{CCR2} exhibited a significantly superior beneficial effect. We also found that Exo^{CCR2} could suppress the CCL2-induced macrophage migration and activation *in vivo* and *in vitro*, compared with Exo^{Ctrl} treated group.

CONCLUSION

CCR2 over-expression enhanced the therapeutic effects of exosomes on the experimental PSCI by promoting M2 microglia/macrophage polarization, enhancing oligodendrogenesis and remyelination. These therapeutic effects are likely through suppressing the CCL2-induced hematogenous macrophage migration and activation.

Key words: Cognitive impairment; Stroke; Exosomes; C-C chemokine receptor type 2; Microglia/macrophage polarization; Remyelination

Core tip: Exosomes have been reported to possess the therapeutic benefit comparable to the therapeutic effects of mesenchymal stromal cells. However, the effects of exosomes derived from human umbilical cord mesenchymal stem cells (Exo^{Ctrl}) on post-stroke cognitive impairment (PSCI) have rarely been reported. Moreover, whether exosomes derived from C-C chemokine receptor type 2 (CCR2)-overexpressing human umbilical cord mesenchymal stem cells (Exo^{CCR2}) have better therapeutic effects on PSCI and the possible mechanisms underlying these effects remained unclear. This study provides new insights into the use of genetically modified exosomes for PSCI treatment, offering new ideas for the clinical application of exosome-based therapies for PSCI.

Citation: Yang HC, Zhang M, Wu R, Zheng HQ, Zhang LY, Luo J, Li LL, Hu XQ. C-C chemokine receptor type 2-overexpressing exosomes alleviated experimental post-stroke cognitive impairment by enhancing microglia/macrophage M2 polarization. *World J Stem Cells* 2020; 12(2): 152-167
URL: https://www.wjgnet.com/1948-0210/full/v12/i2/152.htm
DOI: https://dx.doi.org/10.4252/wjsc.v12.i2.152

INTRODUCTION

Post-stroke cognitive impairment (PSCI) occurs frequently after stroke. The prevalence of PSCI in ischemic stroke patients ranges from 25% to 30%[1], which has been increasing gradually due to the development of modern medicine and the increasing survival rate of stroke patients[2,3]. PSCI imposes a heavy burden on the patients, their families, and societies. However, the treatment of PSCI is still not satisfactory and requires further improvement.

Previous research has shown that mesenchymal stem cell (MSC) therapy faciliates the cognitive recovery after stroke[4,5]. However, the disadvantages of therapies involving MSCs, such as their high *in vivo* clearance rate after transplantion[6,7], limited capacity to cross blood-brain barrier[8,9], potential immunogenicity[10,11], and unpredictability of cell growth and differentiation[12], have emerged with the development of research. Recent studies have indicated that MSCs mostly act via specific paracrine mechanisms, while exosomes play a key role in the general progress and recovery under conditions of disease[13]. MSC-derived exosomes have displayed positive effects in animal models of various ischemic injuries such as stroke[14], myocardial infarction[15], and renal ischemic injury[16]. To a certain extent, MSC-derived exosomes exert therapeutic effects comparable to those of MSCs and overcome the potential risks and disadvantages associated with MSCs[17,18]. However, there are only

a few studies focusing on exosome-based treatments for PSCI.

CC chemokine ligand 2 (CCL2) is highly expressed in the ischemic hemisphere after a stroke; this mediates the migration of C-C chemokine receptor type 2 (CCR2)-positive blood-derived macrophages, thus exacerbating brain tissue damage[19,20]. CCR2 knockout mice[21] or CCL2 knockout[22] mice have shown a significant reduction of macrophage proliferation within 2 wk after a stroke, accompanied by neuronal regeneration and decreased infarct volume, suggesting that inhibition of the CCL2/CCR2 axis may play a neuroprotective role after strokes. In addition, CCR2 antagonism[23] or CCR2 knockout[24] can promote the M2 polarization of microglia/macrophages by inhibiting CCR2+ macrophages and improve cognitive impairment in mice with traumatic brain injury.

It is noticeable that in recent years, exosomes secreted by human umbilical cord MSCs (HUC-MSCs) have shown powerful effects on microglia/macrophage activation and polarization in animal models such as the Alzheimer's disease model[25], hypoxic-ischemic encephalopathy model[26], and the peripheral nerve injury model[27]. However, the effects of HUC-MSC-derived exosomes (Exo^{Ctrl}) on microglia/macrophage polarization and cognitive function after stroke have not yet been reported. Furthermore, we hypothesize that CCR2-overexpressing HUC-MSC-derived exosomes (Exo^{CCR2}) further promote microglia/macrophage M2 polarization by competitively binding to the CCR2 ligand CCL2 and inhibiting the CCL2-mediated infiltration of blood-derived mononuclear macrophages. Particularly, we compared the therapeutic effects of the systemic administration of Exo^{CCR2} and Exo^{Ctrl} on PSCI, which will provide new insights into genetically modified exosome-based therapies for PSCI treatment and serve as a preclinical study on cerebral protection after stroke.

MATERIALS AND METHODS

Establishment of the tMCAO model and animals grouping

Adult Sprague-Dawley rats (male, weighing 280-350 g) were underwent the right transient middle cerebral occlusion (tMCAO) for 2 h in accordance with the method as Longa *et al*[28] described with modifications. Experimental procedures were approved by the Institutional Animal Ethics Committee of Life Sciences School, Sun Yat-sen University. The modified neurological severity score (mNSS) and 2,3,5-Triphenyltetrazolium chloride (TTC) (G3005, Solarbio, China) staining were utilized to confirm the establishment of the tMCAO model. Rats with moderate injury (mNSS values 7-12) were randomly divided into the sham group, tMCAO group, Exo^{Ctrl} treatment group, and Exo^{CCR2} treatment group. As described in a previous study, 100 μg of the exosomes was dissolved in 500 μL of phosphate-buffered saline (PBS)[29]. One day after operation, the rats from sham and tMCAO groups were injected with 500 μL of PBS, the rats in the Exo^{Ctrl} and Exo^{CCR2} treatment groups were injected with equal volumes of the respective exosomal solutions *via* tail vein injections. BrdU (50 mg/kg/d; B5002, Sigma, United States) was injected intraperitoneally for 14 continuous d one day after the induction of tMCAO.

Transfection of HUC-MSCs with lentiviral vectors and comparison of their biological characteristics

HUC-MSCs were obtained from three healthy donors after they signed the informed consent forms. Briefly, the Wharton gum tissues with blood vessels removed were cut up and digested with collagenase II (1 mg/mL, 234155, Millipore) under 37 °C for 30 min with shaking. The cells were filtered from the suspensions with a cell strainer (diameter 70 μm). The cells were washed with Hank's Balanced Salt Solution (SH30031.02, Hyclone) and cultured in low-glucose DMEM (L-DMEM) (C11885500BT, Gibco) containing 10% fetal bovine serum (04-001-1A, Biological Industries, Israel) in a 5% CO2 incubator.

At passage 3, the HUC-MSCs were transfected with lentiviral vectors expressing both the *CCR2* and *eGFP* genes, and vectors expressing the *eGFP* gene in accordance with the manufacturer's instructions. The vector construction is indicated in Supplement Figure 1. Three days after the transfection, the HUC-MSCs transfected with lentiviral vectors encoding CCR2 (namely $HUC\text{-}MSCs^{CCR2}$) or eGFP (namely $HUC\text{-}MSCs^{Ctrl}$), were sorted using fluorescence-activated cell sorting (Influx, Becton Dickinson). The $HUC\text{-}MSCs^{Ctrl}$ and $HUC\text{-}MSCs^{CCR2}$ (passage 6) were identified by microscopic analysis, flow cytometry analysis for detecting the following surface markers: CD13-APC (1:50, 17-0138-41, eBioscience, United States), CD29-APC (1:50, 559883, BD Bioscience, United States), CD44-APC (1:50, 559942, BD Bioscience, United States), CD34-PE (1:50, 550761, BD Bioscience, United States), CD45-PE (1:50, 560975, BD Bioscience, United States), CD73-PE (1:50, 60044, Stemcell Technologies, Canada),

CD90-PE-Cy7 (1:50, 561558, BD Bioscience, United States), CD105-PerCP-Cy5.5 (1:50, 560819, BD Bioscience, USA), HLA-DR-V500 (1:50, 561225, BD Bioscience, United States). Osteogenesis and lipogenesis induction experiments were conducted with modification as described in a previous study[30]. Briefly, for osteogenisis induction experiments, cells were cultured in L-DMEM containing fetal bovine serum (20%), ascorbic acid (100 μg/mL), β-glycerophosphate (10 mmol) and dexamethasone (100 nmol) for three weeks with medium changed every 3 d. For adipogenesis induction experiments, the cells were induced in L-DMEM supplemented with FBS (10%), dexamethasone (100 nmol), indomethacin (0.2 mmol), insulin (10 μg/mL), 3-isobutyl-1-methylxanthine (0.5 mmol). After 3 wk, Osteogenic and adipogenic differentiation were confirmed by oil red O staining and alizarin red staining.

Exosome isolation and identification

The isolation of exosome was performed according to a previous study[31]. Briefly, the exosomes were collected by differential ultracentrifugation, and their morphology was analyzed by transmission electron microscopy. The distribution of the exosomes based on their diameters was performed using a qNano® system (Izon Science, Oxford, United Kingdom). Western blotting was used to detect the CCR2 expression and the exosome-specific markers CD9, CD63, and CD81.

Enzyme-linked immunosorbent assay (ELISA)

To test the CCL2-binding capacity of the exosomes, Exo^{Ctrl} and Exo^{CCR2} were co-incubated with recombinant rat CCL2 (100 ng/well, 400-12, PeproTech, United States). Differential ultracentrifugation was performed to obtain exosome-free supernatants. ELISA kits (CSB-E07429r, Cusabio Biotech, China) were utilized to detect the CCL2-binding capacity of Exo^{CCR2} and Exo^{Ctrl}, according to the protocol of manufacturer.

Cognitive function test

The Morris water maze test was conducted as our previous study described[32]. The test was carried out at 23 d after the induction of tMCAO. The rats were first subjected to five consecutive days of the place navigation test. On day 6, a spatial probe test (60 s) was performed under the same condition without platform. During the test, the latency to the platform and the time recorded in the target quadrants were analysed. The mNSS values were recorded at 1, 4, 14, and 28 d after exosome treatment, as described previously[33]. The rats were tested by an individual blinded to the grouping for three times, and the means of the mNSS results were recorded. The normal score is 0, while the maximal deficit score is 18. Rats with mNSS values ranging from 7-12 were included in the study.

Western blotting

Western blotting was conducted in accordance with the protocol as our previous study described[34]. First, the proteins were obtained from the ischemic cerebral hemisphere or cultured cells by treatment with the kit of protein extraction (KeyGen BioTech, China) according to the protocol of manufacturer. The protein samples were loaded onto 10% polyacrylamide gels and electrophoresed under 120V voltage; the resultant bands were transferred onto polyvinylidene difluoride membranes. Next, the polyvinylidene difluoride membranes were incubated with rabbit anti-CD9 (1:2000, ab92726, Abcam, United Kingdom), rabbit anti-CD63 (1:10000, 25682-1-AP, ProteinTech, United States), rabbit anti-CD81 (1:1000, ab109201, Abcam, United States), rabbit anti-CCR2 (1:1000, DF2711, Affinity Biosciences, United States), rabbit anti-CCL2 (1:1000, ab25124, Abcam, United States), mouse anti-iba-1 (1:500, MABN92, Millipore, United States), rabbit anti-NF-κB (1:1000, ab16502, Abcam, United States), mouse anti-CD68 (1:1000, ab201340, Abcam, United States), rabbit anti-myelin basic protein (anti-MBP) (1:200, ab40390, Abcam, United States), and rabbit anti-β-actin (1:1000, #3700, Cell Signaling Technology, United States) antibodies at 4 °C overnight, and then with peroxidase-conjugated secondary antibodies at 37 °C for 1 h. The protein bands were developed using a specific chromogenic substrate (ECL, KeyGen BioTech, China), according to the manufacturer's instructions.

RNA isolation, reverse transcription, and real-time PCR

Total RNA from the ischemic cerebral hemispheres or cultured cells was extracted by TRIzol (Invitrogen, United States), according to the protocol of manufacturer. Reverse transcription for synthesizing the cDNA was performed using the PrimeScript™ RT Master Mix (Takara, Japan), according to the manufacturer's instructions. The resulting cDNA was then subjected to quantitative real-time PCR for the evaluation of the relative mRNA levels. The real-time PCR amplifications were performed with a final reaction volume of 20 μL using the TB Green™ Premix Ex Taq™ II kit (Takara,

Japan), according to the manufacturer's instructions. The reaction mixtures were preheated at 95°C (30 s) for one cycle and then amplified at 95°C (5 s) and 60°C (34 s) for 40 cycles. The Ct (threshold cycle) value of each sample was analyzed by the 2^{-Ct} method, and the mRNA expression levels of the target genes were normalized to the expression level of β-actin to obtain the relative expression levels. The sequences of the used primers are as follows (Table 1).

Immunofluorescence

Frozen sections for immunofluorescence staining were prepared as described in our previous study[34]. First, the frozen sections were treated for 5 min with hot EDTA-citrate buffer (95 °C) (P0085, Beyotime Biotechnology, China) for antigen retrieval, followed by treatment with a blocking reagent (Beyotime Biotechnology, China) for 1 h at 25 °C. Then, the sections were incubated with mouse anti-iba1 (1:200, MABN92, Millipore, United States), rabbit anti-CD206 (1:200, ab64693, Abcam, United States), rabbit anti-CD16 (1:100, ab211151, Abcam, United States), and rabbit anti-MBP (1:200, ab40390, Abcam, United States) antibodies overnight at 4 °C. The sections were rinsed in PBS for 5 min each for three times, and were then incubated with goat anti-mouse secondary antibodies and goat anti-rabbit secondary antibodies for 1 h at 25 °C. Fluorescence signals were detected using a confocal laser scanning microscope (Dragonfly, Oxford Instruments, United Kingdom). For Brdu/NG2 double immunostaining, rabbit anti-NG2 (1:200, AB5320, Millipore, United States) and rat anti-BrdU (1:200, ab6326, Abcam, United Kingdom) antibodies were used according the protocol described in our previous study[32].

Transwell assays

The transwell assay was performed for examining the migration of mouse macrophages (raw 264.7 cells, CC9001, CELLCOOK, China), according to a previous study[35]. The macrophage suspension (10^6/mL, 100 μL) was transferred into the upper transwell chamber (pore size of 8 μm; Corning, United States). Cells from the CCL2 control, CCL2 + Exo^{Ctrl} and CCL2 + Exo^{CCR2} groups, which were subjected to different treatments, were added into the lower transwell chamber. After co-incubation for 16 h at 37 °C, the macrophages remained in the upper transwell chamber were scraped. The membranes were fixed using 4% paraformaldehyde and stained with DAPI (F6057, Sigma, United States). The macrophages that remained in the lower chamber were observed using a fluorescence microscope (Leica DM6B, Germany).

Statistical Analysis

The results were expressed as the mean ± standard error of mean (SEM). SPSS22.0 for Windows was applied for the statistical analysis. One-way Analysis of Variance (ANOVA), followed by Least Significant Difference (LSD)-*t* test procedure or Student's *T* test, was applied for comparing the statistical differences. $P < 0.05$ was statistically significant.

RESULTS

CCR2-overexpressing HUC-MSCs load the CCR2 receptor into their exosomes

Cultured human MSCs express extremely low levels of the CCR2 receptor during continuous passage[30]. This result was consistent with that of the study by Huang *et al*[30], as indicated by flow cytometry, Western blotting, and quantitative real-time PCR (qRT-PCR) analyses, which indicated that the HUC-$MSCs^{Ctrl}$ (passage 6), following the fluorescent-activated cell sorting analysis, showed a low CCR2 protein and mRNA expression. Moreover, the CCR2 protein and mRNA expression in HUC-$MSCs^{CCR2}$ increased significantly (Figure 1A-1D). Since HUC-MSCs are characterized by specific surface markers such as CD13, CD29, CD44, CD34, CD45, CD73, CD90, CD105, HLA-DR[36,37], and the osteogenesis and lipogenesis capacity[38], we checked the biological characteristics changes by flow cytometry analysis, and osteogenesis and lipogenesis induction experiments. The results showed CCR2 overexpression had no significant effects on the biological characteristics of the HUC-MSCs (Supplementary Figure 2). The morphology and diameter distribution of Exo^{Ctrl} and Exo^{CCR2} were confirmed using transmission electron microscopy and the qNano® system (Izon Science, Oxford, United Kingdom), respectively; there was no significant difference between the Exo^{Ctrl} and Exo^{CCR2} (Figure 1E, 1F). Since exosomes are characterized by specific marker CD9, CD63, and CD81[38,39], we investigated the expressions of them by Western blotting. The results indicated both Exo^{Ctrl} and Exo^{CCR2} expressed CD9, CD63, and CD81(Figure 1G); however, Exo^{CCR2} expressed high amounts of CCR2, while Exo^{Ctrl} expressed extremely low amounts of CCR2 (Figure 1H).

To further compare the CCL2-binding capacity of Exo^{CCR2} and Exo^{Ctrl}, ELISA was

Table 1 Lists of the sequences of the used primers

Gene	Primer sequences (5'-3')			
Human-β-actin	F	GGCTGTATTCCCCTCCATCG	R	CCAGTTGGTAACAATGCCATGT
Human-CCR2	F	TACGGTGCTCCCTGTCATAAA	R	TAAGATGAGGACGACCAGCAT
Rat-β-actin	F	GCCCTGAGGCTCTTTTCCAG	R	TGCCACAGGATTCCATACCC
Rat-CD16	F	TGTGTGTCGTCGTAGACGGT	R	TTCGCACATCAGTGTCACCA
Rat-IL-1β	F	GGCAACTGTCCCTGAACT	R	TCCACAGCCACAATGAGT
Rat-CD206	F	ACTGCGTGGTGATGAAAGG	R	TAACCCAGTGGTTGCTCACA
Rat-Arg-1	F	TGGCGTTGACCTTGTCTTGT	R	TTTGCTGTGATGCCCCAGAT
Mouse-IL-1β	F	TTGTTGCTGTGGAGAAGCTGT	R	AACGTCACACACCAGCAGGTT
Mouse-TNF-α	F	AGCAAACCACCAAGTGAGGA	R	GCTGGCACCACTAGTTGGTTGT

performed. The results suggested that Exo^{CCR2} bound significantly to CCL2, compared to Exo^{Ctrl}, while Exo^{Ctrl} showed little CCL2-binding capacity, compared to the case for the CCL2 control group (Figure 1J).

Exo^{CCR2} showed more beneficial effects against PSCI than Exo^{Ctrl}

The Morris water maze is a common tool for performing cognition tests in animals with experimental stroke[40,41](Figure 2A). The establishment of tMCAO were confirmed mNSS behavioral test and TTC staining at 1 d after surgery, as indicated in Supplementary Figure 3. Compared with the tMCAO group, the rats in both the Exo^{CCR2} and Exo^{Ctrl} treatment groups showed a significant decrease in the escape latency spent finding the platform (indicating spatial learning) from day 4 and day 5 during the navigation test. The latency spent finding the platform in case of the animals from the Exo^{CCR2} treatment group further decreased significantly compared to the case for the animals from the Exo^{Ctrl} treatment group at day 4 and day 5 during the navigation test (Figure 2B). During the spatial probe test, the rats from both the Exo^{CCR2} treatment and Exo^{Ctrl} treatment groups showed a significant increase in the time spent in the target quadrant (indicating spatial memory). Moreover, the rats from the Exo^{CCR2} treatment group showed a further improvement with regards to the time spent in the target quadrant, compared to those from the Exo^{Ctrl} treatment group (Figure 2C). At the same time, the mNSS values of the rats in the Exo^{CCR2} and Exo^{Ctrl} treatment groups decreased significantly compared to those of the rats from the tMCAO group; the mNSS values of the rats from the Exo^{CCR2} treatment group showed a further decrease compared to those of the rats from the Exo^{Ctrl} treatment group (Figure 2D).

Exo^{CCR2} showed more beneficial effects with regards to oligodendrogenesis and remyelination than Exo^{Ctrl}

Oligodendrogenesis and remyelination contribute to the recovery from PSCI[42,43]. Therefore, we examined the fluorescence intensity of MBP indicating the integrity of myelination and the number of BrdU+/NG2+ cells indicating the proliferation status of oligodendrocyte around the ischemic area by immunofluorescence staining; the expression of the MBP protein extracted from the ischemic hemispheres was quantified by Western blotting analysis. Compared to the samples obtained from rats in the tMCAO group, samples from the rats subjected to the Exo^{Ctrl} and Exo^{CCR2} treatments exhibited increased fluorescence intensity and protein expression of MBP at day 28 after tMCAO. Moreover, Exo^{CCR2} treatment showed superior effects on the fluorescence intensity and protein expression of MBP compared to that showed by Exo^{Ctrl} treatment (Figure 3A-D). Compared to the samples from rats in the tMCAO group, the samples obtained from rats in both the Exo^{Ctrl} and Exo^{CCR2} treatment groups showed an increased number of BrdU+/NG2+ cells around the ischemic area at day 28 after tMCAO. Moreover, the changes in samples obtained from rats in the Exo^{CCR2} treatment group were more enhanced than those in the samples obtained from rats in the Exo^{Ctrl} treatment group (Figure 3E, 3F).

Exo^{CCR2} promoted microglia/macrophage M2 polarization and inhibited microglia/macrophage M1 polarization in vivo compared to that by Exo^{Ctrl}

Since microglia/macrophage polarization plays an important role in the process of oligodendrogenesis and remyelination after stroke[40,44], we performed qRT-PCR analysis to quantify the mRNA levels of the M1 markers CD16 and IL-1β and the M2 markers CD206 and Arg-1; we also performed immunofluorescence staining to detect

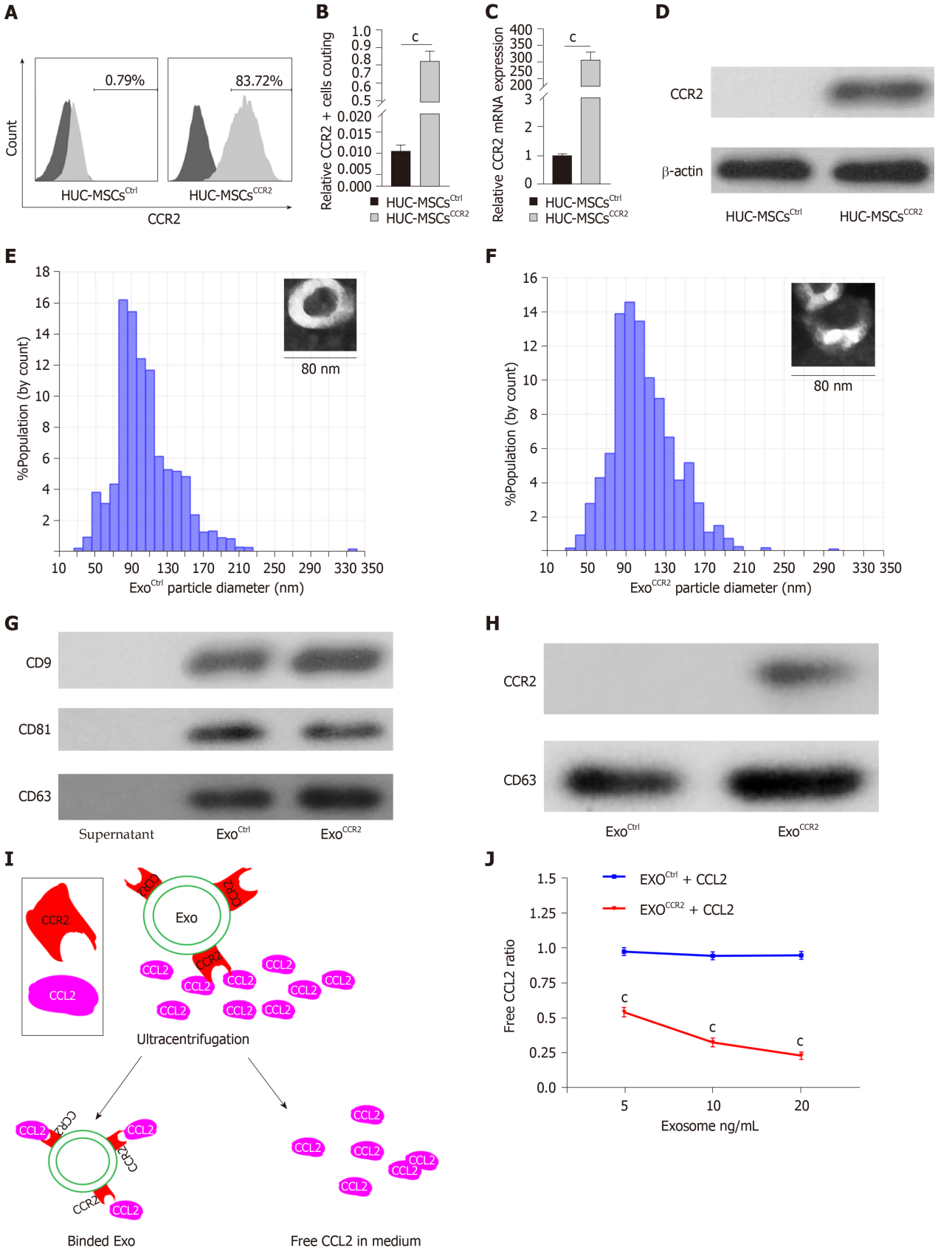

Figure 1 Human umbilical cord mesenchymal stem cells^{CCR2} load the C-C chemokine receptor type 2 receptor into their exosomes. A, B: Flow cytometry analysis of the C-C chemokine receptor type 2 (CCR2) receptor on human umbilical cord mesenchymal stem cells (HUC-MSCs)^{Ctrl} and HUC-MSCs^{CCR2}, n = 3, ^{c}P < 0.001; C: CCR2 mRNA expression in HUC-MSCs^{Ctrl}*vs* HUC-MSCs^{CCR2}, n = 3, ^{c}P < 0.001; D: Western blotting analysis for the quantification of the CCR2 expression in HUC-MSCs^{Ctrl}*vs* HUC-MSCs^{CCR2}, n = 3; E, F: Analysis of the exosomal morphology and diameter distribution of Exo^{Ctrl} and Exo^{CCR2} using transmission electron microscopy and the qNano® system, respectively, n = 3; G: Western blotting analysis for the detection of the exosomal specific markers CD9, CD63, and CD81 in Exo^{Ctrl} and Exo^{CCR2}, n = 3; H: Western blotting analysis for the quantification of the exosomal CCR2 expression in the Exo^{Ctrl} and Exo^{CCR2} samples, n = 3; I: Schematic diagram describing the extraction of the exosomes from the medium; J: Detection of the CCL2-binding ability of the exosomes by ELISA, n = 3, ^{c}P < 0.001.

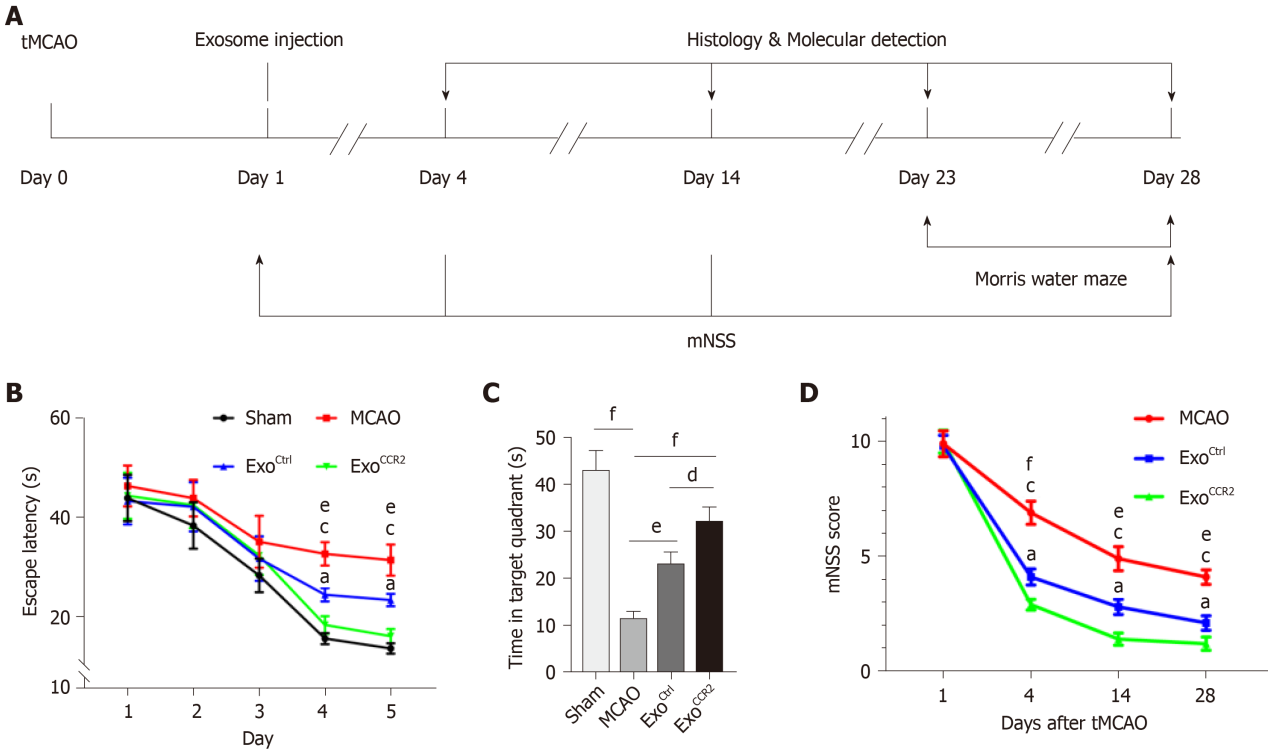

Figure 2 Exo^{CCR2} improved the spatial learning and memory at day 28 after transient middle cerebral occlusion compared to Exo^{Ctrl}. A: Experimental schedule to observe the effects of exosomes on rats with transient middle cerebral occlusion (tMCAO); B: Effect of exosomes on the mean escape latency to find the platform in each group. n = 10, $^{e}P < 0.01$, Exo^{Ctrl} *vs* tMCAO, $^{c}P < 0.001$, Exo^{CCR2} *vs* tMCAO, $^{a}P < 0.05$, Exo^{CCR2} *vs* Exo^{Ctrl}; C: Effect of exosomes on the time spent in the target quadrant in case of rats from each group. n = 10. $^{d}P < 0.05$, $^{e}P < 0.01$, $^{f}P < 0.001$; D: Effect of exosomes on the mNSS values of rats from each group. n = 10. $^{e}P < 0.01$, Exo^{Ctrl} *vs* tMCAO, $^{f}P < 0.001$, Exo^{Ctrl} *vs* tMCAO, $^{c}P < 0.001$, Exo^{CCR2} *vs* tMCAO, $^{a}P < 0.05$, Exo^{CCR2} *vs* Exo^{Ctrl}.

CD16/iba-1 and CD206/iba-1, to compare the effects of Exo^{Ctrl} and Exo^{CCR2} on microglia/macrophage polarization. The CD16 and IL-1β mRNA expression levels in samples obtained from rats after Exo^{CCR2} and Exo^{Ctrl} treatment decreased significantly and the mRNA expression levels of CD206 and Arg-1 increased significantly compared to those in samples obtained from rats in the tMCAO group at day 4 and day 14 after tMCAO. The changes in rats from the Exo^{CCR2} treatment group were more enhanced compared to those in rats from the Exo^{Ctrl} treatment group (Figure 4A-H). These results were validated by immunofluorescence staining for CD16/iba-1 and CD206/iba-1 at day 14 after tMCAO (Figure 4I, 4J).

Exo^{CCR2} suppressed CCL2-induced macrophage migration and activation in vivo and in vitro compared to Exo^{Ctrl}

In pathological conditions such as cerebral ischemia, numerous CCR2+ blood-derived macrophages migrate into the ischemic area due to the high *in situ* expression of CCL2[19,20], which plays a critical role in microglia/macrophage activation and polarization. Downregulation of the CCL2/CCR2 axis inhibits mononuclear macrophage infiltration, which reduces the over-activation and M1 polarization of microglia/macrophages and promotes the alternative M2 activation of microglia/macrophages[21-23,45]. Therefore, we examined the expression of the CCL2, nuclear factor kappa B (NF-κB), ionized calcium-binding adapter molecule 1 (iba-1), and CD68 proteins by Western blotting analysis. The results showed that the expression levels of CCL2, NF-κB, iba-1, and CD68 in samples obtained from rats in the Exo^{CCR2} and Exo^{Ctrl} treatment groups decreased significantly compared to the samples obtained from rats in the tMCAO group; additionally, the changes in samples from rats in the Exo^{CCR2} treatment group were more enhanced compared to those in samples from rats in the Exo^{Ctrl} treatment group (Figure 5A-E).

To further confirm these results *in vitro*, a transwell assay for quantifying the number of migrated macrophages, qRT-PCR analysis for quantifying the mRNA expression levels of IL-1β and tumor necrosis factor α (TNF-α), and Western blotting analysis for quantifying the NF-κB protein expression were performed to evaluate the effects of Exo^{CCR2} and Exo^{Ctrl} on the migration and activation of macrophages *in vitro*. The results indicated that Exo^{CCR2} treatment significantly inhibited macrophage infiltration, and reduced the mRNA expression levels of IL-1β and TNF-α and the

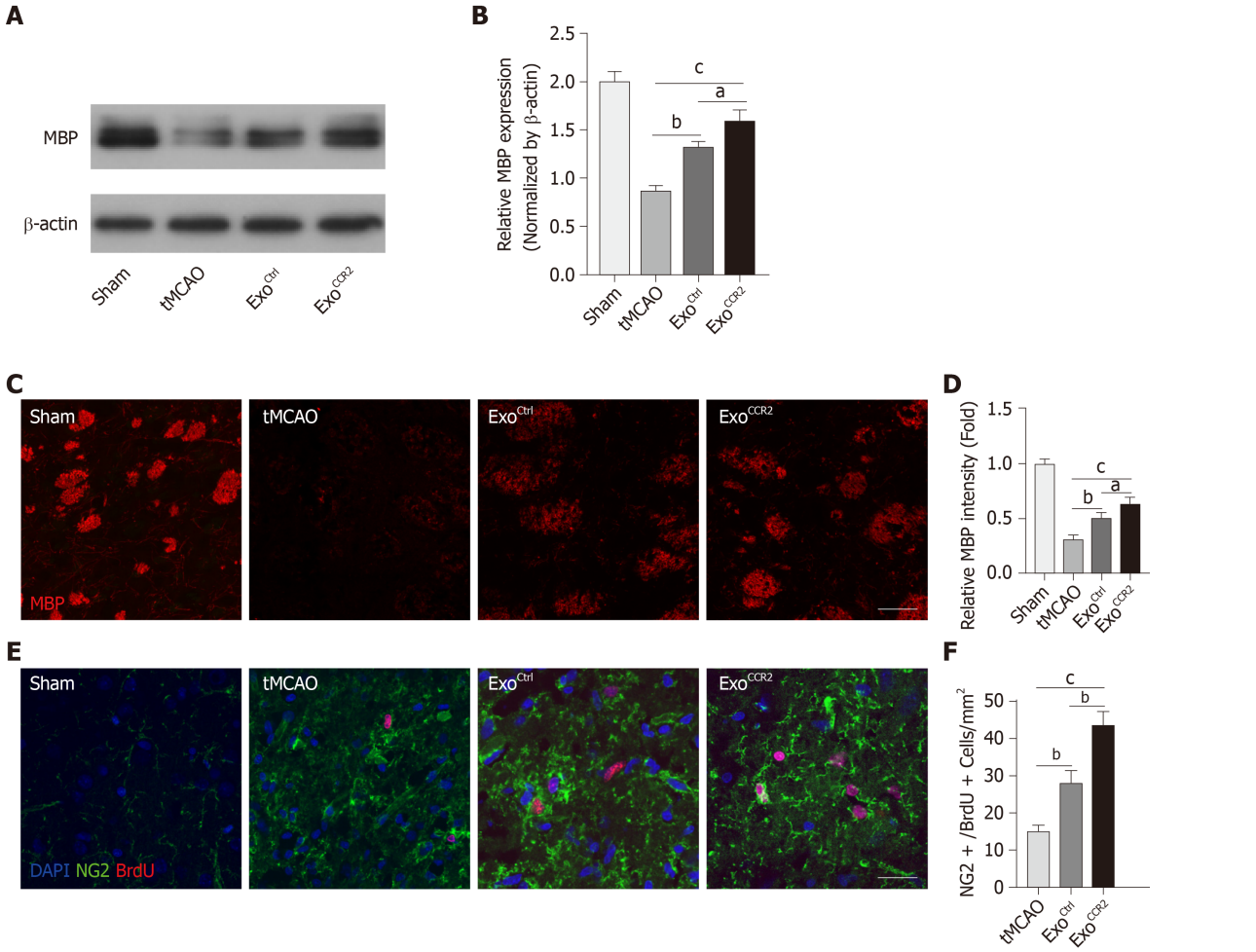

Figure 3 Exo^{CCR2} exerts superior beneficial effects on remyelination and oligodendrogenesis at day 28 after transient middle cerebral occlusion compared to Exo^{Ctrl}. A, B: Western blotting analysis of the MBP expression in samples from rats in each group. n = 5, $^{a}P < 0.05$, $^{b}P < 0.01$, $^{c}P < 0.001$; C, D: Analysis of MBP fluorescence intensity in samples from rats in each group. Scale bar = 50 μm, n = 6, $^{a}P < 0.05$, $^{b}P < 0.01$, $^{c}P < 0.001$; E, F: NG2+/ BrdU+ cell colocalization count by immunofluorescence staining. Scale bar = 50 μm, n = 6. $^{b}P < 0.01$, $^{c}P < 0.001$.

expression levels of the NF-κB protein, compared to the cells from the Exo^{Ctrl} treatment and CCL2 control group; on the contrary, Exo^{Ctrl} showed no significant effects on macrophage migration, the mRNA expression levels of IL-1β and TNF-α, and the expression levels of the NF-κB protein, compared to the case for cells from the CCL2 control group ($P > 0.05$) (Figure 5F-5K).

DISCUSSION

With increasing studies seeking to isolate the specific paracrine factors that mediate the therapeutic effects of MSCs, the therapeutic efficacy of exosomes derived from their parent cells has been found to be comparable to that of MSC therapies[13,14]. Intravenous administration of MSC-derived exosomes to a rodent model of stroke or a rodent model of traumatic brain injury has been shown to substantially promote white matter damage repair, thereby improving the behavioral and cognitive outcomes[29,46]. Moreover, genetically modified exosomes such miR-17-92- or miR-133b-overexpressing exosomes have been found to enhance the therapeutic effects of exosome-based treatment in a model of experimental stroke[47,48]. Exosome-mediated intercellular communications via the transfer of exosomal proteins or RNAs between the source and target cells have been extensively evaluated[49]. However, only a few studies have focused on the surface receptors on exosomes. Ciullo *et al*[50] have found that treatment with C-X-C motif chemokine receptor 4 (CXCR4)-overexpressing exosomes showed more beneficial outcomes in a myocardial infarction animal model than the treatment with control exosomes, suggesting that the receptors on exosomes may also contribute to their therapeutic effects. Shen *et al*[35] have found that CCR2-positive exosomes suppress macrophage migration and alleviate ischemic renal

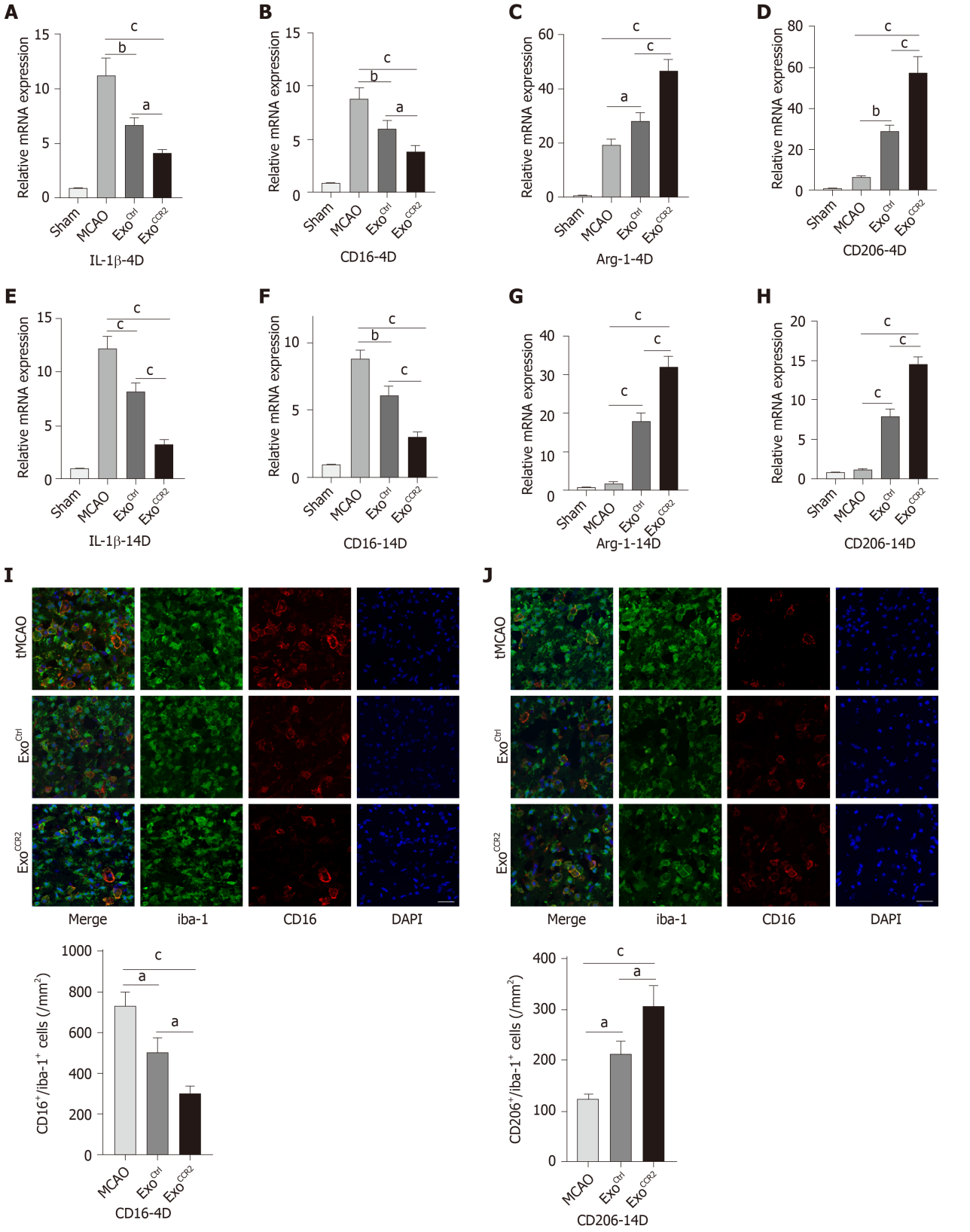

Figure 4 Exo^{CCR2} drove microglia/macrophage M2 polarization and inhibited microglia/macrophage M1 polarization at day 4 and day 14 after transient middle cerebral occlusion compared to Exo^{Ctrl}. A-D: Relative CD16, IL-1β, CD206, and Arg-1 mRNA expression changes in samples obtained from rats in each group on day 4 after transient middle cerebral occlusion (tMCAO), $n = 6$, $^{a}P < 0.05$, $^{b}P < 0.01$, $^{c}P < 0.001$; E-H: Relative CD16, IL-1β, CD206, and Arg-1 mRNA expression changes in samples obtained from rats in each group on day 14 after tMCAO, $n = 6$, $^{b}P < 0.01$, $^{c}P < 0.001$; I: CD16/iba-1 immunofluorescence staining and cell colocalization counts 14 d after tMCAO. Scale bar = 50 μm, $n = 6$, $^{a}P < 0.05$, $^{c}P < 0.001$; J: CT206/iba-1 immunofluorescence staining and cell colocalization counts 14 d after tMCAO. Scale bar = 50 μm, $n = 6$, $^{a}P < 0.05$, $^{c}P < 0.001$.

injury. Since Huang *et al*[30] have demonstrated that CCR2-overexpressing MSCs enhance the therapeutic effects of MSC treatment in rats with tMCAO, we further

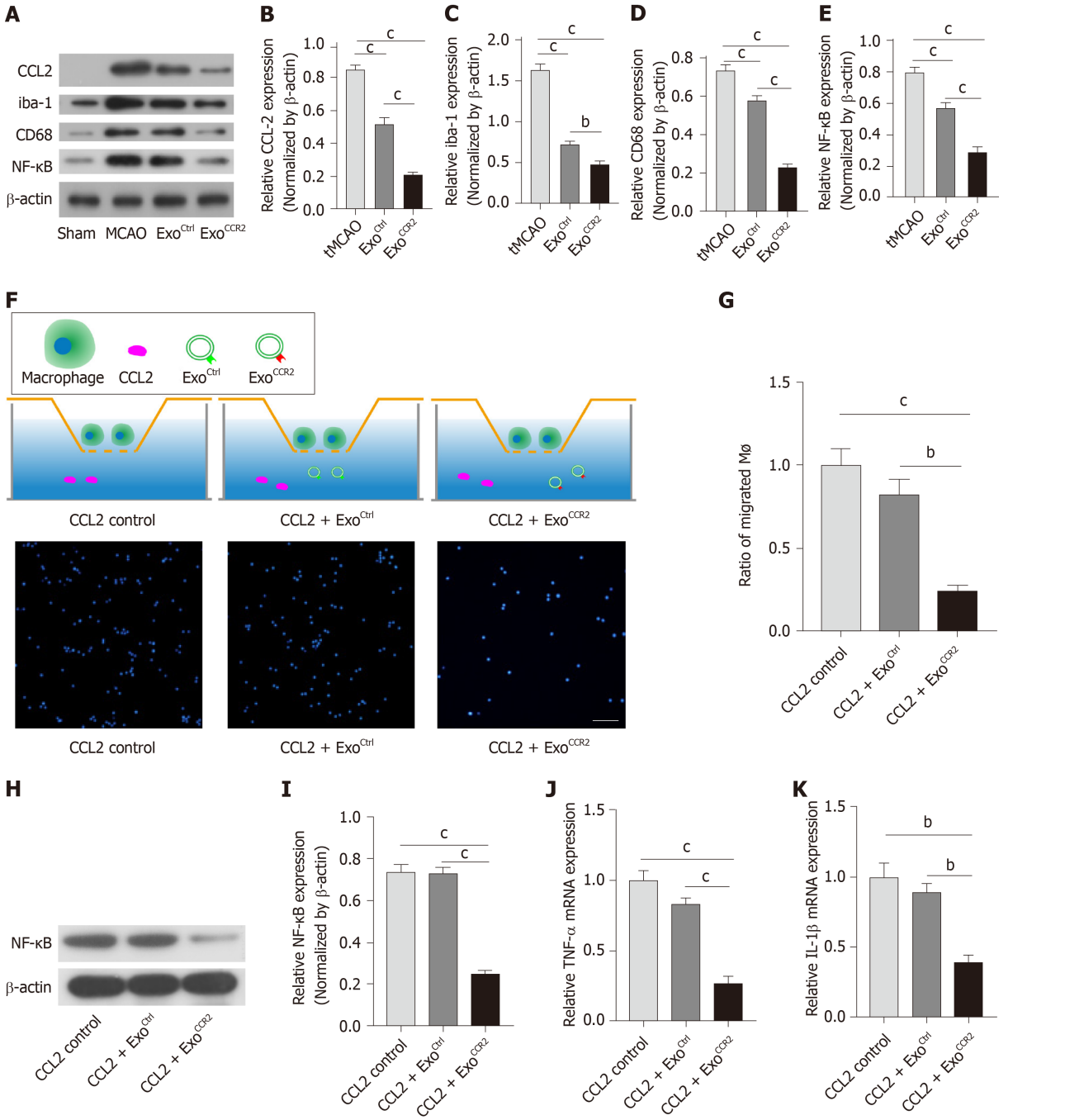

Figure 5 Exo^{CCR2} showed more powerful effects on CCL2-induced macrophage migration and activation *in vivo* and *in vitro* than Exo^{Ctrl}. A-E: Comparison of the expression levels of the CCL2, iba-1, CD68, and NF-κB proteins in samples from rats in each group (*in vivo*) at day 4 after transient middle cerebral occlusion, n = 6, $^{b}P < 0.01$, $^{c}P < 0.001$; F: Schematic diagram of the transwell experiment. Immunofluorescence detection of the migrated macrophages in case of each treatment group (*in vitro*), n = 3; scale bar = 200 μm, $^{b}P < 0.01$, $^{c}P < 0.001$; D-K: Comparison of the mRNA expression levels of TNF-α and IL-1β and the expression levels of the NF-κB protein in cells from each group (*in vitro*), n = 3, $^{b}P < 0.01$, $^{c}P < 0.001$.

explored whether exosomes derived from CCR2-overexpressing MSCs can show enhanced therapeutic effects. The results indicate that HUC-MSCs^{Ctrl} and their secreted Exo^{Ctrl} expressed low amounts of CCR2, while HUC-MSCs^{CCR2} and Exo^{CCR2} showed a high expression of CCR2. Moreover, the results showed that Exo^{CCR2} showed significant binding capacity to the ligand CCL2 *in vitro* compared to Exo^{Ctrl}; this is consistent with the results of the study by Shen *et al*[35], Based on this finding, we hypothesize that when present on exosomes, the CCR2 receptor may exert more powerful therapeutic effects for the treatment of PSCI.

MSC-based treatments have been evaluated to promote cognitive recovery in an animal model of stroke[4] or traumatic brain injury[51]. Previous studies have indicated that exosome treatment can promote the repair of white matter damage after stroke and facilitate the recovery of neurological function after stroke[48,52]. Exosomes

produced by MSCs mediate several therapeutic effects of MSCs; however, reports about the effects of exosome treatment on cognitive impairment after stroke are rare. Since HUC-MSC-derived exosomes have shown potent effects on microglial activation and polarization in animal models such as the hypoxic-ischemic encephalopathy model[26] and the peripheral nerve injury model[27], and improved the cognitive function in an Alzheimer's disease model by modulating microglial polarization[25], we utilized HUC-MSC-derived exosomes in this study. The results showed that the spatial learning and memory in the rats from the Exo^{Ctrl} and Exo^{CCR2} treatment groups were significantly better than those in the rats from the tMCAO group; additionally, Exo^{CCR2} treatment significantly promoted the recovery of spatial learning and memory in rats, compared to that by Exo^{Ctrl} treatment.

Although PSCI is a heterogeneous disease, white matter damage is the most common pathological change observed in almost all cases of vascular dementia[53] and most types of stroke[54]. Both basic medical studies and clinical studies have suggested that white matter damage after stroke is highly correlated with PSCI[43,55,56]. In the acute phase of stroke, oligodendrocyte damage causes the demyelination of the white matter, leading to neurotransmission disorders. During the recovery phase of stroke, oligodendrocytes and their precursor cells proliferate and differentiate into mature oligodendrocytes, which play a key role in remyelination[57]. Thus, facilitating the proliferation of oligodendrocytes and their precursor cells promotes remyelination and cognitive function after stroke[58]. Our finding is consistent with that of Xin *et al*[48,52], who also found that exosomes promote oligodendrogenesis and remyelination following experimental stroke. Another important finding is that Exo^{CCR2} treatment further promoted oligodendrogenesis and remyelination, compared with Exo^{Ctrl} treatment. These results indicate that Exo^{CCR2} treatment notably promoted the recovery from PSCI by enhancing oligodendrogenesis and remyelination compared to that by Exo^{Ctrl} treatment.

Microglia, which are the resident macrophages in the central nervous system, as well as blood-derived macrophages, activate and display dynamic M1 and M2 polarization after stroke[59]. Since activated microglia and blood-derived macrophages are similar with regards to morphology and biological function, and co-express iba-1, CD11b, and F4/80, many scholars have referred to activated microglia and blood-derived macrophages as the same group of cells[60,61]. M1 microglia/macrophage polarization deteriorates oligodendrogenesis and white matter damage by releasing inducible nitric oxide synthase and pro-inflammatory factors such CD16, IL-1β, and TNF-α, while M2 microglia/macrophage polarization facilitates oligodendrogenesis and white matter repair by releasing the mannose receptor CD206 and anti-inflammatory factors such as IL-10, Ym-1 and Arg-1 and engulfing tissue fragments after stroke[40,43,62]. Promoting M2 polarization and inhibiting M1 polarization boosts oligodendrogenesis and remyelination[63,64], and facilitates the recovery from PSCI[40]. The results of our study show that both the Exo^{Ctrl} and Exo^{CCR2} treatments promoted M2 microglia/macrophage polarization and inhibited M1 microglia/macrophage polarization, compared to the case for the rats in the tMCAO group, and Exo^{CCR2} showed enhanced effects compared to Exo^{Ctrl}. Therefore, the enhanced beneficial effects of Exo^{CCR2} against PSCI may be related to their more effective regulation of microglial polarization-mediated oligodendrogenesis and remyelination.

It is well-known that CCL2 is expressed in high amounts in the ischemic hemisphere after stroke, which mediates the infiltration of CCR2+ mononuclear macrophages into the ischemic site and aggravates the excessive activation and M1 polarization of microglia/macrophages[23,45]. Therefore, we postulate that CCR2-overexpressing exosomes may function as endogenous CCL2 sponges binding to these ligands, block the over-infiltration of macrophages, and subsequently inhibit the excessive activation and M1 polarization of microglia/macrophages. These results support the findings from previous studies, which have reported that MSC-derived exosomes downregulate CCL2 overexpression[65] and microglia/macrophage overactivation[27]; Exo^{Ctrl} significantly downregulated the expression of CCL2, iba-1, CD68, and NF-κB *in vivo*, compared to the case for rats in the tMCAO group. Moreover, Exo^{CCR2} further downregulated the expression of CCL2, iba-1, CD68, and NF-κB. To verify this *in vivo* finding, *in vitro* experiments were performed, which showed that Exo^{CCR2} bound significantly to CCL2 *in vitro* compared with Exo^{Ctrl}, while Exo^{Ctrl} showed a low degree of binding to CCL2. Meanwhile, Exo^{CCR2} significantly inhibited *in vitro* macrophage infiltration and the release of inflammatory factors, and reduced the NF-κB expression, compared to Exo^{Ctrl}. Therefore, CCR2 molecules on exosomes may function as endogenous CCL2 sponges that bind to these ligands and inhibit the infiltration of macrophages and the subsequent over-activation and M1 polarization of microglia/macrophages.

In conclusion, the present study demonstrated that both Exo^{Ctrl} and Exo^{CCR2} improved the cognitive function in rats after ischemic stroke by promoting M2

microglia/macrophage polarization, thereby enhancing oligodendrogenesis and remyelination. Furthermore, this study is the first to provide evidence that Exo^{CCR2} have enhanced beneficial effects compared to Exo^{Ctrl}, partially due to the action of CCR2 molecules as endogenous CCL2 sponges, whereby they bind to these ligands and inhibit the infiltration and activation of macrophages. Since we utilized human MSC-derived exosomes, our research serves as a pre-clinical study; further studies on stroke patients are required to confirm our hypothesis.

ARTICLE HIGHLIGHTS

Research background

Post-stroke cognitive impairment (PSCI) is a common sequela of stroke with considerable impact on the health well-being and quality of life to patients, and poses significant financial burden on society. Exosomes have been shown to possess therapeutic effects that are comparable to the mesenchymal stromal cells. However, few studies have focused on the effects of exosomes derived from human umbilical cord mesenchymal stem cells (HUC-MSCs) (Exo^{Ctrl}) on PSCI. Here in this study, we aimed to explore the if exosomes derived from C-C chemokine receptor type 2 (CCR2)-overexpressing HUC-MSCs (Exo^{CCR2}) have any therapeutic effects on PSCI, and clarify the possible underlying mechanisms.

Research motivation

Effective treatment strategies for PSCI in stroke patients are an unmet clinical need.

Research objectives

In the present study, we aimed to: (1) Investigate whether CCR2 over-expressing exosomes possess improved therapeutic effects on PSCI; and (2) The possible underlying mechanisms involved in the therapeutic benefits of exosomes.

Research methods

The morphology of Exo^{Ctrl} and Exo^{CCR2} were determined by transmission electron microscopy and qNano® particles analyzer; the CCR2 expression in the Exo^{Ctrl} and Exo^{CCR2} was evaluated by Western blotting; the binding capacity of exosomes to CC chemokine ligand 2 (CCL2) *in vivo* was examined by ELISA; the effects of Exo^{Ctrl} and Exo^{CCR2} on PSCI in experimental stroke rats were assessed by Morris water maze. Remyelination and oligodendrogenesis was analyzed by Western blotting and immunofluorescence microscopy, and microglia/macrophage polarization were investigated by qRT-PCR and immunofluorescence imaging. The infiltration and activation of hematogenous macrophages were analyzed by transwell migration analysis and Western blotting.

Research results

CCR2-overexpressing HUC-MSCs could deliver CCR2 receptor rich exosomes. There were not significant difference in the size and morphology between Exo^{Ctrl} and Exo^{CCR2}. Exo^{CCR2} showed more powerful binding capacity to CCL2, while Exo^{Ctrl} hardly bound to CCL2. Exo^{CCR2} enhanced the beneficial effects of Exo^{Ctrl} on PSCI through further promoting microglia/macrophage polarization-mediated oligodendrogenesis and remyelination. Compared with Exo^{Ctrl}, Exo^{CCR2} showed more powerful suppression on CCL2-induced macrophage migration and activation *in vivo* and *in vitro*.

Research conclusions

CCR2 over-expressing on exosomes showed enhanced therapeutic benefits on PSCI through more powerful modulation on microglia/macrophage polarization-mediated oligodendrogenesis and remyelination. The additional therapeutic effect maybe related to the suppression on CCL2-induced macrophage infiltration and activation.

Research perspectives

Our study provides great insight in the application of stem cells-based therapies for neural degenerative disorders. Comparisons of the therapeutic effects of Exo^{Ctrl} and Exo^{CCR2} on more clinically relevant animal models of stroke are warranted.

ACKNOWLEDGEMENTS

Authors are grateful to the generous support of the Center for Stem Cell Biology and Tissue Engineering, Sun Yat-sen University.

REFERENCES

1 **Kalaria RN**, Akinyemi R, Ihara M. Stroke injury, cognitive impairment and vascular dementia. *Biochim Biophys Acta* 2016; **1862**: 915-925 [PMID: 26806700 DOI: 10.1016/j.bbadis.2016.01.015]
2 **Qu Y**, Zhuo L, Li N, Hu Y, Chen W, Zhou Y, Wang J, Tao Q, Hu J, Nie X, Zhan S. Prevalence of post-

stroke cognitive impairment in china: a community-based, cross-sectional study. *PLoS One* 2015; **10**: e0122864 [PMID: 25874998 DOI: 10.1371/journal.pone.0122864]
3 **Béjot Y**, Giroud M. Mean age at stroke onset: an instructive tool from epidemiological studies. *Eur J Neurol* 2009; **16**: e3 [PMID: 19087137 DOI: 10.1111/j.1468-1331.2008.02360.x]
4 **Sammali E**, Alia C, Vegliante G, Colombo V, Giordano N, Pischiutta F, Boncoraglio GB, Barilani M, Lazzari L, Caleo M, De Simoni MG, Gaipa G, Citerio G, Zanier ER. Intravenous infusion of human bone marrow mesenchymal stromal cells promotes functional recovery and neuroplasticity after ischemic stroke in mice. *Sci Rep* 2017; **7**: 6962 [PMID: 28761170 DOI: 10.1038/s41598-017-07274-w]
5 **Moisan A**, Favre I, Rome C, De Fraipont F, Grillon E, Coquery N, Mathieu H, Mayan V, Naegele B, Hommel M, Richard MJ, Barbier EL, Remy C, Detante O. Intravenous Injection of Clinical Grade Human MSCs After Experimental Stroke: Functional Benefit and Microvascular Effect. *Cell Transplant* 2016; **25**: 2157-2171 [PMID: 26924704 DOI: 10.3727/096368916X691132]
6 **Fischer UM**, Harting MT, Jimenez F, Monzon-Posadas WO, Xue H, Savitz SI, Laine GA, Cox CS. Pulmonary passage is a major obstacle for intravenous stem cell delivery: the pulmonary first-pass effect. *Stem Cells Dev* 2009; **18**: 683-692 [PMID: 19099374 DOI: 10.1089/scd.2008.0253]
7 **Barbash IM**, Chouraqui P, Baron J, Feinberg MS, Etzion S, Tessone A, Miller L, Guetta E, Zipori D, Kedes LH, Kloner RA, Leor J. Systemic delivery of bone marrow-derived mesenchymal stem cells to the infarcted myocardium: feasibility, cell migration, and body distribution. *Circulation* 2003; **108**: 863-868 [PMID: 12900340 DOI: 10.1161/01.CIR.0000084828.50310.6A]
8 **Gervois P**, Wolfs E, Ratajczak J, Dillen Y, Vangansewinkel T, Hilkens P, Bronckaers A, Lambrichts I, Struys T. Stem Cell-Based Therapies for Ischemic Stroke: Preclinical Results and the Potential of Imaging-Assisted Evaluation of Donor Cell Fate and Mechanisms of Brain Regeneration. *Med Res Rev* 2016; **36**: 1080-1126 [PMID: 27439773 DOI: 10.1002/med.21400]
9 **Acosta SA**, Tajiri N, Hoover J, Kaneko Y, Borlongan CV. Intravenous Bone Marrow Stem Cell Grafts Preferentially Migrate to Spleen and Abrogate Chronic Inflammation in Stroke. *Stroke* 2015; **46**: 2616-2627 [PMID: 26219646 DOI: 10.1161/STROKEAHA.115.009854]
10 **Huang XP**, Sun Z, Miyagi Y, McDonald Kinkaid H, Zhang L, Weisel RD, Li RK. Differentiation of allogeneic mesenchymal stem cells induces immunogenicity and limits their long-term benefits for myocardial repair. *Circulation* 2010; **122**: 2419-2429 [PMID: 21098445 DOI: 10.1161/CIRCULATIONAHA.110.955971]
11 **Barry FP**, Murphy JM, English K, Mahon BP. Immunogenicity of adult mesenchymal stem cells: lessons from the fetal allograft. *Stem Cells Dev* 2005; **14**: 252-265 [PMID: 15969620 DOI: 10.1089/scd.2005.14.252]
12 **Gomzikova MO**, Rizvanov AA. Current Trends in Regenerative Medicine: From Cell to Cell-Free Therapy. *BioNanoScience* 2017; **7**: 240-245 [DOI: 10.1007/s12668-016-0348-0]
13 **Phinney DG**, Pittenger MF. Concise Review: MSC-Derived Exosomes for Cell-Free Therapy. *Stem Cells* 2017; **35**: 851-858 [PMID: 28294454 DOI: 10.1002/stem.2575]
14 **Zhang ZG**, Buller B, Chopp M. Exosomes - beyond stem cells for restorative therapy in stroke and neurological injury. *Nat Rev Neurol* 2019; **15**: 193-203 [PMID: 30700824 DOI: 10.1038/s41582-018-0126-4]
15 **Suzuki E**, Fujita D, Takahashi M, Oba S, Nishimatsu H. Therapeutic Effects of Mesenchymal Stem Cell-Derived Exosomes in Cardiovascular Disease. *Adv Exp Med Biol* 2017; **998**: 179-185 [PMID: 28936740 DOI: 10.1007/978-981-10-4397-0_12]
16 **Farzamfar S**, Hasanpour A, Nazeri N, Razavi H, Salehi M, Shafei S, Nooshabadi VT, Vaez A, Ehterami A, Sahrapeyma H, Ai J. Extracellular micro/nanovesicles rescue kidney from ischemia-reperfusion injury. *J Cell Physiol* 2019; **234**: 12290-12300 [PMID: 30609022 DOI: 10.1002/jcp.27998]
17 **Phinney DG**, Di Giuseppe M, Njah J, Sala E, Shiva S, St Croix CM, Stolz DB, Watkins SC, Di YP, Leikauf GD, Kolls J, Riches DW, Deiuliis G, Kaminski N, Boregowda SV, McKenna DH, Ortiz LA. Mesenchymal stem cells use extracellular vesicles to outsource mitophagy and shuttle microRNAs. *Nat Commun* 2015; **6**: 8472 [PMID: 26442449 DOI: 10.1038/ncomms9472]
18 **Zagrean AM**, Hermann DM, Opris I, Zagrean L, Popa-Wagner A. Multicellular Crosstalk Between Exosomes and the Neurovascular Unit After Cerebral Ischemia. Therapeutic Implications. *Front Neurosci* 2018; **12**: 811 [PMID: 30459547 DOI: 10.3389/fnins.2018.00811]
19 **Rajan WD**, Wojtas B, Gielniewski B, Gieryng A, Zawadzka M, Kaminska B. Dissecting functional phenotypes of microglia and macrophages in the rat brain after transient cerebral ischemia. *Glia* 2019; **67**: 232-245 [PMID: 30485549 DOI: 10.1002/glia.23536]
20 **Chen Y**, Hallenbeck JM, Ruetzler C, Bol D, Thomas K, Berman NE, Vogel SN. Overexpression of monocyte chemoattractant protein 1 in the brain exacerbates ischemic brain injury and is associated with recruitment of inflammatory cells. *J Cereb Blood Flow Metab* 2003; **23**: 748-755 [PMID: 12796723 DOI: 10.1097/01.WCB.0000071885.63724.20]
21 **Dimitrijevic OB**, Stamatovic SM, Keep RF, Andjelkovic AV. Absence of the chemokine receptor CCR2 protects against cerebral ischemia/reperfusion injury in mice. *Stroke* 2007; **38**: 1345-1353 [PMID: 17332467 DOI: 10.1161/01.STR.0000259709.16654.8f]
22 **Hughes PM**, Allegrini PR, Rudin M, Perry VH, Mir AK, Wiessner C. Monocyte chemoattractant protein-1 deficiency is protective in a murine stroke model. *J Cereb Blood Flow Metab* 2002; **22**: 308-317 [PMID: 11891436 DOI: 10.1097/00004647-200203000-00008]
23 **Morganti JM**, Jopson TD, Liu S, Riparip LK, Guandique CK, Gupta N, Ferguson AR, Rosi S. CCR2 antagonism alters brain macrophage polarization and ameliorates cognitive dysfunction induced by traumatic brain injury. *J Neurosci* 2015; **35**: 748-760 [PMID: 25589768 DOI: 10.1523/JNEUROSCI.2405-14.2015]
24 **Hsieh CL**, Niemi EC, Wang SH, Lee CC, Bingham D, Zhang J, Cozen ML, Charo I, Huang EJ, Liu J, Nakamura MC. CCR2 deficiency impairs macrophage infiltration and improves cognitive function after traumatic brain injury. *J Neurotrauma* 2014; **31**: 1677-1688 [PMID: 24806994 DOI: 10.1089/neu.2013.3252]
25 **Ding M**, Shen Y, Wang P, Xie Z, Xu S, Zhu Z, Wang Y, Lyu Y, Wang D, Xu L, Bi J, Yang H. Exosomes Isolated From Human Umbilical Cord Mesenchymal Stem Cells Alleviate Neuroinflammation and Reduce Amyloid-Beta Deposition by Modulating Microglial Activation in Alzheimer's Disease. *Neurochem Res* 2018; **43**: 2165-2177 [PMID: 30259257 DOI: 10.1007/s11064-018-2641-5]
26 **Thomi G**, Surbek D, Haesler V, Joerger-Messerli M, Schoeberlein A. Exosomes derived from umbilical cord mesenchymal stem cells reduce microglia-mediated neuroinflammation in perinatal brain injury. *Stem Cell Res Ther* 2019; **10**: 105 [PMID: 30898154 DOI: 10.1186/s13287-019-1207-z]

27 **Shiue SJ**, Rau RH, Shiue HS, Hung YW, Li ZX, Yang KD, Cheng JK. Mesenchymal stem cell exosomes as a cell-free therapy for nerve injury-induced pain in rats. *Pain* 2019; **160**: 210-223 [PMID: 30188455 DOI: 10.1097/j.pain.0000000000001395]

28 **Longa EZ**, Weinstein PR, Carlson S, Cummins R. Reversible middle cerebral artery occlusion without craniectomy in rats. *Stroke* 1989; **20**: 84-91 [PMID: 2643202 DOI: 10.1161/01.str.20.1.84]

29 **Otero-Ortega L**, Laso-García F, Gómez-de Frutos MD, Rodríguez-Frutos B, Pascual-Guerra J, Fuentes B, Díez-Tejedor E, Gutiérrez-Fernández M. White Matter Repair After Extracellular Vesicles Administration in an Experimental Animal Model of Subcortical Stroke. *Sci Rep* 2017; **7**: 44433 [PMID: 28300134 DOI: 10.1038/srep44433]

30 **Huang Y**, Wang J, Cai J, Qiu Y, Zheng H, Lai X, Sui X, Wang Y, Lu Q, Zhang Y, Yuan M, Gong J, Cai W, Liu X, Shan Y, Deng Z, Shi Y, Shu Y, Zhang L, Qiu W, Peng L, Ren J, Lu Z, Xiang AP. Targeted homing of CCR2-overexpressing mesenchymal stromal cells to ischemic brain enhances post-stroke recovery partially through PRDX4-mediated blood-brain barrier preservation. *Theranostics* 2018; **8**: 5929-5944 [PMID: 30613272 DOI: 10.7150/thno.28029]

31 **Ouyang X**, Han X, Chen Z, Fang J, Huang X, Wei H. MSC-derived exosomes ameliorate erectile dysfunction by alleviation of corpus cavernosum smooth muscle apoptosis in a rat model of cavernous nerve injury. *Stem Cell Res Ther* 2018; **9**: 246 [PMID: 30257719 DOI: 10.1186/s13287-018-1003-1]

32 **Jiang T**, Zhang L, Pan X, Zheng H, Chen X, Li L, Luo J, Hu X. Physical Exercise Improves Cognitive Function Together with Microglia Phenotype Modulation and Remyelination in Chronic Cerebral Hypoperfusion. *Front Cell Neurosci* 2017; **11**: 404 [PMID: 29311834 DOI: 10.3389/fncel.2017.00404]

33 **Liu N**, Zhang Y, Fan L, Yuan M, Du H, Cheng R, Liu D, Lin F. Effects of transplantation with bone marrow-derived mesenchymal stem cells modified by Survivin on experimental stroke in rats. *J Transl Med* 2011; **9**: 105 [PMID: 21733181 DOI: 10.1186/1479-5876-9-105]

34 **Zheng HQ**, Zhang LY, Luo J, Li LL, Li M, Zhang Q, Hu XQ. Physical exercise promotes recovery of neurological function after ischemic stroke in rats. *Int J Mol Sci* 2014; **15**: 10974-10988 [PMID: 24945308 DOI: 10.3390/ijms150610974]

35 **Shen B**, Liu J, Zhang F, Wang Y, Qin Y, Zhou Z, Qiu J, Fan Y. CCR2 Positive Exosome Released by Mesenchymal Stem Cells Suppresses Macrophage Functions and Alleviates Ischemia/Reperfusion-Induced Renal Injury. *Stem Cells Int* 2016; **2016**: 1240301 [PMID: 27843457 DOI: 10.1155/2016/1240301]

36 **Yan Y**, Xu W, Qian H, Si Y, Zhu W, Cao H, Zhou H, Mao F. Mesenchymal stem cells from human umbilical cords ameliorate mouse hepatic injury in vivo. *Liver Int* 2009; **29**: 356-365 [PMID: 19141029 DOI: 10.1111/j.1478-3231.2008.01855.x]

37 **Monguió-Tortajada M**, Roura S, Gálvez-Montón C, Pujal JM, Aran G, Sanjurjo L, Franquesa M, Sarrias MR, Bayes-Genis A, Borràs FE. Nanosized UCMSC-derived extracellular vesicles but not conditioned medium exclusively inhibit the inflammatory response of stimulated T cells: implications for nanomedicine. *Theranostics* 2017; **7**: 270-284 [PMID: 28042333 DOI: 10.7150/thno.16154]

38 **Xiong ZH**, Wei J, Lu MQ, Jin MY, Geng HL. Protective effect of human umbilical cord mesenchymal stem cell exosomes on preserving the morphology and angiogenesis of placenta in rats with preeclampsia. *Biomed Pharmacother* 2018; **105**: 1240-1247 [PMID: 30021360 DOI: 10.1016/j.biopha.2018.06.032]

39 **Zhang Y**, Hao Z, Wang P, Xia Y, Wu J, Xia D, Fang S, Xu S. Exosomes from human umbilical cord mesenchymal stem cells enhance fracture healing through HIF-1α-mediated promotion of angiogenesis in a rat model of stabilized fracture. *Cell Prolif* 2019; **52**: e12570 [PMID: 30663158 DOI: 10.1111/cpr.12570]

40 **Han L**, Cai W, Mao L, Liu J, Li P, Leak RK, Xu Y, Hu X, Chen J. Rosiglitazone Promotes White Matter Integrity and Long-Term Functional Recovery After Focal Cerebral Ischemia. *Stroke* 2015; **46**: 2628-2636 [PMID: 26243225 DOI: 10.1161/STROKEAHA.115.010091]

41 **Bouët V**, Freret T, Toutain J, Divoux D, Boulouard M, Schumann-Bard P. Sensorimotor and cognitive deficits after transient middle cerebral artery occlusion in the mouse. *Exp Neurol* 2007; **203**: 555-567 [PMID: 17067578 DOI: 10.1016/j.expneurol.2006.09.006]

42 **Dufouil C**, Godin O, Chalmers J, Coskun O, MacMahon S, Tzourio-Mazoyer N, Bousser MG, Anderson C, Mazoyer B, Tzourio C; PROGRESS MRI Substudy Investigators. Severe cerebral white matter hyperintensities predict severe cognitive decline in patients with cerebrovascular disease history. *Stroke* 2009; **40**: 2219-2221 [PMID: 19390070 DOI: 10.1161/STROKEAHA.108.540633]

43 **Suenaga J**, Hu X, Pu H, Shi Y, Hassan SH, Xu M, Leak RK, Stetler RA, Gao Y, Chen J. White matter injury and microglia/macrophage polarization are strongly linked with age-related long-term deficits in neurological function after stroke. *Exp Neurol* 2015; **272**: 109-119 [PMID: 25836044 DOI: 10.1016/j.expneurol.2015.03.021]

44 **Wang G**, Zhang J, Hu X, Zhang L, Mao L, Jiang X, Liou AK, Leak RK, Gao Y, Chen J. Microglia/macrophage polarization dynamics in white matter after traumatic brain injury. *J Cereb Blood Flow Metab* 2013; **33**: 1864-1874 [PMID: 23942366 DOI: 10.1038/jcbfm.2013.146]

45 **He S**, Liu R, Li B, Huang L, Fan W, Tembachako CR, Zheng X, Xiong X, Miyata M, Xu B, Li Y, Fang W. Propagermanium, a CCR2 inhibitor, attenuates cerebral ischemia/reperfusion injury through inhibiting inflammatory response induced by microglia. *Neurochem Int* 2019; **125**: 99-110 [PMID: 30794846 DOI: 10.1016/j.neuint.2019.02.010]

46 **Zhang Y**, Chopp M, Meng Y, Katakowski M, Xin H, Mahmood A, Xiong Y. Effect of exosomes derived from multipluripotent mesenchymal stromal cells on functional recovery and neurovascular plasticity in rats after traumatic brain injury. *J Neurosurg* 2015; **122**: 856-867 [PMID: 25594326 DOI: 10.3171/2014.11.JNS14770]

47 **Xin H**, Katakowski M, Wang F, Qian JY, Liu XS, Ali MM, Buller B, Zhang ZG, Chopp M. MicroRNA cluster miR-17-92 Cluster in Exosomes Enhance Neuroplasticity and Functional Recovery After Stroke in Rats. *Stroke* 2017; **48**: 747-753 [PMID: 28232590 DOI: 10.1161/STROKEAHA.116.015204]

48 **Xin H**, Li Y, Liu Z, Wang X, Shang X, Cui Y, Zhang ZG, Chopp M. MiR-133b promotes neural plasticity and functional recovery after treatment of stroke with multipotent mesenchymal stromal cells in rats via transfer of exosome-enriched extracellular particles. *Stem Cells* 2013; **31**: 2737-2746 [PMID: 23630198 DOI: 10.1002/stem.1409]

49 **Zhang ZG**, Chopp M. Exosomes in stroke pathogenesis and therapy. *J Clin Invest* 2016; **126**: 1190-1197 [PMID: 27035810 DOI: 10.1172/JCI81133]

50 **Ciullo A**, Biemmi V, Milano G, Bolis S, Cervio E, Fertig ET, Gherghiceanu M, Moccetti T, Camici GG, Vassalli G, Barile L. Exosomal Expression of CXCR4 Targets Cardioprotective Vesicles to Myocardial Infarction and Improves Outcome after Systemic Administration. *Int J Mol Sci* 2019; 20 [PMID: 30678240 DOI: 10.3390/ijms20030468]

51 **Zhao Y**, Gibb SL, Zhao J, Moore AN, Hylin MJ, Menge T, Xue H, Baimukanova G, Potter D, Johnson EM, Holcomb JB, Cox CS, Dash PK, Pati S. Wnt3a, a Protein Secreted by Mesenchymal Stem Cells Is Neuroprotective and Promotes Neurocognitive Recovery Following Traumatic Brain Injury. *Stem Cells* 2016; **34**: 1263-1272 [PMID: 26840479 DOI: 10.1002/stem.2310]

52 **Xin H**, Li Y, Cui Y, Yang JJ, Zhang ZG, Chopp M. Systemic administration of exosomes released from mesenchymal stromal cells promote functional recovery and neurovascular plasticity after stroke in rats. *J Cereb Blood Flow Metab* 2013; **33**: 1711-1715 [PMID: 23963371 DOI: 10.1038/jcbfm.2013.152]

53 **Kalaria RN**. Neuropathological diagnosis of vascular cognitive impairment and vascular dementia with implications for Alzheimer's disease. *Acta Neuropathol* 2016; **131**: 659-685 [PMID: 27062261 DOI: 10.1007/s00401-016-1571-z]

54 **Deramecourt V**, Pasquier F. Neuronal substrate of cognitive impairment in post-stroke dementia. *Brain* 2014; **137**: 2404-2405 [PMID: 25125586 DOI: 10.1093/brain/awu188]

55 **Molad J**, Kliper E, Korczyn AD, Ben Assayag E, Ben Bashat D, Shenhar-Tsarfaty S, Aizenstein O, Shopin L, Bornstein NM, Auriel E. Only White Matter Hyperintensities Predicts Post-Stroke Cognitive Performances Among Cerebral Small Vessel Disease Markers: Results from the TABASCO Study. *J Alzheimers Dis* 2017; **56**: 1293-1299 [PMID: 28157096 DOI: 10.3233/JAD-160939]

56 **Jokinen H**, Kalska H, Mäntylä R, Ylikoski R, Hietanen M, Pohjasvaara T, Kaste M, Erkinjuntti T. White matter hyperintensities as a predictor of neuropsychological deficits post-stroke. *J Neurol Neurosurg Psychiatry* 2005; **76**: 1229-1233 [PMID: 16107356 DOI: 10.1136/jnnp.2004.055657]

57 **Itoh K**, Maki T, Lok J, Arai K. Mechanisms of cell-cell interaction in oligodendrogenesis and remyelination after stroke. *Brain Res* 2015; **1623**: 135-149 [PMID: 25960351 DOI: 10.1016/j.brainres.2015.04.039]

58 **Wang Y**, Liu G, Hong D, Chen F, Ji X, Cao G. White matter injury in ischemic stroke. *Prog Neurobiol* 2016; **141**: 45-60 [PMID: 27090751 DOI: 10.1016/j.pneurobio.2016.04.005]

59 **Hu X**, Li P, Guo Y, Wang H, Leak RK, Chen S, Gao Y, Chen J. Microglia/macrophage polarization dynamics reveal novel mechanism of injury expansion after focal cerebral ischemia. *Stroke* 2012; **43**: 3063-3070 [PMID: 22933588 DOI: 10.1161/STROKEAHA.112.659656]

60 **Ginhoux F**, Greter M, Leboeuf M, Nandi S, See P, Gokhan S, Mehler MF, Conway SJ, Ng LG, Stanley ER, Samokhvalov IM, Merad M. Fate mapping analysis reveals that adult microglia derive from primitive macrophages. *Science* 2010; **330**: 841-845 [PMID: 20966214 DOI: 10.1126/science.1194637]

61 **Wang J**. Preclinical and clinical research on inflammation after intracerebral hemorrhage. *Prog Neurobiol* 2010; **92**: 463-477 [PMID: 20713126 DOI: 10.1016/j.pneurobio.2010.08.001]

62 **Lan X**, Han X, Li Q, Yang QW, Wang J. Modulators of microglial activation and polarization after intracerebral haemorrhage. *Nat Rev Neurol* 2017; **13**: 420-433 [PMID: 28524175 DOI: 10.1038/nrneurol.2017.69]

63 **Miron VE**, Boyd A, Zhao JW, Yuen TJ, Ruckh JM, Shadrach JL, van Wijngaarden P, Wagers AJ, Williams A, Franklin RJM, Ffrench-Constant C. M2 microglia and macrophages drive oligodendrocyte differentiation during CNS remyelination. *Nat Neurosci* 2013; **16**: 1211-1218 [PMID: 23872599 DOI: 10.1038/nn.3469]

64 **Miron VE**, Franklin RJ. Macrophages and CNS remyelination. *J Neurochem* 2014; **130**: 165-171 [PMID: 24601941 DOI: 10.1111/jnc.12705]

65 **Yu B**, Shao H, Su C, Jiang Y, Chen X, Bai L, Zhang Y, Li Q, Zhang X, Li X. Exosomes derived from MSCs ameliorate retinal laser injury partially by inhibition of MCP-1. *Sci Rep* 2016; **6**: 34562 [PMID: 27686625 DOI: 10.1038/srep34562]

Published By Baishideng Publishing Group Inc
7041 Koll Center Parkway, Suite 160, Pleasanton, CA 94566, USA
Telephone: +1-925-3991568
E-mail: bpgoffice@wjgnet.com
Help Desk: https://www.f6publishing.com/helpdesk
https://www.wjgnet.com